Effect of secondary current on flow prediction in an open channel flow

Jnana Ranjan Khuntia

Department of Civil Engineering

National Institute of Technology, Rourkela

Effect of Secondary Current on Flow Prediction in an Open Channel Flow

Dissertation submitted in partial fulfilment

of the requirement for the degree of

Master of Technology

in

Water Resources Engineering

of

Civil Engineering Department

by

Jnana Ranjan Khuntia

(Roll No: 214CE4382)

Based on research carried out

Under the supervision of

Prof. Kishanjit Kumar Khatua

May, 2016

Department of Civil Engineering

National Institute of Technology, Rourkela

Department of Civil Engineering

National Institute of Technology, Rourkela

May 27, 2016

Certificate of Examination

Roll Number: *214CE4382*

Name: *Jnana Ranjan Khuntia*

Title of dissertation: *Effect of Secondary Current on Flow Prediction in an Open Channel Flow*

We the below signed, after checking the dissertation mentioned above and the official record book (s) of the student, hereby state our approval of the dissertation submitted in partial fulfilment of the requirements of the degree of *Master in Technology* in *Civil Engineering Department* at *National Institute of Technology Rourkela*. We are satisfied with the volume, quality, correctness, and originality of the work.

Place: Prof. K. K. Khatua

Date: (Supervisor)

Prof. R. K. Panda

External Examiner

Department of Civil Engineering

National Institute of Technology, Rourkela

Prof. Kishanjit Kumar Khatua

Associate Professor

May 27, 2016

Supervisors' Certificate

This is to certify that the work presented in the dissertation entitled *Effect of Secondary Current on Flow Prediction in an Open Channel Flow* submitted by *Jnana Ranjan Khuntia*, Roll Number 214CE4382, is a record of original research carried out by him under my supervision and guidance in partial fulfilment of the requirements of the degree of *Master in Technology* in *Civil Engineering Department*. Neither this dissertation nor any part of it has been submitted earlier for any degree or diploma to any institute or university in India or abroad.

Place: Prof. K. K. Khatua

Date: (Supervisor)

Dedicated To

My Family and Dear Friends

Jnana Ranjan Khuntia

Declaration of Originality

I, Jnana Ranjan Khuntia, Roll Number 214CE4382 hereby declare that this dissertation entitled Effect of Secondary Current on Flow Prediction in an Open Channel Flow presents my original work carried out as a Master student of NIT Rourkela and, to the best of my knowledge, contains no material previously published or written by another person, nor any material presented by me for the award of any degree or diploma of NIT Rourkela or any other institution. Any contribution made to this research by others, with whom I have worked at NIT Rourkela or elsewhere, is explicitly acknowledged in the dissertation. Works of other authors cited in this dissertation have been duly acknowledged under the section “Reference” or “Bibliography”. I have also submitted my original research records to the External Examiner for evaluation of my dissertation.

I am fully aware that in case of any non-compliance detected in future, the senate of NIT Rourkela may withdraw the degree awarded to me on the basis of the present dissertation.

May 27, 2016 *Jnana Ranjan Khuntia*

NIT Rourkela

Acknowledgement

Although an M.Tech constitutes a period of individual study, a number of persons have impacted on it directly or indirectly and without them this piece of research work would not have been successfully completed.

First and foremost I would like to express my sincere thanks to my supervisor **Prof. Kishanjit Kumar Khatua**, Associate Professor in the department if Civil Engineering of NIT, Rourkela guided me throughout this research with his valuable instruction and inspiration. He is a great person with his personality, knowledge with academic curriculums, positive motivational guidance and also have a good patients. I am grateful to him not only for his supervision, but his major contribution in the information of my character and skills for future study required as a young researcher. I eagerly hope to have another chance to work under his supervision.

I also have to thank **Prof. K. C. Patra**, **Prof. A. Kumar** and **Prof. S. N. Sahoo** who assisted and supported me throughout the research work.

I also acknowledge **Prof. S. K. Sarangi**, Director of NIT, Rourkela and **Prof. S. K. Sahu**, H.O.D of Civil Engineering Department who made good accademic environment for study and research throughout two years of my study.

Also my sincere thanks to Ph.D scholar **Ms. Kamalini Devi** for supporting me throughout the research to providing technical knowledge and expertise. I also have to thank to Ph.D scholar Mr. Bhabani Shankar Das for his cooperation as a good friend.

I would also like to thanks to my dear friends Srusti, Subhalaxmi, Sabya who make my life easier by spending valuable time with my research work. I wished for all of my friends for their bright future. I would like to thank Balaram, lab assistant to help me during experiment and also always supplied drinking water for us.

My most sincere and affectionate thanks to my parents, sister and brother for their good patient and a valuable time spent with me during the saddest moment in my life. Also one person who helped me a lot to overcome all the sorrow in that period and never leave me alone.

I would like to attribute my success to the almighty God, my supportive parent, Daddy, Mummy, my younger brother, my elder sister, my friends, my guide and all of them who supported me direct and indirect way to reach up to this.

Jnana Ranjan Khuntia

Abstract

The present thesis is an outcome of physical and numerical research of secondary current effects in open channel flows with both smooth and rough configuration in prismatic cross-sections.

Experiments have been conducted for open channel flows of rectangular and trapezoidal cross-section with four different roughnesses to develop models and also to find calibrating coefficients. Using micro-ADV we have been collected 3-D data sets and evaluated Reynolds stress and calibrating coefficients (i.e. secondary flow parameter Γ, eddy viscosity coefficient λ, friction factors f). These coefficients play an important role in prediction of depth averaged velocity and boundary shear stress of an open channel flows. These are found to vary with flow depth, geometry, roughness and hydraulic conditions.

A mathematical expressions have been formulated to predict these variables in terms of non-dimensional geometry and hydraulic parameters such as aspect ratio, lateral distances along width of the channel and vertical distances above bed are $b/h, y/b$ and z/H respectively. The new expressions are expected to improve the Shiono and Knight method (SKM) and accurately predict depth averaged velocity distribution in an open channel flows for different geometry, surface and flow conditions.

The predictions of depth averaged velocity using new expressions obtained from multi-linear regression were found to provide better results as compared to SKM. The prediction capability of model has been also well validated against experimental data sets, FCF data series and natural river data series.

Keywords: Open channel flow; Secondary Current; Secondary cells; Eddy viscosity; Depth averaged velocity; Multi linear regression

Contents

List of Figures

List of tables

Nomenculture

b	half width of channel
A	wetted area of cross-section
2b	total width of the channel
u, v, w	components of velocity along x, y, z directions respectively
$u', v'w'$	components of turbulence intensity along x, y, z directions respectively
$\bar{u}, \bar{v}, \bar{w}$	time averaged mean velocity along x, y, z directions respectively
U	Point / local velocity
ρ	density of water
ψ	stream function
ξ	component of vorticity in the X direction
ν	kinetic viscosity of water
μ	dynamic viscosity
λ	dimensionless eddy viscosity
Γ	secondary flow parameter
z	vertical coordinate above the bed of channel along depth of flow
y	lateral co-ordinate along the width of the channel
x	longitudinal co-ordinate
S_0	bed slope/longitudinal slope
s	side slope
R^2	coefficient of determination
R	hydraulic radius of channel = A/P
Q	discharge of the channel
P	wetted perimeter of the channel
n	Manning's roughness co-efficient
K_2	secondary flow coefficient at variable flow domain
K_1	secondary flow coefficient at constant flow domain
H	flow depth
g	acceleration due to gravity
f	Darcy-weisbach friction factor

τ^R	Reynolds stress
μ_t	dynamic turbulent viscosity
μ_l	dynamic laminar viscosity
$-\overline{uv}, -\overline{uw}$ &$-\overline{vw}$	components of Reynolds stress
$\bar{U}$or U_m	mean velocity
τ_b	boundary shear stress
U_*	global average boundary shear velocity = $\sqrt{\frac{\tau_b}{\rho}}$
$\bar{\tau}_{yx}$	depth-averaged Reynolds stress on a vertical interface
$\bar{\epsilon}_{yx}$	depth-averaged eddy viscosity
$(\rho UV)_d$	secondary flow term

Abbreviations

ADV	Acoustic Doppler velocimeter
FCF	Flood Channel Facility
RANS	Reynolds averaged Navier-Stoke's equation

Chapter-1

Introduction

1.1 Background

From the beginning of ancient and modern times water has been indispensable to mankind as an essential source for life. This is why human beings settled nearby the river coasts, despite the possibility of periodic flooding. In fact, these regions mesmerize mankind because of the advantages and benefits related to soil fertility for agriculture, the availability of water for different uses and transportation. The balance between the possible risk of damage and the likely benefits is more difficult to make, people must now accept, understand and learn how to live with natural disasters due to permanent urbanization. This is crucial for both survival and for reducing any threat, Knight & Shameseldin (2005).

Rivers have been used as a source of water, for procuring food, for transport and also as a source of hydropower to operate machinery, for bathing and for navigation. Generally the water in a river is restricted to a channel, made up of a stream bed between banks. The main river channel consisting of two banks with a bed where the water is flowing towards the downstream. The term left bank refers to the left bank in the direction of flow and right bank is to the right of main channel.

Open channel flow, a branch of hydraulics and fluid mechanics, is a type of flow within a conduit with a free surface, is known as a channel. Open channel can be said to be as the deep hollow surface generally having the top surface open to the atmosphere. These free surface flows obtain in engineering practice and include both large-scale geophysical flows (i.e. rivers and estuaries) and artificial flows (i.e., irrigation channels, sewers and laboratory channels).These flows are may be laminar or turbulent, steady or unsteady and uniform or varied. We can said to be as open channel is a way for flow of fluid (water) having pressure equal to the atmospheric pressure, while on the other hand flow under pressure is said to be as pipe flow.

In order to approximate prediction, control and make more efficient use of rivers and open channels, measurements of different properties (e.g. depth, discharge, velocity, boundary shear stress) of the hydrodynamic flow are most required. These measurements are taken into design consideration by two methods. Firstly, using measurement techniques, the flow properties are measured with sophisticated instruments as direct method and secondly, using numerical models to predict the nature and properties of flow as an indirect source of method.

1.2 Classification of open channel

Classification of open channel based on different criteria as given below:

I. Classification Type 1

1. *Natural Channels:* These channels are exits naturally on the earth surafce. Generally very un even and non-uniform in size and shape.
   Examples: Rivers, tidal estuaries etc.
2. *Artificial Channels:* These channels are human made and generally constructed with regular geometric size and shape.
   Examples: Irrigation canals, laboratory flumes, spillway chutes, drops, culverts etc.

II. Classification Type 2

1. *Prismatic Channels:* A channel of uniform cross-section and constant bottom slope is called prismatic channel. All artificial channels are usually prismatic.
   Examples: Most commonly used prismatic channels are Rectangular, trapezoidal, circular and parabola.
2. *Non-prismatic Channels:* A channel with non-uniform cross-section and constant bottom slope is called non-prismatic channel. The natural channels are generally non-prismatic.

III. Classification Type 3

1. *Rigid Boundary Channels:* A channel with rigid (not moveable) bed and sides is known as a rigid boundary channel.
   Examples: Lined canals, sewers and non-erodible unlined canals.
2. *Mobile boundary Channels:* If a channel boundary is composed of loose sedimentary particles moving under the action of flowing water, the channel is called as mobile or movable boundary channel.

Examples: An alluvial channel is a mobile boundary channel transporting the same type of material that comprising the channel perimeter.

IV. Classification Type 4

1. *Small Slope Channels:* An open channel having a bottom slope less than 1 in 10 is called a channel of small slope (Chow, 1959).The slopes of ordinary channels, natural or artificial, are far less than 1 in10.
2. *Large Slope Channels:* An open channel having a bottom slope greater than 1 in 10 is called a channel of large slope (Chow, 1959).The slopes of ordinary channels, natural or artificial, are far more than 1 in10.

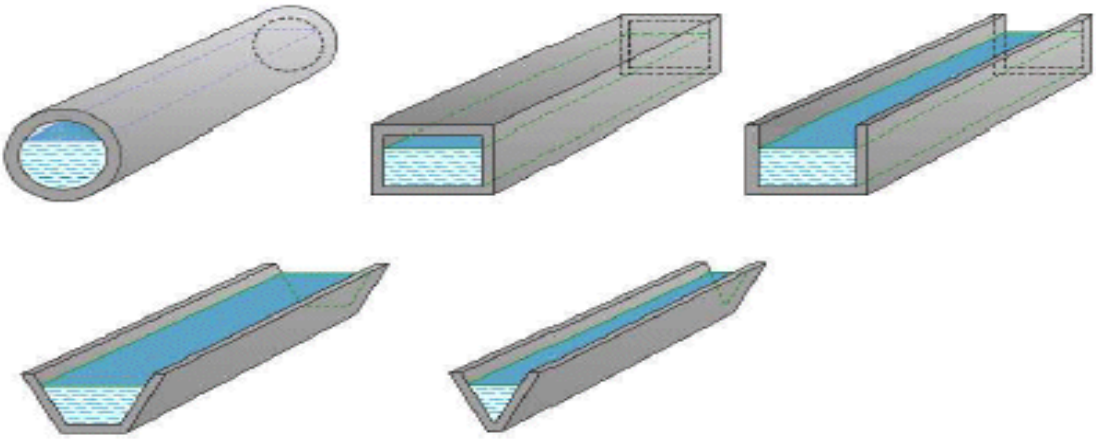

Figure 1.1: Different types of open channels based on geometry

1.3 Classifications of flow

The flow in an open channel can be classified depending upon the change in flow depth with respect to space and time. These are:

1.3.1 Time as the criterion

Steady flow: When the depth of water remains constant over time, that means the depth does not change with respect to any time.

Unsteady flow: When the depth of water in a flowing liquid changes time to time, then the flow is known as unsteady flow.

1.3.2 Space as criterion

Uniform flow: According to space, if the depth of flow does not change along the longitudinal distance of the channel and remain same for every individual location, then

the flow is said to be as uniform flow. This uniform flow may be of steady flow if in a total system, the depth of flow does not vary at any location over a time. But it is said to be unsteady, if the water depth remain same at every location but it changes uniformly after a certain period of time.

Varied flow: When, the depth of water changes throughout the longitudinal distance of the channel, the flow varies along the channel. These varied flows are also classified as rapidly varied or gradually varied.

Rapidly varied flow: This type of flow occurs, when a sudden changes in water depth over a short distance occurs within a channel.

Gradually varied flow: This is defined as the change in water depth along a large distance.

Continuous flow: When the flow in a channel remains same along the entire length, this is termed as continuous flow. Often it is known considered as steady flow. Also, this flow obeys the equation of continuity.

Spatially varied or discontinuous flow: When a steady flow is non uniform along the longitudinal dimension of the channel, the flow is considered as spatially varied. This flow is generally occurred along the length of flow when the water enters to the channel and leaves from the channel.

Based on Coordinate system or plane of flow

One-dimensional (1D) flow: All the flow parameters may be expressed as function of time and one space coordinate only. The single space coordinate is usually the distance along the centre-line (not compulsory straight) in which the fluid is flowing. In reality, flow is never one-dimensional because viscosity causes the velocity to decrease to zero at the solid boundaries. Sometimes valuable results may be obtained from a "one-dimensional flow"

Two-dimensional (2D) flow: All the flow parameters are function of time and two space coordinates (say x and y), no variation in z direction.

Three-dimensional (3D) flow: The hydrodynamic parameters are functions of three space coordinates and time. Fluid flow is generally three dimensional in nature. The flow parameters like velocity, pressure etc. vary in all three coordinate directions.

Sometimes simplification is made in the analysis of different fluid flow problems by selecting the appropriate coordinate directions so that reasonable variation of the hydrodynamic parameters take place in only two or one direction.

Factors influencing the flow in open channel:

1. *Channel shape*
2. *Fluid depth*
3. *Fluid velocity*
4. *Slope of channel*

1.4 State of flow

The behaviour of open channel flow is governed by the effect of viscosity and gravity relate to the inertial forces of the flow. Surface tension has a minor contribution, but does not play a significant enough role in most circumstances to be a governing factor. Depending on the effect of viscosity relative to inertia, as represented by the Reynolds number, the flow can be laminar, turbulent, or transitional.

1.5 Properties of Open Channels

In open channel flow usually occur due to the slope of channel bottom and the slope of liquid surface. The main difference in the open channel flow and pipe flow usually the cross section of channel is fixed and confined while on the other hand open channel flow is unconfined. Open channel is difficult to analyse than pipe flow. So that in open channel flow measurement empirical approach is adopted. Most elementary open channel hydraulics is based upon three fundamental assumptions: (1) the fluid is incompressible; (2) the flow is steady; and (3) the pressure distribution is hydrostatic at all control sections. In three-dimensional flow field, the flow is usually consisting of two components i.e., primary flow and secondary flow. The primary flow is parallel to the longitudinal direction of flow and the secondary flow is perpendicular to the primary flow direction. These types of flow are generally produced by the effect of drag in the boundary (i.e. side walls and bed). In nature, laminar flow is rarely or never encountered, but, instead of turbulent flow or turbulence occurred. The turbulence depends upon different factors, such as the average velocity of the flow, the average velocity gradients and the boundaries of the system.

1.6 Secondary (Transverse) Flow

It is important that in bank flow (i.e. flow within the main channel) is modelled accurately, since flow is present in the main channel all of the time and during flood only water inundates on the flood plain (s). In three-dimensional flow field, the flow is usually consisting of two components i.e., primary flow and secondary flow. The primary flow is parallel to the longitudinal direction of flow and the secondary flow is perpendicular to the primary flow direction. Flow component along the direction of flow is called longitudinal velocity or primary flow and other two components of flow (i.e. transverse or y and vertical or z direction) comprising another flow is called secondary flow. Secondary flow is the resultant vector or velocity of flow component along y and z direction. The anisotropy of turbulences causes secondary currents to be generated and modified. This anisotropy is caused by the boundary conditions of the bed, side wall, the free surface as well as the aspect ratio and channel geometry. These secondary currents are approximately only 2-3% of the mean stream wise velocity, but which makes the total flow extremely difficult to measure accurately. Secondary current is very important component for all numerical analysis to accurate prediction of flow in simple open channel flow with different roughness.

In rectangular prismatic channels, the free surface causes the secondary currents to flow toward the side wall along the horizontal plane and the pattern of secondary currents is affected by the free surface of open channel. The horizontal plane is separated by a pair of vortices which is generated at near the side walls, so the upper vortex is known as “free surface vortex” and the lower side vortex is called the “bottom vortex” (Tominaga et al.,1989).

In trapezoidal prismatic channels, the pattern of secondary flow cells is quite different from that of rectangular channel flows. But in this case the horizontal plane is separated by three vortices which are generated within the depth of flow. These three vortices are named as the bottom vertex (i.e. the lower side vortex), the longitudinal vortex (i.e. near the side walls) and the free surface vortex (i.e. occurs between bottom and longitudinal vortex). These patterns are depending upon the side slope angles. Mainly the longitudinal vortices are becoming stronger and weaker depends on the angle of side slopes. The complex motion of turbulent flows in open channel flows shown in figure 1.2 and

schematic influence of secondary flows in rectangular and trapezoidal cross-section shown in figure 1.3.

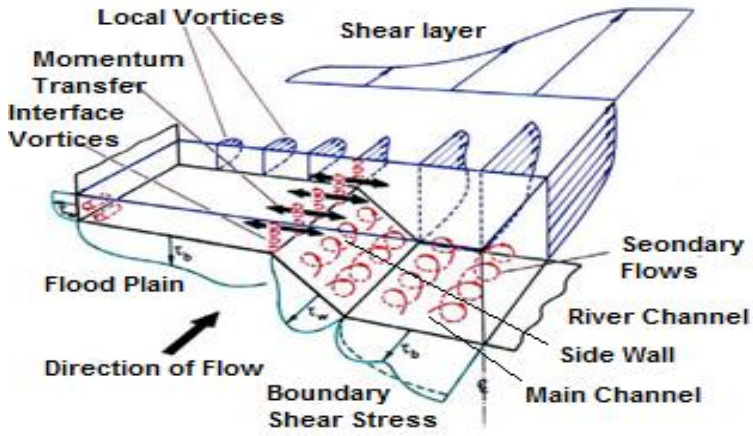

Figure 1.2: Complex 3D structures in open channel flows (Shiono and Knight, 1991)

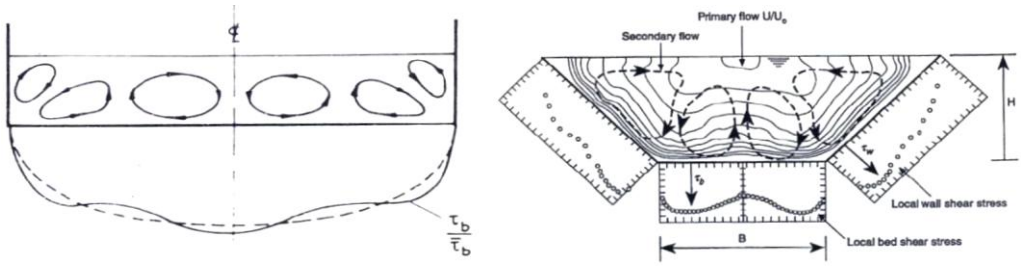

(a) Rectangular Cross-section (Knight et al., 1983) (b) Trapezoidal Cross-section (Knight et al., 1994)

Figure 1.3: Schematic influence of secondary flow cells

1.6.1 Some causes of vortices in channels

Vortices can also be induced due to the natural form of the channel or by man-made obstructions. Some following causes are:

- Berms affect the structure of secondary flows and their orientation with depth.
- Simple channels have different channel circulations as the side walls affect the both sides of the main channel.
- Compound channels also have different channel circulations as the floodplain only affects one side or both sides of the main channel.
- Natural channels tend to have large width to depth ratios which results in non-homogeneous turbulence.
- Vegetation in simple channels may reduce or remove the vertical interfacial turbulent exchanges as it acts a stream wise barrier between the main channel and the side walls.

1.7 Eddy viscosity in simple open channels

Eddy viscosity is an imaginary concept. Eddy viscosity is introduced to simplify the modelling of the momentum and the energy transfer due to the formation of turbulence eddies. The hypothesis concept of eddy viscosity is caused for making simpler, in the sense that the turbulent Reynolds stresses are simplified to be proportional to the gradients of the mean velocity, as happens in the Newtonian laminar flows. This coefficient of proportionality termed the eddy viscosity, which being a constant or property of fluid is a magnitude dependant on the flow field and its solution.

1.8 Classification of flow models

Mathematical modelling: This model is a comprehensive methodof representing the flow process in terms of mathematical equations.These models are built on the existing physical laws and known relations associated with the flow system.

Numerical modelling: An alternate procedure for complex mathematical models is to solve the sets of equations using a step wise approximation. These solutions are obtained by performing iterations with appropriate step size by descritizing at each successive step and continue until the numerical solution satisfies all the solutions. Numerical modelling is a rigorous task to work on it, but once the model is set up and established a range of similar criteria maybe investigated with relatively little effort. Finite difference and finite element methods are the most popular numerical modelling techniques.

Physical modelling: This type of modelling are developed in similar flow conditions at a smaller scale. The observations and measurements are carried out in the physical model provide useful information of the process. The main aim of physical modelling is whether these observations and measurements at a different scale can be generalised to the natural models. The results of this modelling process can be used to modify other mathematical models and obtain the value of some internal empirical parameters.

Statistical Modelling: This is a special class of mathematical modelling which is specified by some mathematical equations, some of variables have no specific value. Statistical modelling is used even when the physical process being modelled is deterministic. There are three main purpose of statistical modelling are predictions, extraction of information and description of stochastic structures.

1.9 Objective of research work

1. Analytical and Numerical solutions of Shiono and Knight Method to predict Depth-Averaged velocity in an open channel flow.
2. Experimental investigation on evaluation of three calibrating coefficients (friction factor, eddy viscosity coefficient and secondary flow coefficient) required for solution of SKM and also to propose mathematical expressions to evaluate these calibrating coefficients.
3. To calibrate the secondary flow parameters (i.e. K_1, K_2) and eddy viscosity for different zones for simple trapezoidal and rectangular channels of both smooth and rough surfaces, this will lead to predict the secondary flow and depth averaged velocity for any symmetric and un-symmetric simple trapezoidal channel.
4. To study the lateral variation of these calibrating coefficients in different flow and roughness conditions.Validation of proposed method with the experimental data sets of other researchers and natural river data sets.
5. To plot the variation of velocity distribution along the whole cross-section at a different vertical section (i.e. 0.2H, 0.4H, 0.6H, 0.8H, H,) and to model using multiple regression. This will be helpful to determine the local velocities at any point for a known geometry of any simple open channels.

1.10 Dissertation Layouts

The dissertation has been divided into seven chapters including Introduction. Chapter 1 consists of general introduction, overview of previous literatures are given in chapter 2, experimental setup and procedures are explained in chapter 3, experimental results and discussions are presented in chapter 4, chapter 5 comprises theoretical analysis and discussions, method are used and model development are included in methodology of chapter 6, chapter 7 consists of concluding remark and scope of future work.

Chapter 1 presents a brief introduction to open channel flow importance and different criteria of flow. The objective of the present research work has been presented along with important background information regarding secondary flow, eddy viscosity and also gives an overview of the work presented in the dissertation.

Chapter 2 presents literature reviews of the previous work of pioneer investigators. This chapter includes previous work already carried out in straight prismatic channels having smooth and rough surface: based on secondary current, eddy viscosity and different calibrating coefficients applied in SKM which are responsible for evaluating depth averaged velocity and boundary shear stress.

Chapter 3 describes experimental investigation and procedures, which includes experimental channel design with different roughness surfaces, determination of bed slope, measurements depth of flow and discharge and three directional velocity measurements by micro-ADV.

Chapter 4 include experimental results concerning stage-discharge curve, stream wise velocity contour, dimensionless velocity profiles with vertical and lateral variations and depth averaged velocity.

Chapter 5 describes theoretical analysis and discussions concerning variation of eddy viscosity and secondary flow mechanism from experimental results.

Chapter 6 consists of methodology used in this dissertation. Derivations of Shiono and Knight Method and development of calibrating coefficients for prediction of depth averaged velocity of an open channel flow for different geometry, flow and hydraulic conditions. Also validation has been made with SKM, FCF data series, other researcher's data series and well comparison with natural data series.

Chapter 7 included the concluding remarks and future scope if the research works.

Previous works carried out by other investigators have been cited in references are provided at the last preceding the publication from present research work.

Chapter-2

Literature Reviews

2.1 General

The past research findings from each researchers is an extensive research for future investigation. This race has never end whether it is continued from preceding runner to the successor. The research in the field of science and technology continuum where research findings and information of past research are contributed to the next advance research in form of published literature.

2.2 Straight Prismatic channel

This section contained the past research on secondary current effect and turbulence study in simple trapezoidal and rectangular open channel flow to quantify the flow characteristics by some prominent researchers. These are summarised below:

Sarma et al.(1983) studied lateral velocity distribution in smooth rectangular channel for four regions. This model included some experimental parameters of the aspect ratio of 1, froude numbers of 0.2 and 0.3 and range of Reynolds number in between 10^4 and 7×10^4.The froude number and aspect ratio were found no significant effect on the form of the equation for the velocity distribution in the outer region of the side wall close to the bed.

Steffler et al.(1985) presented mean velocity and measures turbulence for uniform subcritical flow in a smooth rectangular channel for three aspect ratios of 5.08, 7.83 and 12.3.They studied the departure of the velocity measurements to the velocity from logarithmic law in the respective regions. They also carried out the measurements of turbulent shear stress profile in the central as well as wall regions. The longitudinal velocity measurements in the viscous sub layer were found to agree well with the linear form of the law of the wall. Near the side wall region, the velocity profiles were found to drop off from the log-law line, so a significant dip in the velocity profile near the water surface.

Tominaga et al.(1989) initiated the secondary currents and also modified the turbulence anisotropy, which affects by the different factors like: boundary conditions of the bed, the side walls and the free surface, as well as the aspect ratio of the channel and the channel geometry. This model also demonstrated that primary flow affected by secondary current effects which initiated from three dimensional structures. They observed a secondary currents phenomena in open channel flows are different from closed channel flows. The scales of vortex increases as the ratio of the side wall shear to bottom wall shear increases. But the basic structure of the secondary currents was not changed significantly although the boundary roughness conditions were varied in the given flow field. In every case the three-dimensional structure of the primary mean velocity, which produces the Reynolds stresses and also boundary shear stress, depth averaged velocity distribution along the span were mainly affected by secondary currents.

Nezu et al.(1997) conducted experiments for measurement of turbulence successfully for the first time over a smooth wall in non-uniform unsteady open-channel flows were considered and use of a two-component laser Doppler anemometer (LDA) as velocity measuring device to measure two components of flow. This paper also evaluated the shear velocity independently of the log-law. The von Karman constant k was calculated using this friction velocity and turbulence characteristics were investigated across the whole flow from the near-wall region up to the free surface. Mean velocity profiles and turbulent characteristics were revealed in both the rising and falling stages of the flood period. The maximum velocity and shear attained just below the free surface due to the air friction at the top of the water surface.

Shiono and Feng (2003) presented the turbulence measurements of velocity and tracer concentration using a combination of Laser Doppler anemometer (LDA) and laser induced fluorescence (LIF) in rectangular and compound channels simultaneously. They also investigated the effect of secondary flow on passive contaminant diffusion processes that in the rectangular channel relatively weak secondary flow and relative strong secondary flow in compound channels.

Omran (2005) implemented the SKM in both inbank and overflows condition to a number of laboratory channels and also in natural rivers. A model was developed for boundary conditions for simple trapezoidal channels were re-examined and version of two

layer model developed for compound channels. Also developed analytical expressions for secondary flow parameter Γ across the channel, the use of SKM is reduced to allocating friction factor values to a different domain of cross-sections.

Liao and Knight(2007) derived three analytical models which were suitable for hand calculation for finding out stage-discharge relationship in prismatic open channels. These three types of prismatic cross sections were simple rectangular, symmetric and asymmetric rectangular compound channels. The three calibrating coefficients include three key parameters that are the friction factor, eddy viscosity coefficient and secondary flow. The individual influences of*f*, λ, and Γ on the stage-discharge curves had been analysed. The friction factor, *f*, had been found to be the most important influence, followed by the secondary flow term, Γ. In general, the discharge would be decreased as increased of any of the parameters *f*, λ, and Γ.

Knight et al. (2007) proposed a philosophy for characterizing the appropriate panel structure in view of the number and position of secondary cells in trapezoidal channels. This model incorporated the impacts of secondary flows by determining a appropriate value for the Γ parameter relying upon the ability to know the direction of secondary flows. It was shown that by utilizing the approach, back ascertaining the friction values from measured information, keeping λ constant value 0.07 and calculating Γ, the depth averaged velocity and boundary shear could be precisely assessed for simple trapezoidal channels.

Zarrati et al.(2008) determined semi- analytical equations for distribution of shear stress in straight open channels with rectangular, trapezoidal, and compound cross sectional areas. These equations are based on improved stream wise vorticity condition that incorporates secondary Reynolds stress. Reynolds stresses were demonstrated and their distinctive terms were assessed based on experimental data and different reseachers work. Substitution of these terms into rearranged vorticity equation yielded the relative shear stress distribution equation along the lateral cross-sections of various channels.

Sharifi (2008) analyzed the utilization of two evolutionary computation techniques to two unique parts of open channel flow. The quasi 2D profundity depth averaged Reynolds Averaged Navier Stokes (RANS) model connected with three primary impacting

parameters to demonstrate the stream in prismatic channels. The RANS model was adopted by the Shiono and Knight Method (SKM) which required three information parameters so as to give acceptable results, i.e. the friction factor (*f*), dimensionless eddy viscosity (λ) and effect of secondary flow parameter (Γ).

Sterling et al.(2008) examined the use of data obtained from large eddy simulations in exploring the instantaneous characteristics of boundary shear stress. This model has been used an integrated approach which provides ideal results and also an efficient method of analysis.

Tang and Knight (2008) reviewed on a model of two-dimensional analytical solution developed by Shiono and Knight (1988) for a compound channel. Two new analytical solutions were also compared with the traditional solution for three simple channel shapes and one trapezoidal compound channel to highlight their differences and the significance of the secondary flow and plan structure vorticity term. They additionally proposed two assumptions to depict the commitment of the stream wise vortices to the flow taking into account the experimental data with respect to the seconday flow.

Aydin (2009) introduced a nonlinear turbulence model for numerical solution of uniform channel flow is exhibited. Turbulent stresses are assessed from a nonlinear mixing length model that relates turbulent stresses to quadratic results of the mean rate of strain and the mean velocity. The author also recommended that the mixing length, based on a three-dimensional integral measure of boundary proximity, eliminates the need of arrangement of extra transport conditions for turbulence quantities. This paper likewise processed velocity field and wall shear stresses influenced by secondary stream vortices.

Ansari et al.(2011) exhibited the utilization of computational liquid dynamics (CFD) to decide the bed shear and wall shear stresses in trapezoidal channels. The shear stress information can be specifically yield from the CFD models at the limits, yet they can likewise be inferred utilizing the Guo and Julien equations average wall and bed shear stresses. The outcomes show significant contribution from the secondary flow and internal shear stresses on the overall shear stress at the boundaries. They also examined the effect of the variety of the inclination point of the side walls, aspect ratio and composite roughness on the shear stress distribution. Guo and Julien equations were computed the shear stress as an function of three componentss i.e., gravitational, secondary flow and

interfacial shear stress on the bed and side walls separately. The variety of inclination angle and aspect ratio conveyed significant changes to the distribution of the shear stress at the boundaries, predictable with changes in the flow structures as previously shown by Morvan and Hargreaves (2009), specifically for low aspect ratio channels.

Jesson et al.(2013) simulated the open channel flow over a heterogeneously roughened bed and also inspected physically and numerically. The velocity field was mapped at four distinctive cross sections by utilizing an Acoustic Doppler Velocimeter (ADV) and the boundary shear stress ontained from both the velocity data and use of a Preston tube. This paper has been presented the primary endeavor at utilizing Shiono-Knight method to to depth-averaged velocity and boundary shear stress distribution.

Yang et al.(2013) proposed the depth-averaged equation of flow by analyzing the forces acting on the natural water body and utilizing Newton's second law as a part of a rectangular compound channel with secondary flow. The analytical solution for the transverse variation of depth-averaged velocity was presented that incorporates the impacts of lateral momentum exchange and secondary flow in addition to bed friction. This paper also introduced distinctive type of boundary conditions at the internal wall between the rectangular main channel and the adjoining flood plain. The outcomes also demonstrate that the secondary flow and boundary conditions have impacts on them.

2.3 Research Gap

1 Many researchers have studied velocity distribution in a smooth rectangular channel and also described the analytical solution of SKM in simple channel as well as in compound channels.

2 Some researchers also have demonstrated the three calibrating coefficients (friction factor, eddy viscosity coefficient and secondary flow coefficient) with smooth simple and compound channels.

3 Some investigators developed their models for predicting velocity using experimental data sets and used aspect ratio , froud number and Reynolds number as independent parameters.

4 Similarly for evaluation of boundary shear, many expressions have been derived by a lot of researchers. also some of them presented the use of computational fluid

dynamics(CFD) to determine the distribution of the bed and side wall shear stresses in trapezoidal channels.

5 There are less work found regarding the mathematical model for predicting the calibrating coefficients of open channel flow for different roughness.

Chapter-3

Experimental Setup and Procedures

3.1 Experimental Setup

In experimental setup, some important arrangements should be required before conduct an experiment in laboratory as well as in the field survey. In this section an experimental setup were described with some experimental photographs.

3.1.1 Fabrication of flumes and accessories

The experimental flumes were made up of mild steel bars and plates. For supplying water into the experimental channels a large reinforced cement concrete (R.C.C) overhead tank was constructed on the upstream side of the flume inside the laboratory. A volumetric tank was built at the downstream end of the flume for measuring the discharge of each flow depth. A large underground sump located outside was used for maintaining continues water supply to the overhead tank. Two centrifugal pumps of 10 HP capacities each fitted with suction and delivery pipes completed the recirculation system of water supply to the channels in the flume. A stilling chamber fitted with an adjustable head gate and flow straigtheners were provided in the entrance region of the flume to maintain the flow uniform and laminar entering the channel. On the downstream side of the channel an adjustable tail gate was fitted to control depth of flow and to maintain the uniformity of the flow. Figure 3.1 to figure 3.10 show the photographs of important components in different roughness of rectangular and trapezoidal simple channel experimental setups. Figure 3.7 to 3.9show the schematic layout diagrams of overall experimental setup and plan view for straight simple rectangular and trapezoidal channels respectively.

3.1.2 Fabrication of Channels

Both the straight simple channels were having different in dimensions i.e., width of main channels, depth of main channels and other geometry also.The cross section of main channel in **first case** is rectangular in shape with bottom (*2b*) dimension of 0.34m, height (*h*) of 0.113m. The overall width of the channel is 2m with symmetric flood plain laying both side of centre of the main channel over a length of 14m. The cross section of main

Flow analysis in the both prismatic simple channels with different roughness being the primary aim of the present research work. Experiments were carried out in rectangular smooth channel, by using Perspex acrylic sheets (6 to 10mm thick and having manning's *n* value 0.01) and in trapezoidal channel three different roughness were used (i.e., smooth cement concrete surface having manning's *n*value0.011, small gravel of size 7 to20mm having manning's *n* value 0.02 and plastic mat of thickness 15mm having manning's *n*value0.024).The Perspex sheets were used in rectangular steel flume by cutting in designed shape and size, glued with chemicals and put in their desired locations to make the channel for the experimental purpose. Then cement concrete trowel finished surface were used as another smooth surface in case of trapezoidal cross section of channel inside the flume for this research purpose and other two roughnesses (i.e., small gravel and plastic mat) were glued and put on the bed and side wall of the trapezoidal channel for experimental purposes. The roughness were maintained uniform in whole main channel and side slope (where applicable) to investigate the momentum transfer and secondary current effect in simple channels between main channel and side walls. The model was developed and results were compared after the experiments were completed in both trapezoidal and rectangular channels.

Figure 3.1: Photo of fabricated experimental channels (a) Trapezoidal (b) Rectangular

Figure 3.2: Photo of Centrifugal Pumps (10HP capacity each)

Figure 3.3: Photo of Overhead Tank

Figure 3.4: Photo of Experimental channel with arrangement of stilling chambers and baffle walls

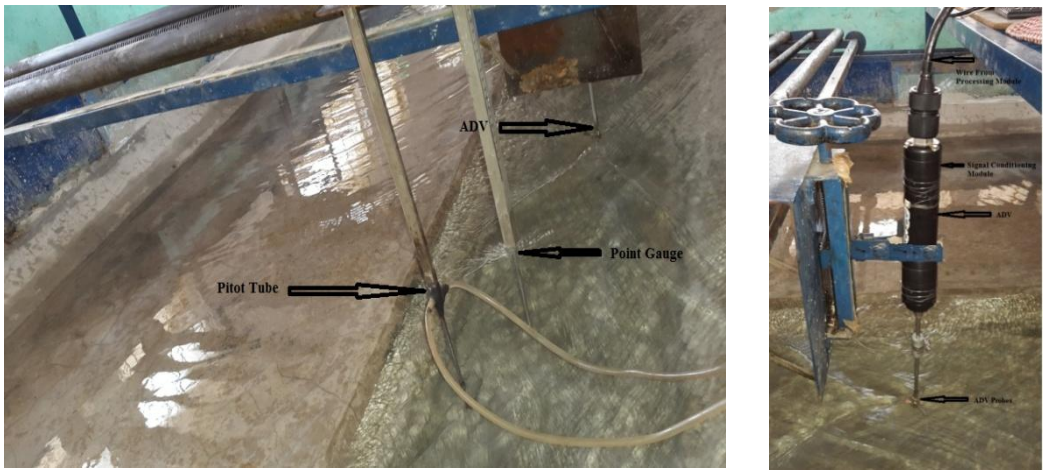

Figure 3.5: Photo of measuring instruments usedin experimentation (Pointer Gauge, Pitot tube and ADV)

Figure 3.6: Photo of Volumetric tank and vertical piezometer

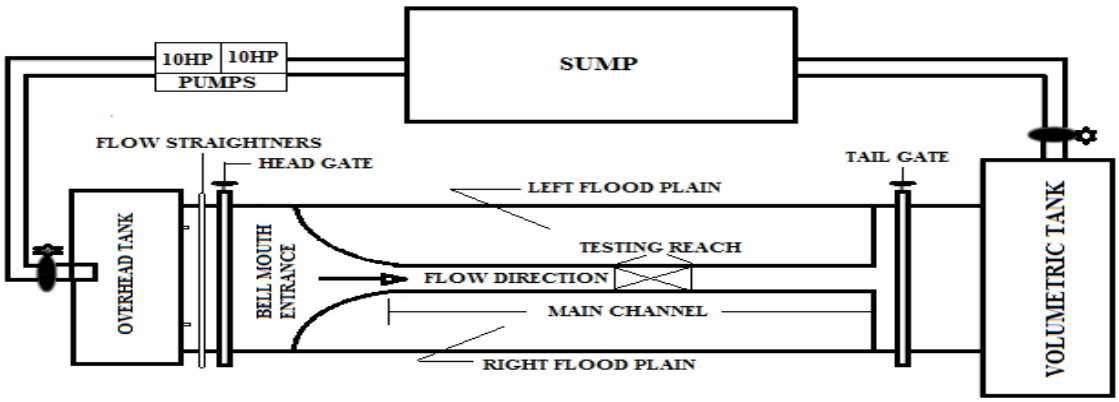

Figure 3.7: Layout of Experimental setup for Rectangular channel

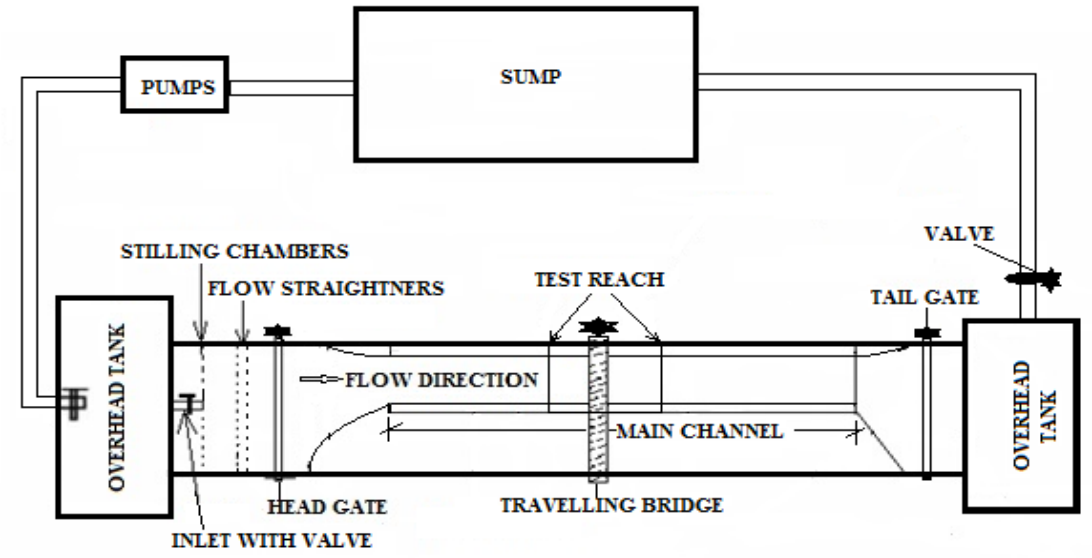

Figure 3.8: Layout Experimental setup for Trapezoidal channel

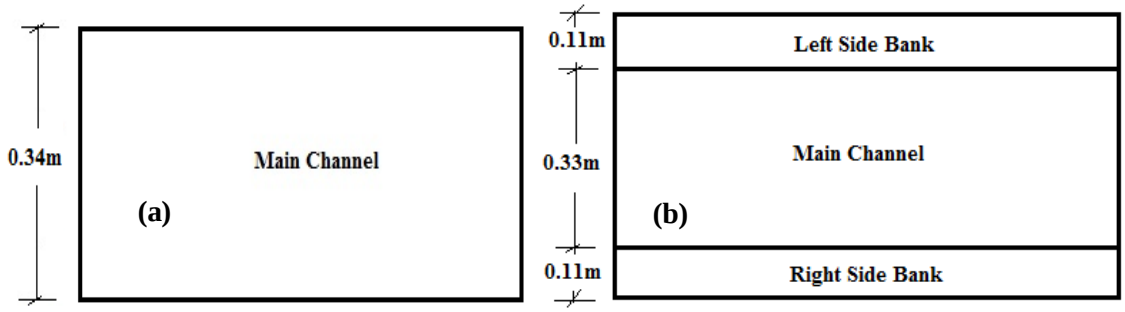

Figure 3.9: Plan view of Experimental Channels (a) Rectangular (b) Trapezoidal

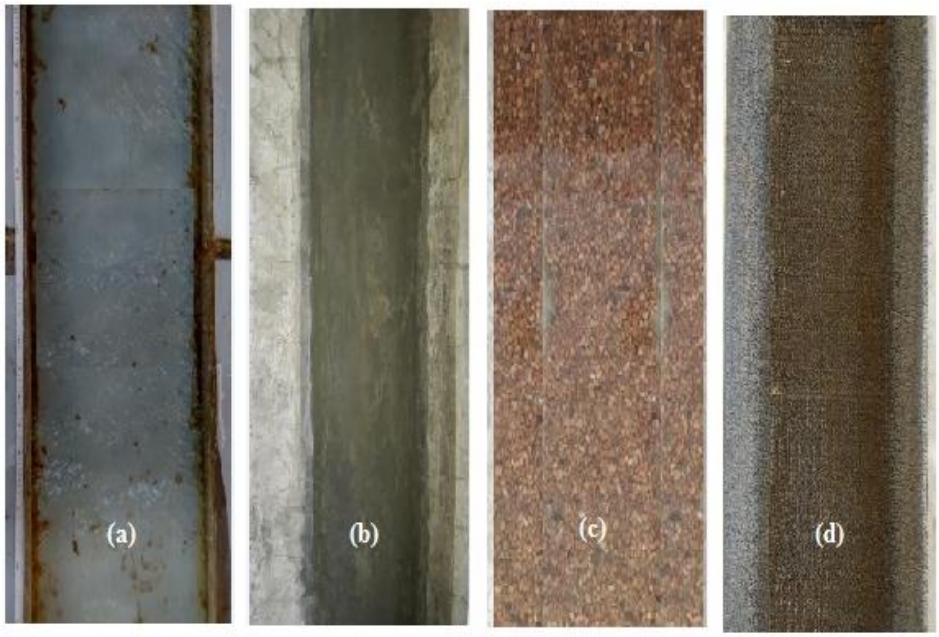

Figure 3.10: Photo of Plan view of Experimental Channels used for Experimentation

3.1.1.1 Trapezoidal Channel

The experiments were carried out in a mild steel body with glass-walled tilted flume of 12m long, 2m wide, 0.5m deep and bed slope of 0.001 as smooth roughness configuration at the fluid mechanics laboratory, Civil Engineering Department, NIT, Rourkela. The smooth rectangular channel casted of having dimensions 12m long, 0.33m width (*2b*) and 0.11 deep (*h*) with bed materials of trowel finished cement concrete surface (*n* =0.01) as smooth roughness. The test section was considered 8m away toward the downstream from the bell mouthed entrance. In this same geometry of trapezoidal channel other two roughness were used as small gravel of size 7 to 20mm having manning's *n* value 0.02 and plastic mat of thickness 15mm having manning's *n* value 0.024 for experimental purposes.

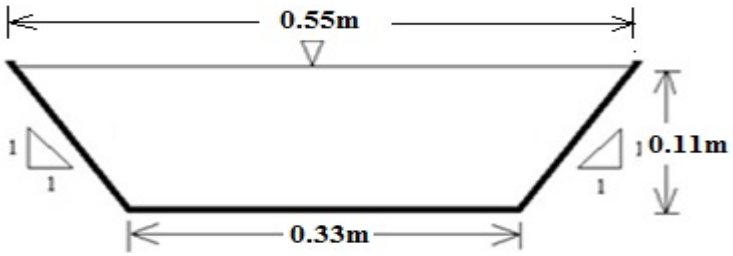

Figure 3.11: Cross-section of experimental trapezoidal channel

Figure 3.12: Different roughness materials used in trapezoidal channel (a)cement concrete trowel finished (b)Small Gravel (size 7 to 20 mm) (c) Plastic mat (15mm thick)

3.1.1.2 Rectangular Channel

The experiments were carried out in a mild steel body with glass-walled tilted flume of 22m long, 2m wide, 0.6m deep and bed slope of 0.0015 as smooth roughness configuration at the fluid mechanics laboratory, Civil Engineering Department, NIT, Rourkela. The smooth rectangular channel casted of having dimensions 15 m long, 0.34m width (*2b*) and 0.113 deep (*h*) with Perspex acrylic sheet (n = 0.011) as smooth roughness.

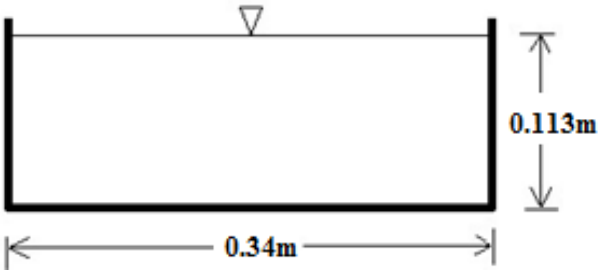

Figure 3.13:Cross-section of experimental rectangular channel

A point gauge was used along the centreline of the flume for water depth measurements. All depths were measured with respect to the bottom of the flume or to the top surface of the roughness material. The discharge was measured volumetrically at different flow depths using vertical single tube manometer fitted to volumetric tank by measuring rise with time. Then product of volumetric tank plan area and height of 1 cm water in vertical single tube manometer divided by average time taken for 1 cm rise was given the discharge of a particular flow depth.

Table 3.1: Detailed Geometric parameters of experimental channels

Sl. No.	Item Description	Experimental Channels	
		Trapezoidal	**Rectangular**
1	Channel Type	Straight Prismatic	Straight Prismatic
2	Roughness Criteria	Rigid Smooth and Rough	Rigid and Smooth
3	Main Channel Width (*2b*)	0.33 m	0.34 m
4	Side Slope	1V:1H	0
5	Depth of Main Channel (*h*)	0.11 m	0.113 m
6	Top Width	0.55 m	0.34 m
7	Bed Slope	0.001325	0.003
8	Aspect Ratio (*2b/h*)	3	3.01
9	Flume Size	12m×2m×0.5m	22m×2m×0.65m

3.2 Experimental Procedures

In this section experimental procedures were described with important steps which helped successfully measured velocity, discharge and other findings by using some sophisticated instruments.

3.2.1 Determination of Bed slope

All the experiments in straight simple prismatic channels were to be conducted under subcritical flow (i.e., Froude No (Fr) <1) conditions. Accordingly the flume was given a mild slope of value of 0.001 to 0.0015 so that water could flow under gravity within the main channels. For obtaining this desired slope different methods could be adopted. In this research work we used two methods for measuring the bed slope of the channels. First method was conducted with following steps. The tail gate of the channel was closed to impound the main channel with water at a certain depth. Then two end points were fixed of length of 6m and heights of the water at the two positions were recorded with the help of a point gauge having least count 0.1mm. A travelling bridge was fitted with a point gauge which was able to move back and forth in transverse as well as longitudinal directions of the channel. The slope of the bed was obtained by dividing the depth of water difference at two ends fixed earlier by the reach length. From measurements, the bed slope was obtained 0.0015, 0.001325 and 0.001 for rectangular smooth, trapezoidal smooth and trapezoidal rough channel respectively. In second method it was a common and easier method by measuring the piezometric height. So opened the water from inlet valve at required depth, a pipe was filled with water laid on the main channel up to a certain length and fixed the two ends of the pipe above the water level. Then we measured the difference of two piezometric heights. For obtaining the bed slope dividing the piezometric difference by the length of the two pipe ends. In this case also the bed slope was obtained closer to the above method for the same.

3.2.2 Determination of base *n* value for different surfaces

Roughness of a material is generally gives resistance to flow and expressed in terms of roughness coefficient. For evaluating the actual flow capacity, the appropriate value of roughness coefficient will be required to be determined accurately. Roughness coefficient was generally determined as Manning's *n* in every cases of an open channel flow. In the present study Manning's *n* calculated from inbank flow experiments and then mean *n*value considered for a particular channel geometry and surface condition. In this process Manning's *n* was determined for rectangular and trapezoidal cross sections with different roughness surfaces i.e., Perspex sheet, cement concrete trowel finish, small gravel (rough type-1) and plastic mat (rough type-2). For determination of base *n* value, the Manning's formula was used of these materials:

$$n = \frac{1}{U} R^{2/3} S_0{}^{1/2} \quad (1)$$

3.2.3 Measurements of flow depth and discharge

The experiments were carried out with some limitation always, without those limitation and rules we could not performed any experiments. So one of the limitation was to obtain the flow in experimental channels should be uniform and laminar. The flow of water passed through stilling chambers, baffle walls and flow straighteners to reduce the turbulence in flow and maintain the uniformity throughout the channel. So to obtain that condition, the flow of water in the channel was allowed to run continuously for a sufficient time (about 4 to 5 hours) while the desired behaviours of flow of water obtained in the experimental channels. Then the depth of flow measured by using point gauge along the centre line of the main channel for each flow depth.

The discharge for each flow depth is an important to determine by the following procedures. After obtaining the desired conditions of flow, the outlet valve was closed to increase the water level in the volumetric tank. After at a constant rise in the piezometer provided near to the volumetric tank, 1 cm rise in piezometer in a certain time was recorded by stopwatch for 15 to 20 times. To obtain the measured discharge, by dividing the multiplication of volumetric tank area with 1 cm rise to average time was taken by stopwatch. All the discharges were measured with respect to flow depths for rectangular and trapezoidal channel with smooth and rough surfaces. The details of hydraulic parameters of experimental channels are given in table3.2.

Table 3.2: Detailed Hydraulic parameters of experimental channels

Material	nnel Geometr	Flow Depth, H (m)	Area of flow, A (m^2)	Wetted Perimeter, P (m)	Discharge, Q (m^3/s)	Mean Velocity, U_m(m/s)	Bed Slope, S_0	Average Manning's n
Perspex Sheet	Rectangular	0.076	0.026	0.492	0.0117	0.4520	0.0015	0.011
		0.083	0.028	0.506	0.0143	0.5067	0.0015	
		0.090	0.031	0.520	0.0160	0.5225	0.0015	
		0.099	0.034	0.538	0.0178	0.5288	0.0015	
		0.107	0.036	0.554	0.0201	0.5525	0.0015	
Cement Concrete	Trapezoidal	0.080	0.033	0.556	0.0158	0.4824	0.0013	0.01
		0.090	0.038	0.585	0.0160	0.4229	0.0013	
		0.100	0.043	0.613	0.0241	0.5603	0.0013	
		0.110	0.048	0.641	0.0256	0.5289	0.0013	

Small Gravel@ size7-20mm	**Trapezoidal**	0.070	0.028	0.528	0.0057	0.2025	0.0010	0.02
		0.080	0.033	0.556	0.0079	0.2396	0.0010	
		0.085	0.035	0.570	0.0087	0.2473	0.0010	
		0.090	0.038	0.585	0.0096	0.2547	0.0010	
Mat Surface (Plastic)	**Trapezoidal**	0.070	0.028	0.528	0.0047	0.1689	0.0010	0.024
		0.075	0.030	0.542	0.0059	0.1929	0.0010	
		0.080	0.033	0.556	0.0066	0.1997	0.0010	
		0.085	0.035	0.570	0.0073	0.2061	0.0010	
		0.090	0.038	0.585	0.0080	0.2122	0.0010	

3.2.4 Measurement of three directional velocity using Micro-ADV (Acoustic Doppler Velocimeter)

For experimental purposes Micro-ADV was used for measuring the three directional velocities. The measurement of accurate velocities measured by micro ADV for study of secondary current flow should be required because secondary flow components are very small as compared to primary flow component. In this present work micro-ADV was used to measure the velocities *u*, *v* and *w* along x, y and z directions respectively.

3.2.4.1 Micro ADV

The velocity field was measured by a SonTek Micro 16-MHz acoustic Doppler velocimeter (ADV). The sampling rate is 50 Hz (the maximum).Sampling volume of ADV is located approximately 5 cm below the probe and was set to be minimum of 0.09 cm^3.The 5 cm distance between the probe and sampling volume minimizes the flow interference. A total of 2, 97,000 data points were recorded (at 50 Hz) for a total recording length of 99 minutes for simple rectangular channel and 2, 97,000 data points were recorded (at 50 Hz) for a total recording length of 129 minutes for simple trapezoidal channel. Correlation was used to monitor data quality during collection and to edit data in post processing. Ideally, correlation should be between 70 to 100%.Low correlation values affect the short term variability of velocity data, but do not prejudice mean velocity measurement. For mean velocity measurements, correlation values as low as 30% can be used. Signal strength is a measure of the strength of the return reflection from water; it can be accessed as signal amplitude in internal logarithmic units called signal to noise ratio (SNR) in dB. The SNR (signal to noise ratio) value of range higher than 20dB for 16-MHz

micro ADV. It was necessary to maintain the value of SNR. Short term uncertainty in the velocity measurement increases as SNR decreases. For higher sampling rate (e.g.50 Hz), SNRs higher than about 30 dB are recommended (SonTek).

Micro-ADV used in Experimental work:

Three directional velocities were measured by ADV at the test section which was taken 8m towards the downstream from the bell mouth entrance. ADV recorded the three directional velocitiesV_1, V_2 and V_3in X-direction, Y-direction and Z-direction respectively in the first section 1 of the figure3.14 shown below. The (Signal to Noise Ratio) SNR in dB and the correlation (%) with respect to sample in section 2 and section 3 respectively. In our laboratory three different types of Micro-ADV were used for experimental purposes. Generally down prove and up prove ADV are used in a particular vertical section along the lateral direction of the channel. Sometimes near the side wall regions, it was not detected any value in down and up prove of ADV. So in these regions side prove ADV will be used to take accurate data for analysis of turbulence in both rectangular and trapezoidal channel with smooth and rough surfaces in an open channel flow. Figure 3.14 shows the screen shot at the time of data accusation by SonTek software of micro-ADV.

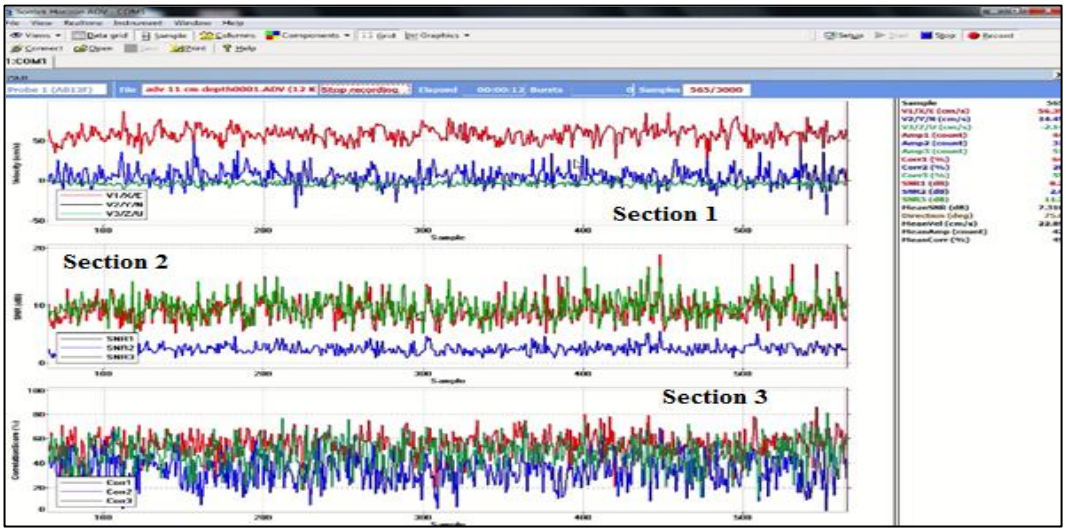

Figure 3.14: Data accusations in Sontek ADV software

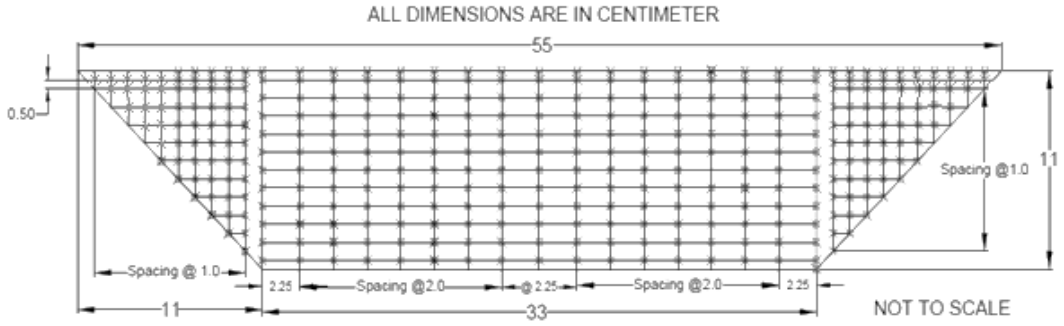

Figure 3.15: Grid points for measuring three dimensional velocities in trapezoidal channel

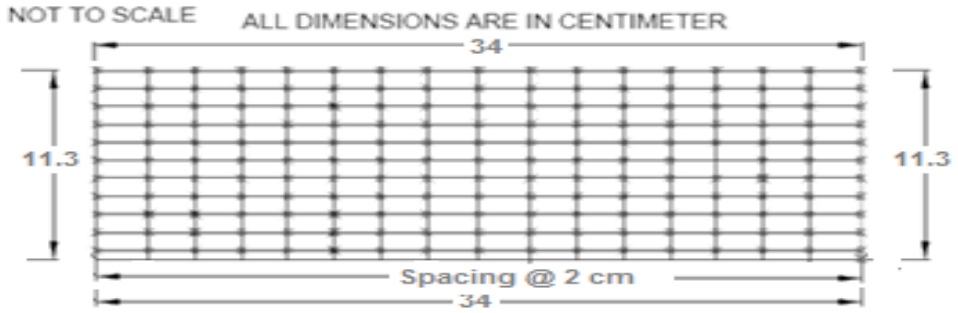

Figure 3.16: Grid points for measuring three dimensional velocities in rectangular channel

Chapter 4

Experimental Results and Discussions

4.1 General

In this section all results regarding stage-discharge curves, longitudinal velocities, depth averaged velocities etc. from the new experiments conducted in the channels of NIT, Rourkela are presented. All the experiments are conducted by using different smooth and rough roughness in two different geometry of rectangular and trapezoidal straight channels, so accordingly separate subsections are mentioned for deal with the results of each type.

4.2 Stage-Discharge Curve

The stage-discharge relation curve is also known as rating curve for the channels are in the form of discharge (Q) varying as power function of flow depth (H). The stage-discharge relationships for rectangular and trapezoidal channel geometry of smooth and rough channels are plotted in figure 4.1.

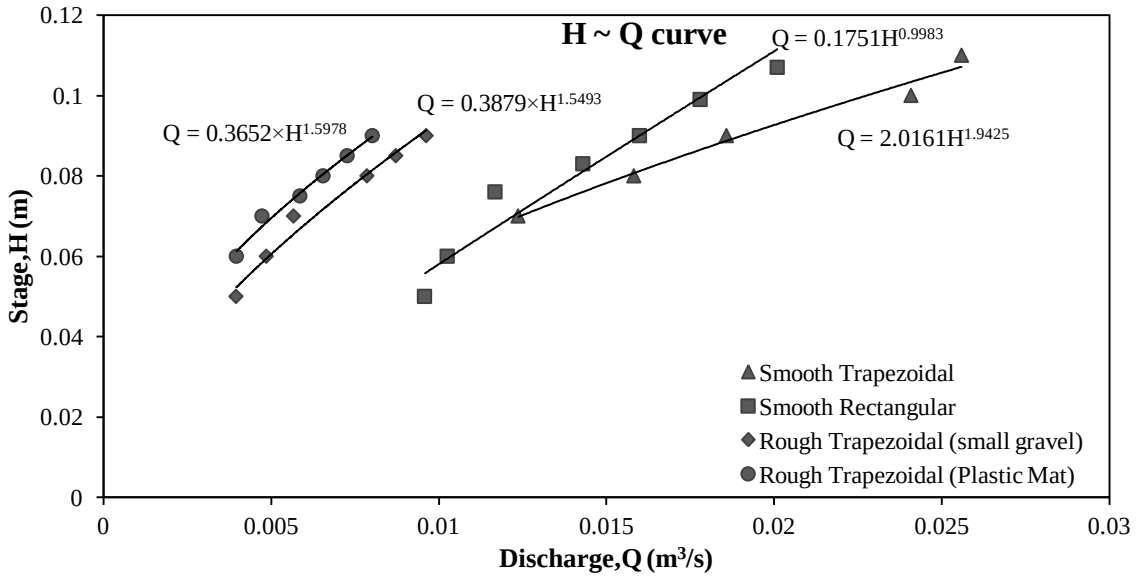

Figure 4.1: Stage-Discharge curve for experimental channels

For all cases, the discharge increases as stage increases. Their relationship follows power function with higher R^2 value more than 0.9. The coefficient of power function equations are tabulated in table 3. For the same discharge depth of flow of rougher channel is less as compared to smooth channels because of larger friction reduces velocity. Looking to the

stage-discharge curves of smooth rectangular and smooth trapezoidal channel, it can be observed that the discharge in trapezoidal channel is higher as compared to rectangular channel for approximately same slope and same roughness condition, because in trapezoidal cross-section, due to presence of sloping bank, the flow of water does not get so much obstruction as found in vertical wall in rectangular channel. Trapezoidal channels provide less turbulence as compared to rectangular channels of vertical walls.

Table 4.1: Stage-Discharge Relationship for experimental channels

Channel Geometry	Materials Used	Stage-Discharge Relationship	Regression Coefficient(R^2)
Smooth Rectangular channel	Perspex sheet	$Q= 0.1751\times H^{0.9983}$	0.9338
Smooth Trapezoidal channel	Cement concrete	$Q = 2.0161\times H^{1.9425}$	0.9749
Rough Trapezoidal channel (Type-1)	Small gravel	$Q = 0.3879\times H^{1.5493}$	0.9735
Rough Trapezoidal channel (Type-2)	Plastic mat	$Q = 0.3652\times H^{1.5978}$	0.9814

4.3 Vertical Velocity Profiles

The variations of velocities with vertical dimensions of a channel needs to be investigated for it's importance characteristics for finding out the distribution of discharge in terms of velocity in every vertical section along the cross channel distance.

4.3.1 Rectangular channel

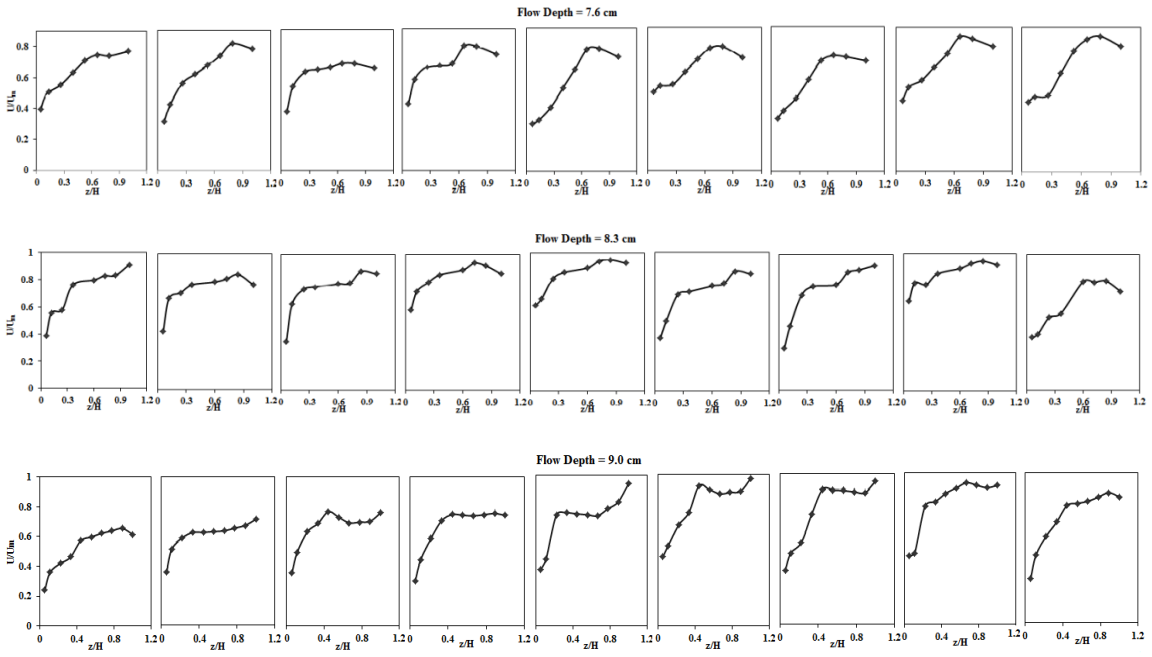

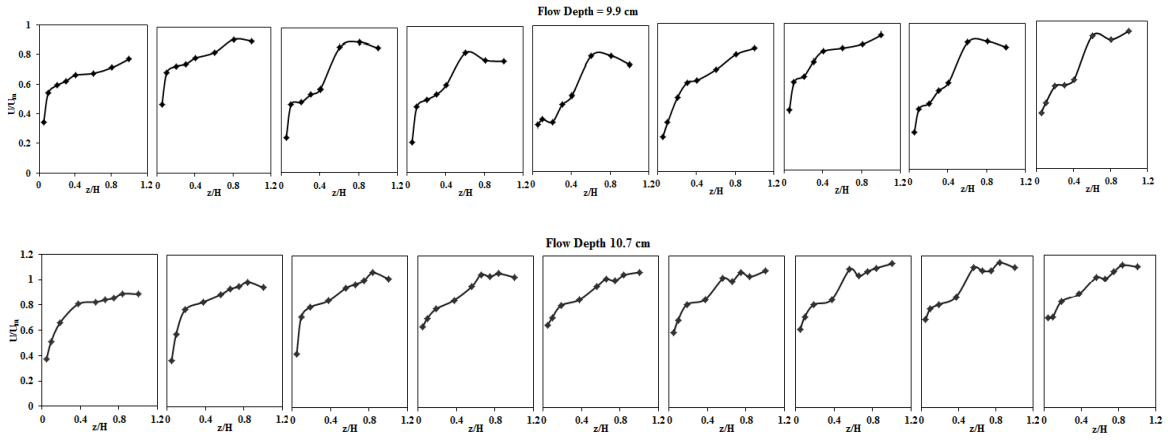

Figure 4.2: Vertical profiles for different flow depths of rectangular experimental channel

4.3.2 Trapezoidal channel

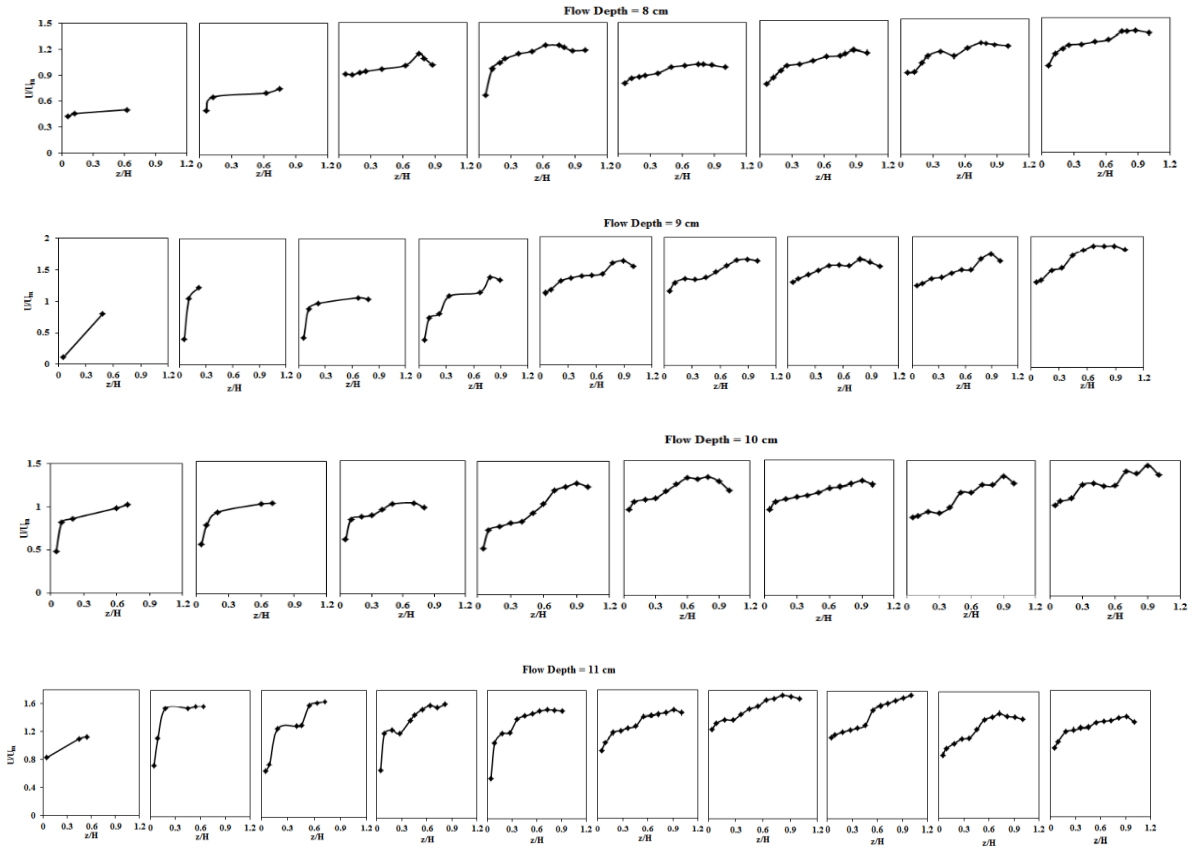

Figure 4.3: Vertical profiles for different flow depths of trapezoidal experimental channel

The nature of stream wise velocity has been found to flatten towards water surface. However at bottom region, the flow acquires a minimum value of velocity. The reason is due to the existence of boundary friction at bottom. Also towards corner region of channel, the vertical distribution of velocity get minimum value as compared to the

velocity distribution exists at centre. It's because of the development of friction at wall and boundary.

4.4 Lateral Velocity Profiles

The velocity varies in three coordinate axes. When this variation of velocity in transverse coordinate is considered, then the distribution of velocity is known as the lateral velocity distribution or lateral velocity profile. Lateral velocity profiles were plotted between two non-dimensional parameters of U/U_m and y/b along the half width of the channels. The experimental lateral velocity profile results found for rectangular and trapezoidal channels for various flow depths have been graphically presented below.

4.4.1 Rectangular channel

In rectangular channel, the distribution of lateral velocity in five vertical positions measuring from bottom i.e., 0.95H, 0.8H, 0.6H, 0.4 H and 0.2H are selected and considered. Where H refers as the respective flow depth in channel. The results from the Figure 4.4 give an idea regarding the aspects of flow for every depth. The velocity is growing to reach maximum value at centre. For a given flow depth, the velocity acquires minimum value at low vertical distance and it becomes high near the surface. When the flow depth increases, the velocity profile for a same vertical position also increases. Profiles in each vertical positions show a similar trend bearing power function.

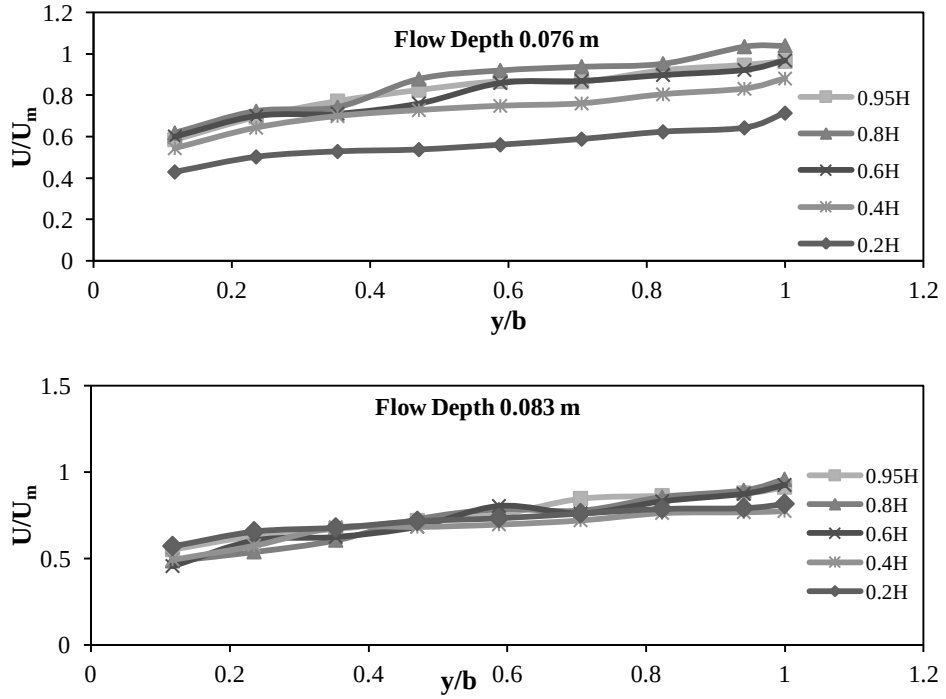

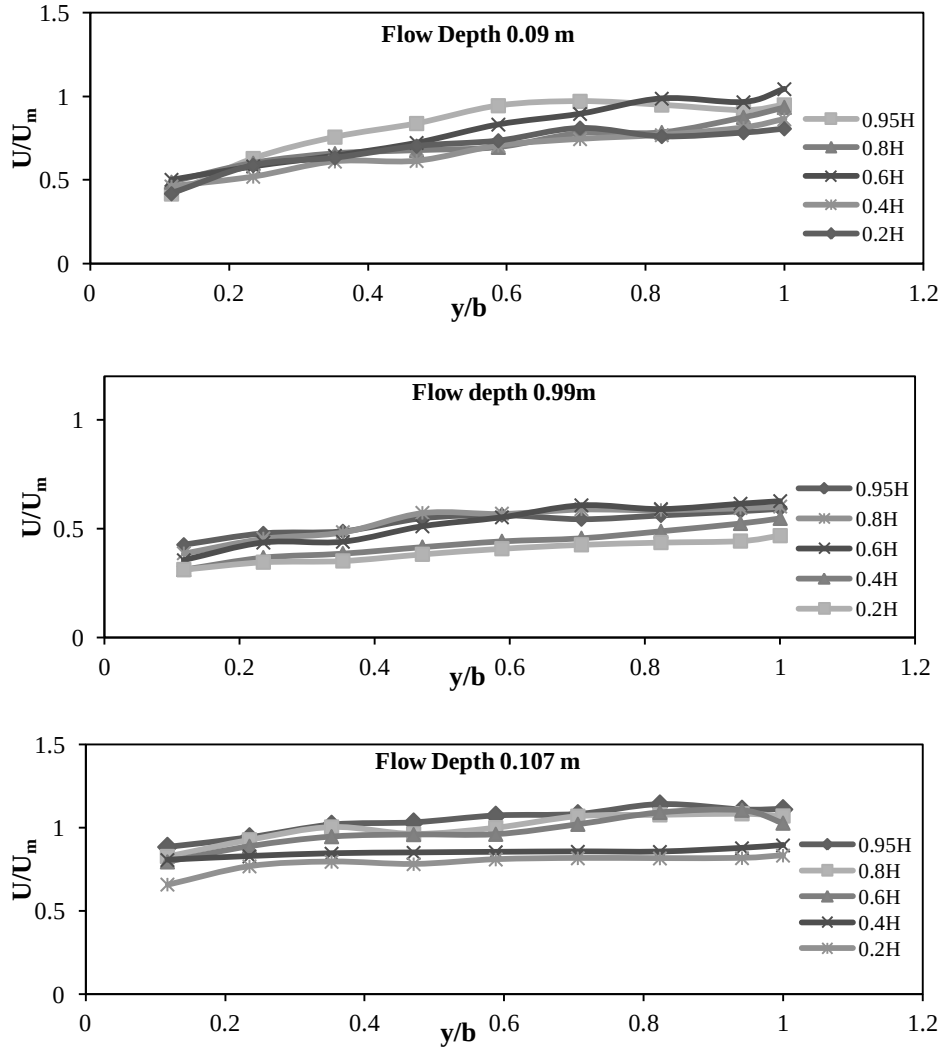

Figure 4.4: Lateral Velocity profiles for Rectangular Channel of different flow depths

4.4.2 Trapezoidal channel

In trapezoidal channel, the same procedure of taking measurements of lateral velocity in five vertical positions is considered as taken for rectangular cases. The same results are also obtained for trapezoidal channel. But a deviation of profiles has been found at transition region showing a clear existence of turbulence.

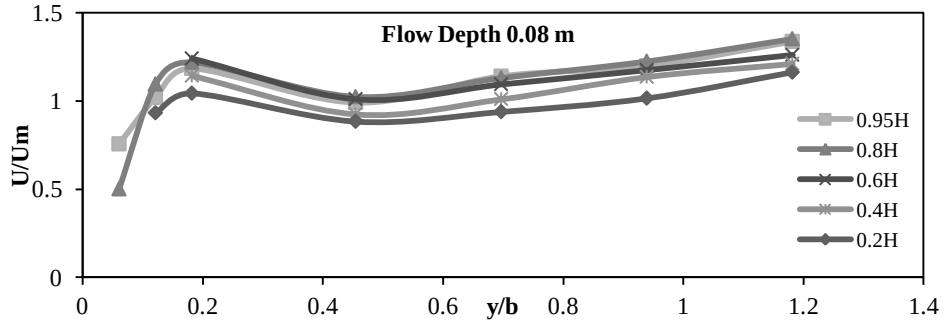

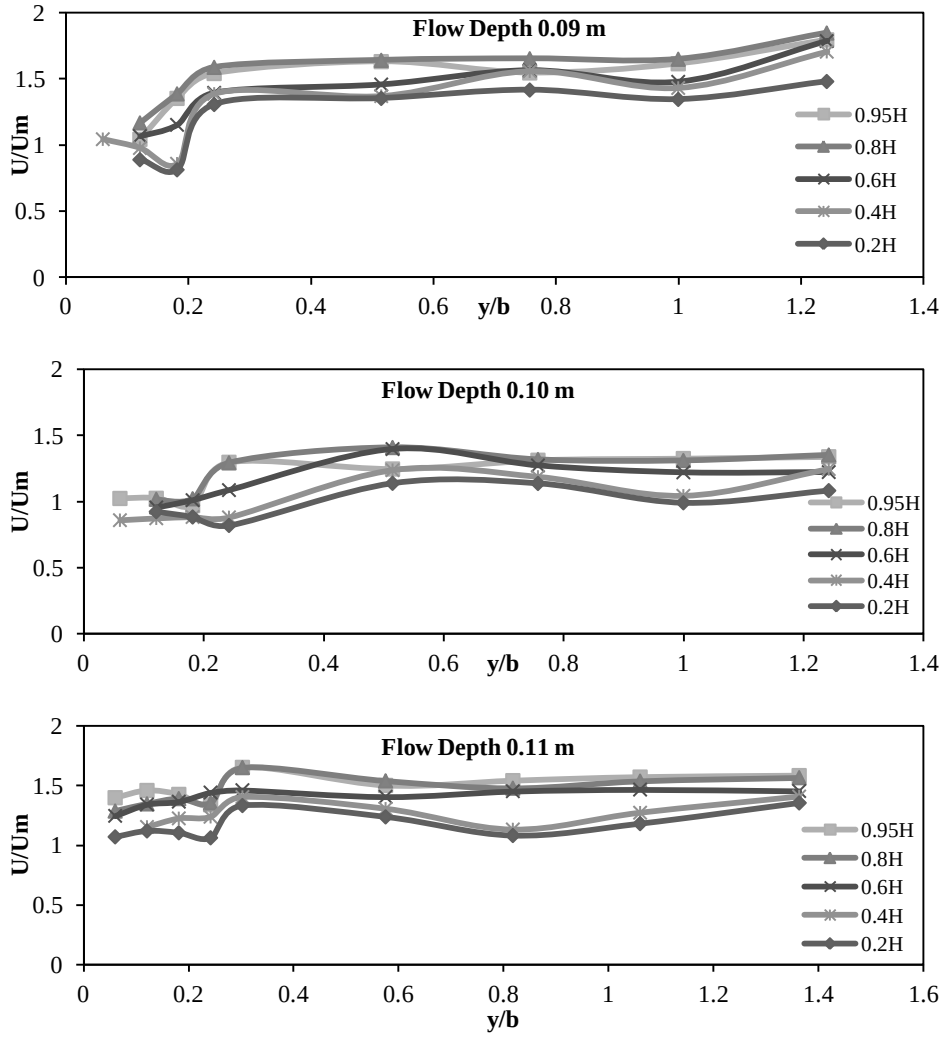

Figure 4.5: Lateral Velocity profiles for Trapezoidal Channel of different flow depths

4.5 Depth Averaged Velocity Distributions

The depth averaged velocity U_d for the entire in bank cases were calculated for both simple and rough of rectangular and trapezoidal channels. Using the equation

$$U_d = \frac{1}{H}\int_0^H U dz \qquad (6)$$

Where: U is the point velocity at a vertical line. U_d is calculated by integrating local point stream wise velocities (U) over a flow depth H.

Depth averaged velocity distribution is a plot which is plotted by joining the obtained value of U_d along the lateral direction of the channel.

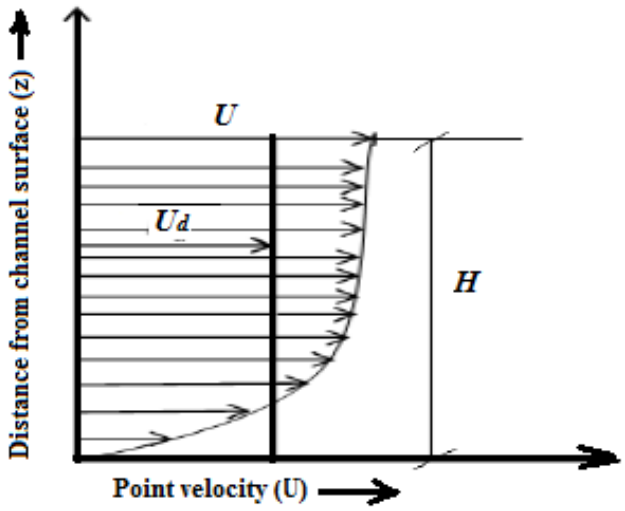

Figure 4.6: Velocity profile and depth averaged velocity at a section

The experimental results of depth averaged velocity distribution along the lateral distance of the channel for smooth rectangular and trapezoidal channel with both smooth and rough channel are given below respectively.

4.5.1 Smooth Rectangular Channel

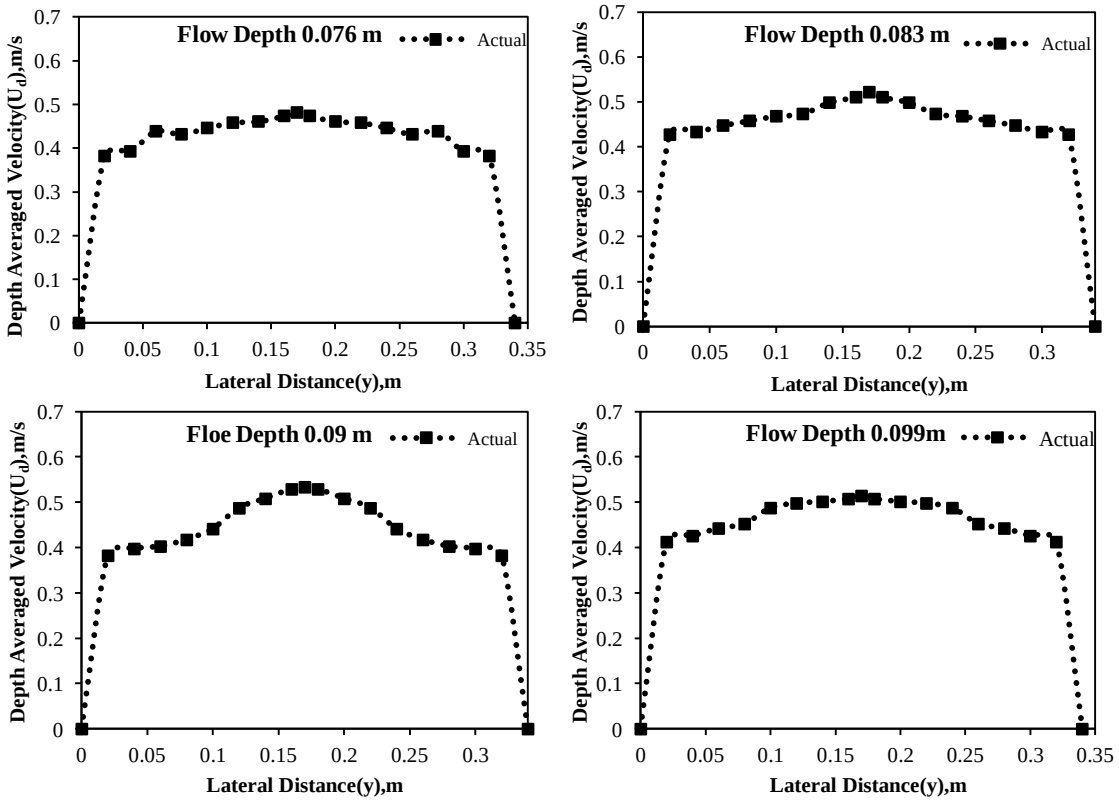

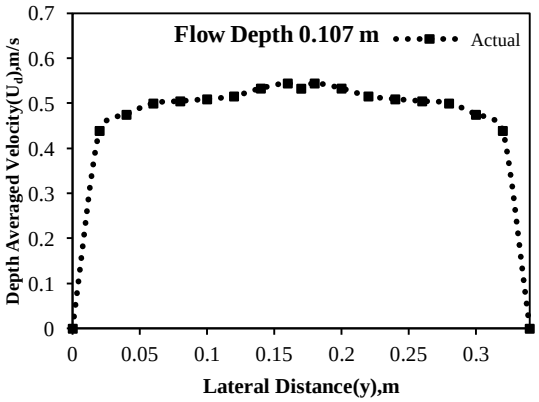

Figure 4.7: Depth Averaged velocity for rectangular channel of different flow depths

4.5.2 Trapezoidal smooth Channel

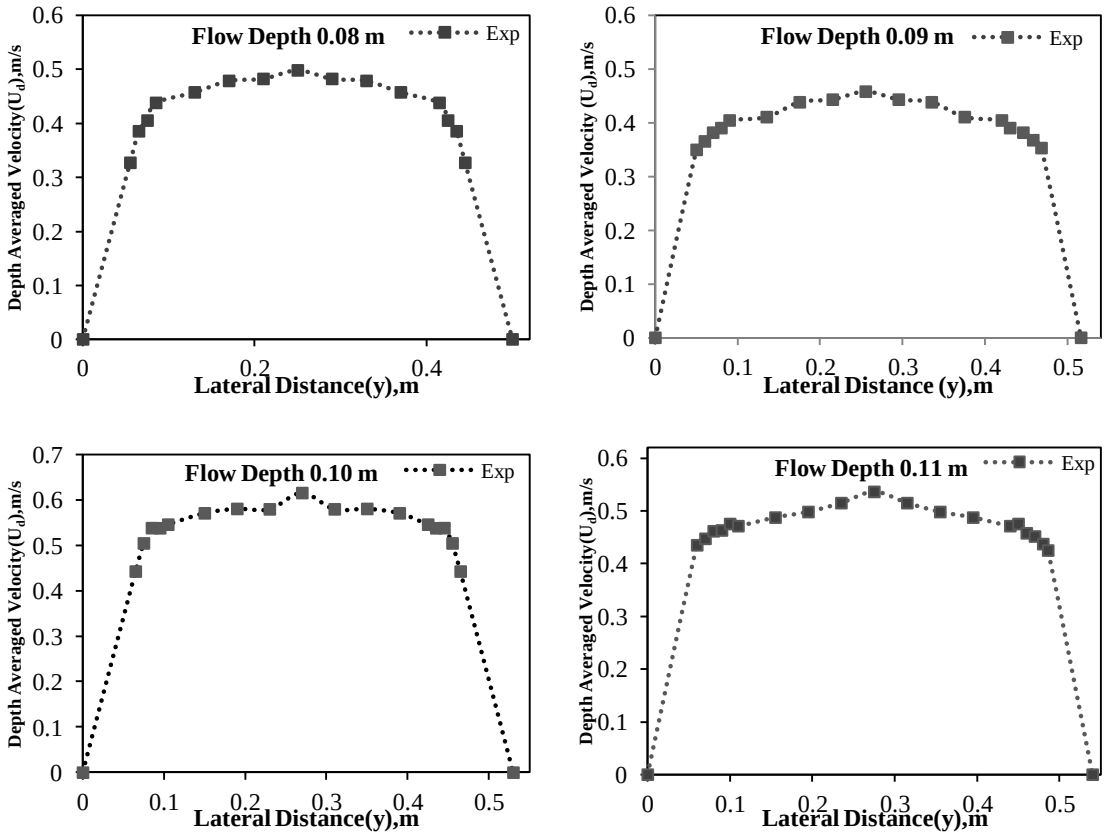

Figure 4.8: Depth Averaged velocity for trapezoidal smooth channel of different flow depths

4.5.3 Trapezoidal Rough Channel (Type-1)

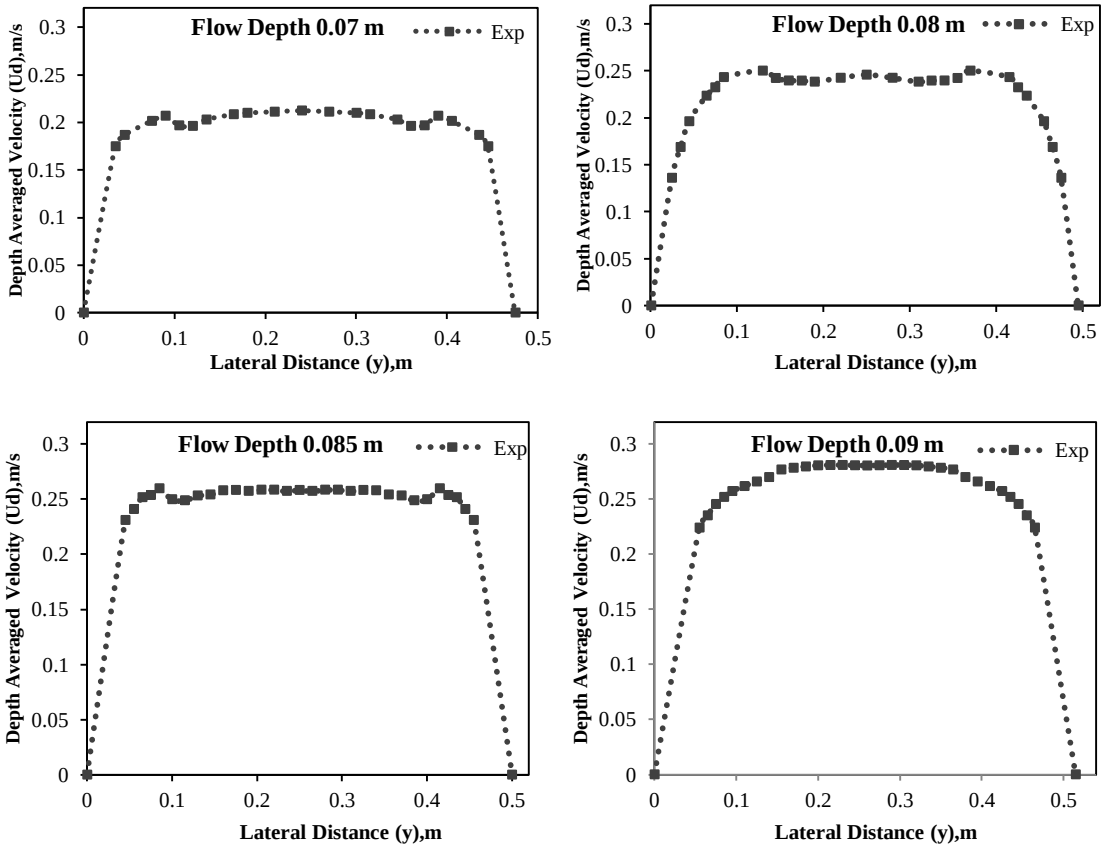

Figure 4.9: Depth Averaged velocity for trapezoidal rough channel (Type-1) of different flow depths

4.5.4 Trapezoidal Rough Channel (Type-2)

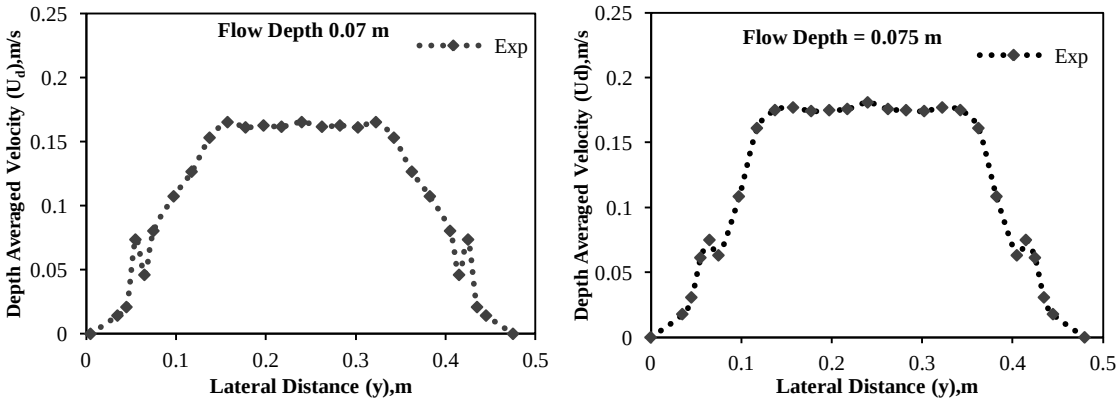

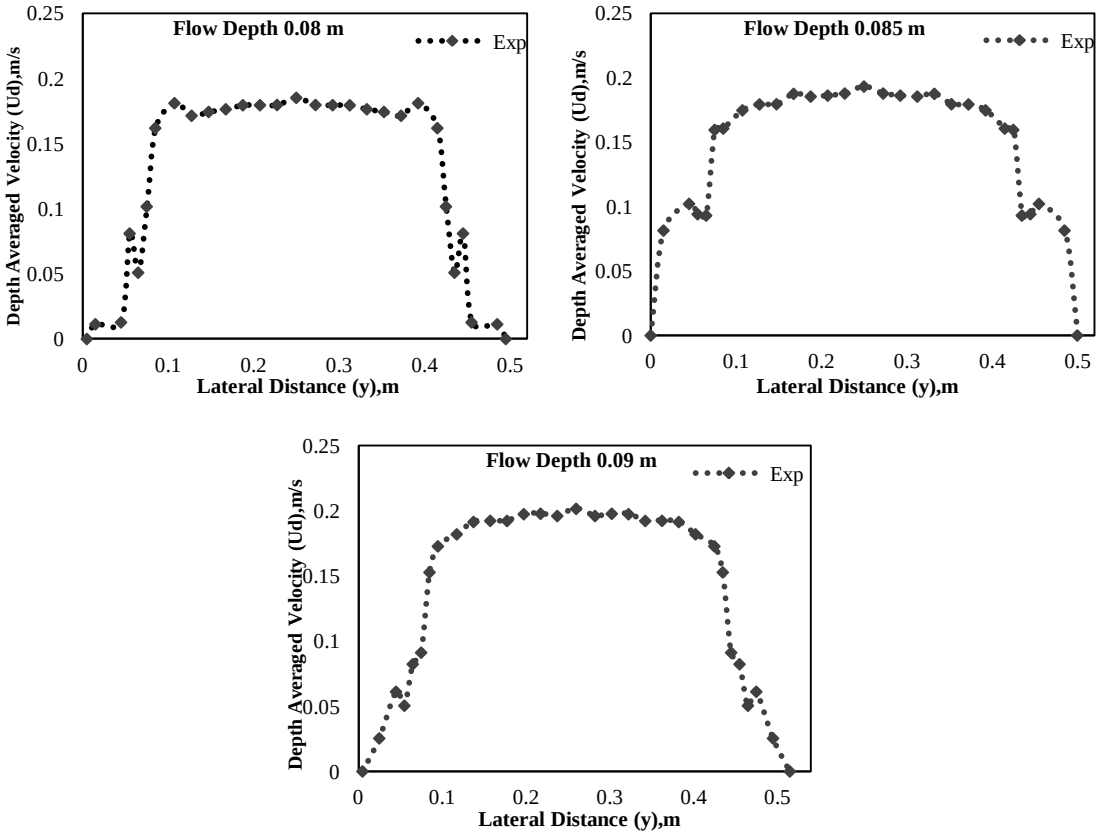

Figure 4.10: Depth Averaged velocity for trapezoidal rough channel (Type-2) of different flow depths

4.6 Discussions

From the results of depth averaged velocity for smooth rectangular channel, it is observed that when depth of flow increases the magnitude of depth averaged velocity also increases. For lower depth of flow depth averaged velocity remains uniform s compared to the higher depth of flow. It has been seen that magnitude of depth averaged velocity minimum at boundary and maximum at centre. When depth of flow increases the range of maximum velocity also increases along the lateral direction of the channel and reaches maximum at centre.

Similar observations are found for trapezoidal smooth channel. However for low depth the maximum velocity is found to occur at the junction between wall and bed. But for higher flow depth maximum velocities are found to be centre of the channel.

For the same trapezoidal channel with rough surface the magnitude of depth averaged velocity are found to be less, this is because of consumption of energy due to friction. For rough trapezoidal channel (type-2) shown in fig the magnitude of depth averaged velocity

is further less because of higher roughness (n=0.024). For channels of higher roughness the depth averaged velocity in central region are found to be more uniform as compared to lower depths. Another peculiar observation were found in rough trapezoidal channel (type-2), there is a sudden fall in depth averaged velocity occurs at the middle of side wall of trapezoidal channel and then increased maximum at the centre. For very high flow depths the maximum velocity distributed along the central portions of the channel.

4.7 Introduction to Surfer

4.7.1 General

Surfer is a powerful contouring, gridding, and surface mapping package for scientists, engineers, educators, or anyone who needs to generate maps quickly and easily. Maps can be displayed and enhanced in Surfer. Surfer is a grid-based mapping program that interpolates irregularly spaced XYZ data into a regularly spaced grid. The grid is used to produce different types of maps including contour, vector, image, watershed, 3D surface, and 3D wireframe maps. Many gridding and mapping options are available allowing us to produce the map that best represents our data. An extensive suite of gridding methods is available in Surfer. The variety of available methods provides different interpretations of data, and allows choosing the most appropriate method for our needs. In addition, data metrics allow us to gather information about our gridded data. Surface area, projected planar area, and volumetric calculations can be performed quickly in Surfer. Cross-sectional profiles can also be computed and exported.

4.7.2 Velocity Contours for Smooth Rectangular Channel

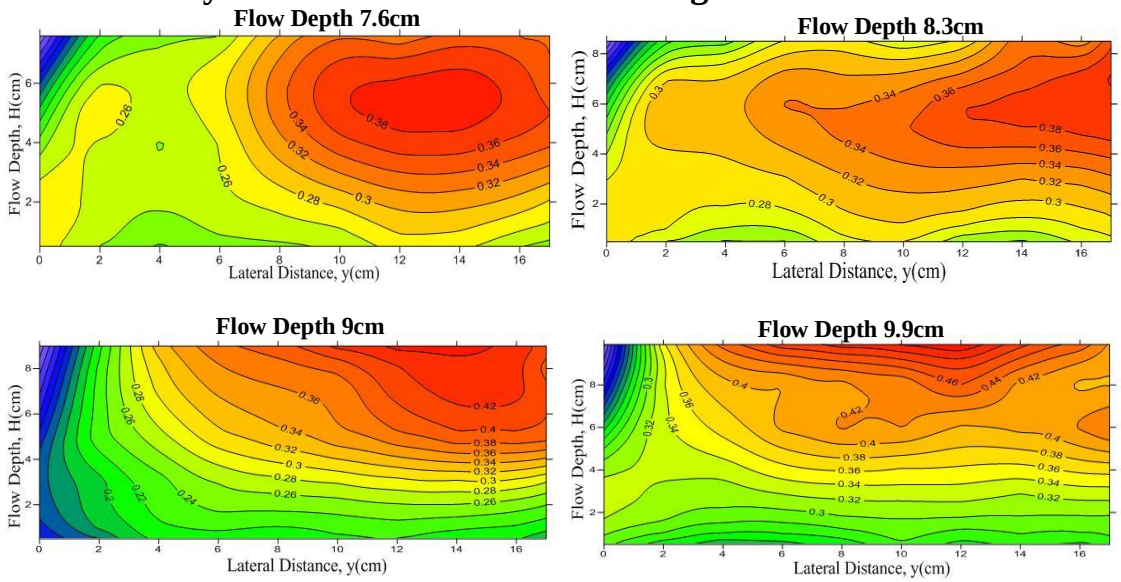

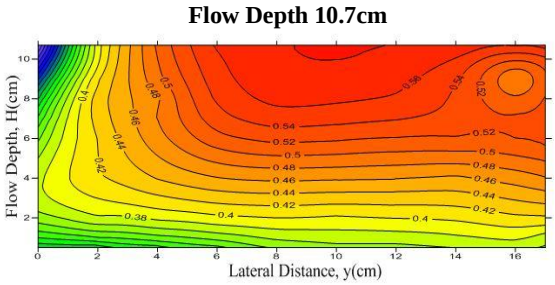

Figure 4.11: Velocity contours in X-direction (along the flow direction)

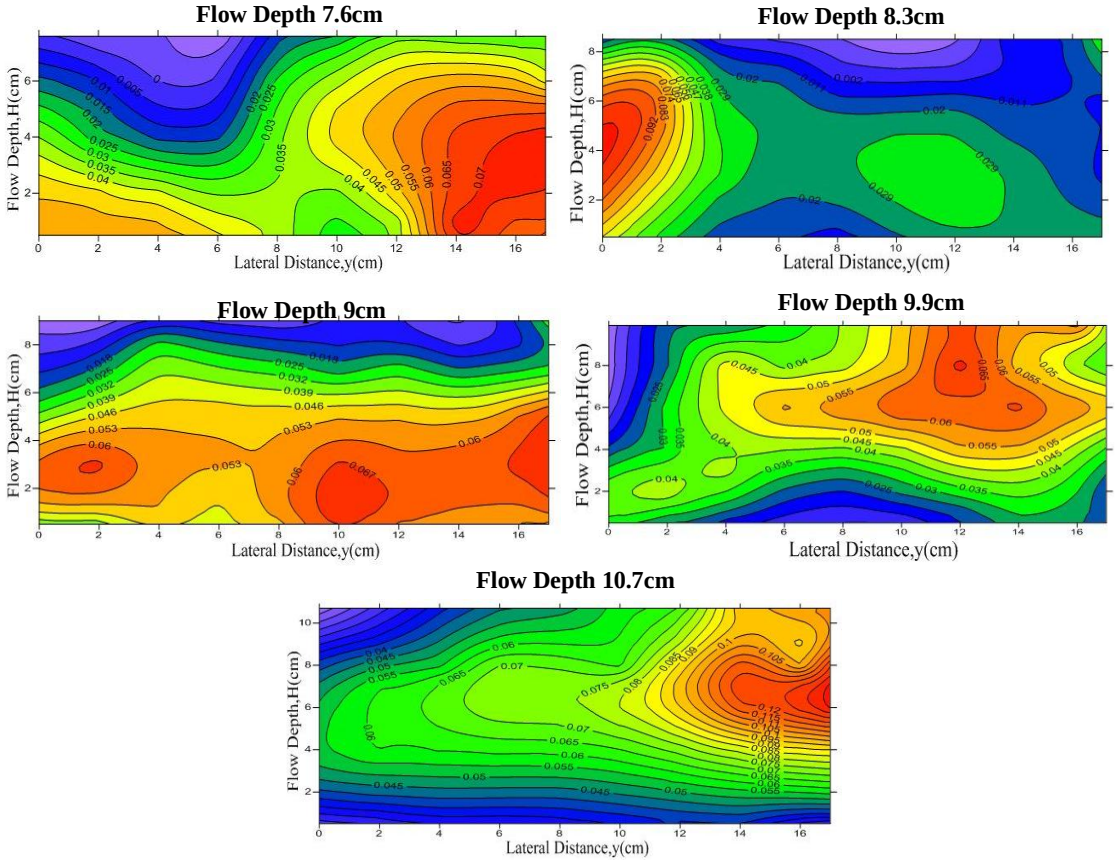

Figure 4.12: Velocity contours in Y-direction (along the transverse direction)

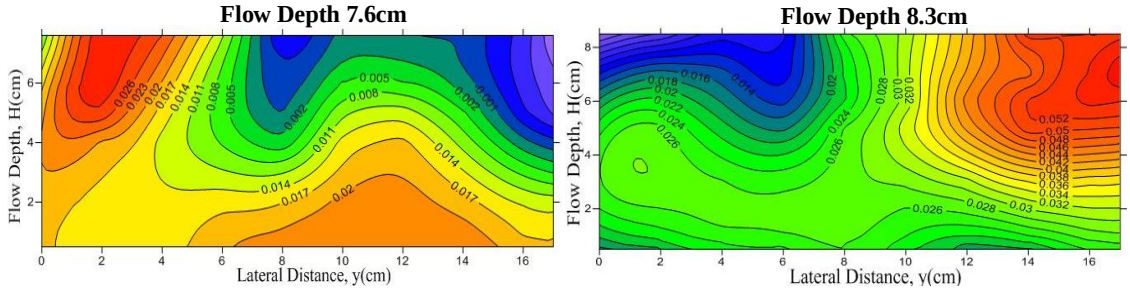

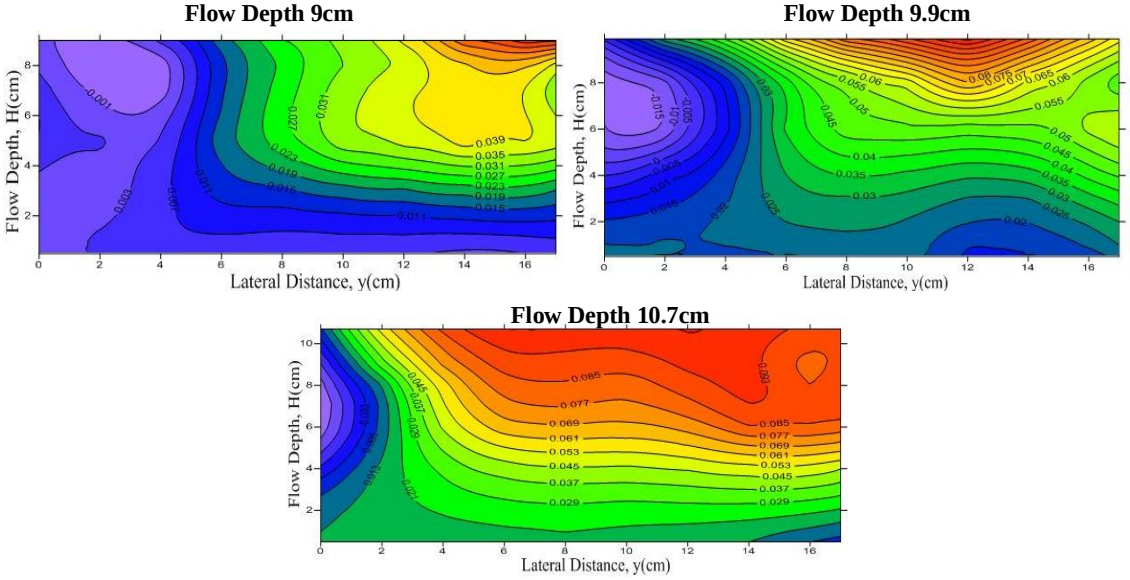

Figure 4.13: Velocity contours in Z-direction (along the vertical direction)

- Using surfer software the longitudinal velocity contours in x direction, transverse velocity contours in both y direction and z direction for smooth rectangular channel from experimental observation have been graphically presented in figure 4.11 to 4.13.It has been observed that for smooth rectangular channel the maximum longitudinal velocity in X-direction occurs in central upper portion of the channel and the minimum velocities occur near the side wall of flow for all cases.
- Regarding transverse velocity in y-direction a peculiar results have been observed. As the longitudinal velocity is higher in upper portion the transverse velocity is found to decrease in this region and rises towards side wall and bottom. The directions of velocity are not constant and appears as negative (i.e., towards central region). The minimum velocity occurs at the upper near to the side wall.
- The velocity in Z-direction are found to maximum (positive) near to the central portion of channel and side wall due to the occurrence of higher turbulence at this region. For lower depth of flow also the maximum velocity occurs at upper central region as well as at side wall because of friction from all three sides.

4.7.3 Velocity Contours for Smooth Trapezoidal Channel

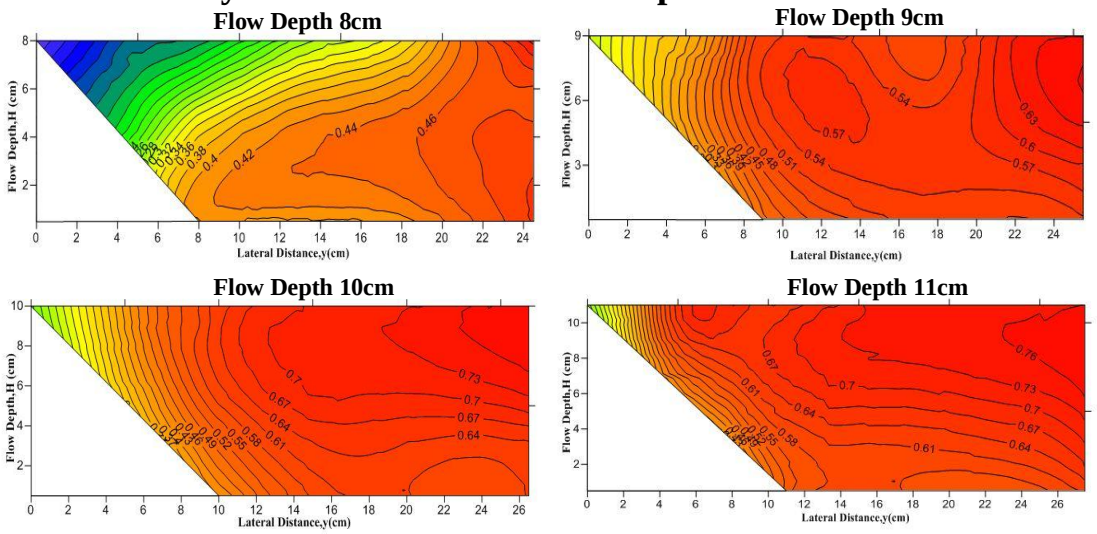

Figure 4.14:.Velocity contours in X-direction (along the flow direction)

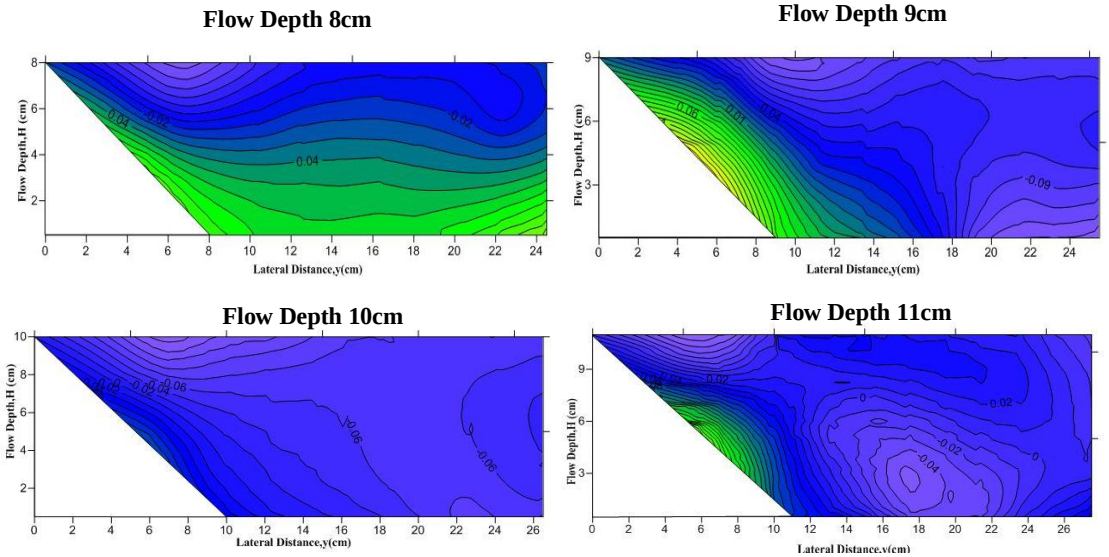

Figure 4.15: Velocity contours in Y-direction (along the transverse direction)

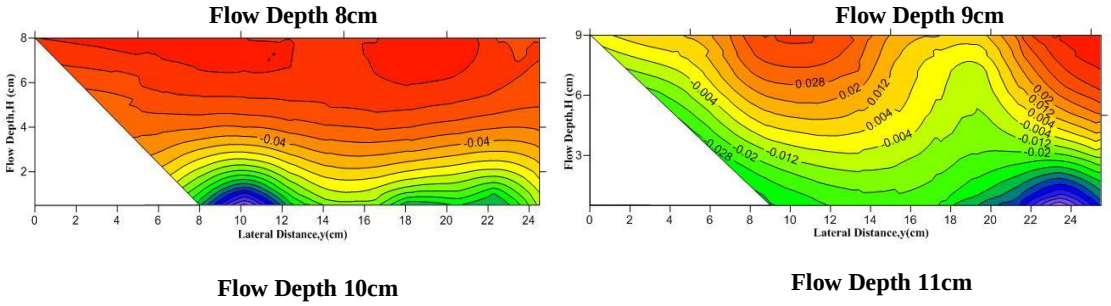

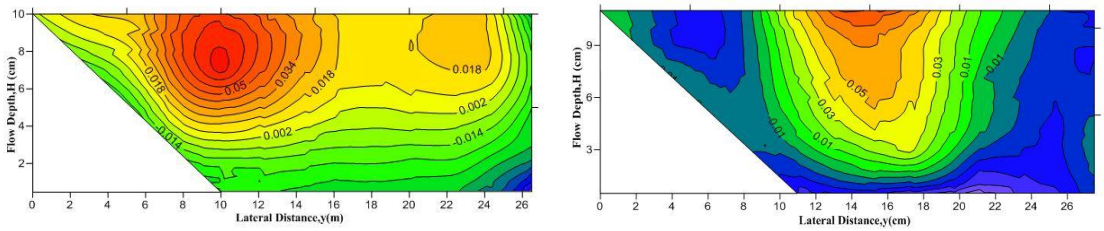

Figure 4.16: Velocity contours in Z-direction (along the vertical direction)

- Using surfer the longitudinal velocity contours in x direction, transverse velocity contours in both y direction and z direction for smooth trapezoidal channel from experimental observation have been graphically presented in figure 4.14 to 4.16. It has been observed that for smooth channel the maximum longitudinal velocity in X-direction occurs in central upper portion of the channel and the minimum velocities occur at upper edge of side slope due to the smaller depth of flow for all cases.
- Regarding transverse velocity in y-direction a peculiar results have been observed. As the longitudinal velocity is higher in upper portion the transverse velocity is found to decrease in this region and rises towards side banks and bottom. The directions of velocity are not constant and appears as negative (i.e., towards central region). The minimum velocity occurs at the upper part of interface.
- The velocity in Z-direction are found to maximum(positive) at interface of main channel and side bank due to the occurrence of higher turbulence at this region. For lower depth of flow also the maximum velocity occurs at upper central region as well as at interface because of friction from all three sides.

4.7.4 Velocity Contours For Rough trapezoidal Channel (Type-1)

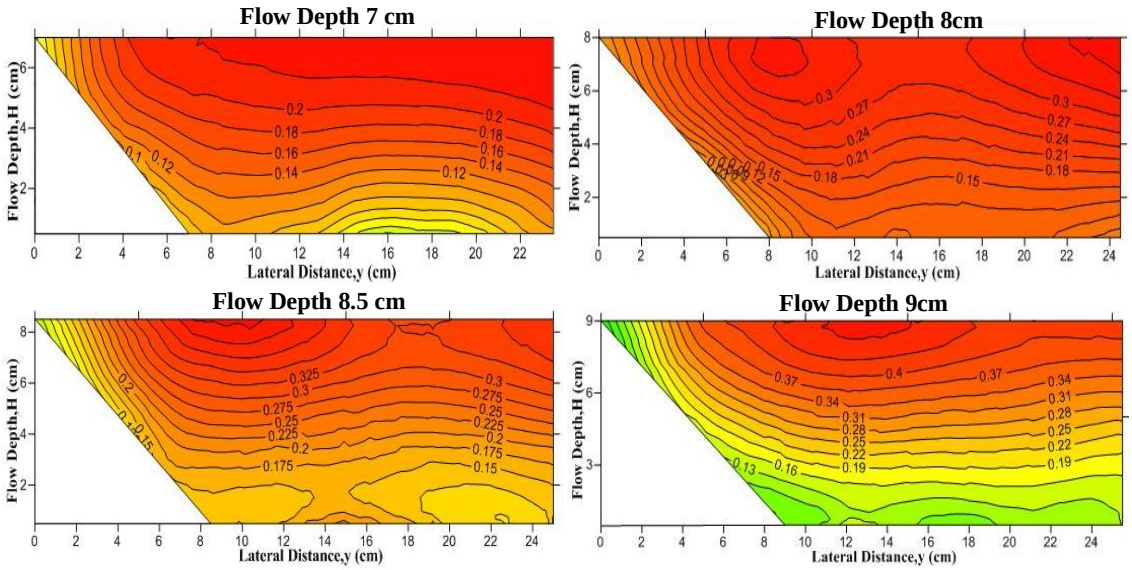

Figure 4.17: Velocity contours in X-direction (along the flow direction)

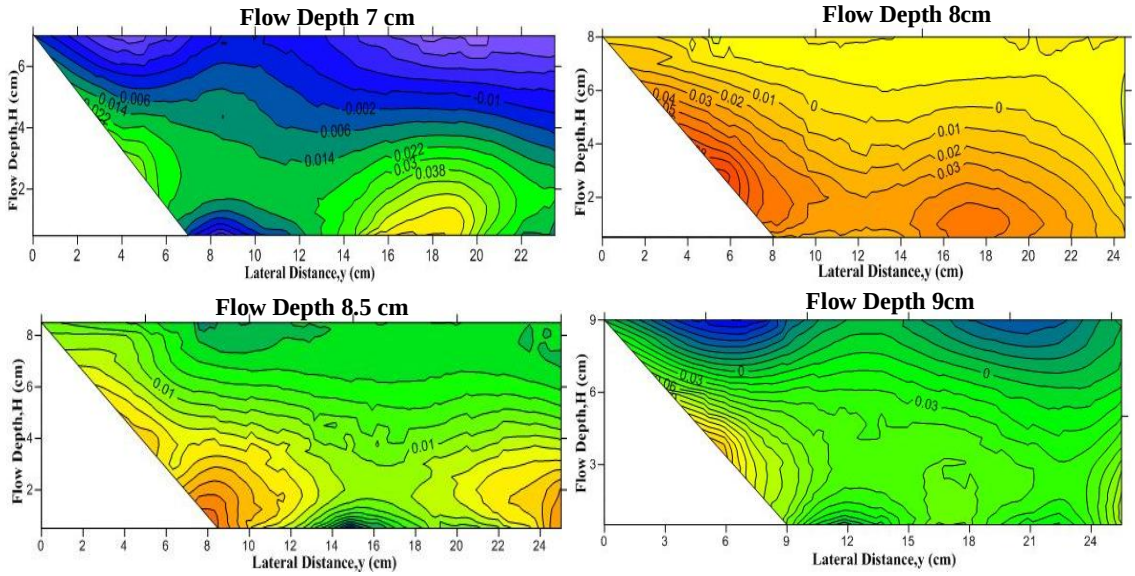

Figure 4.18: Velocity contours in Y-direction (along the transverse direction)

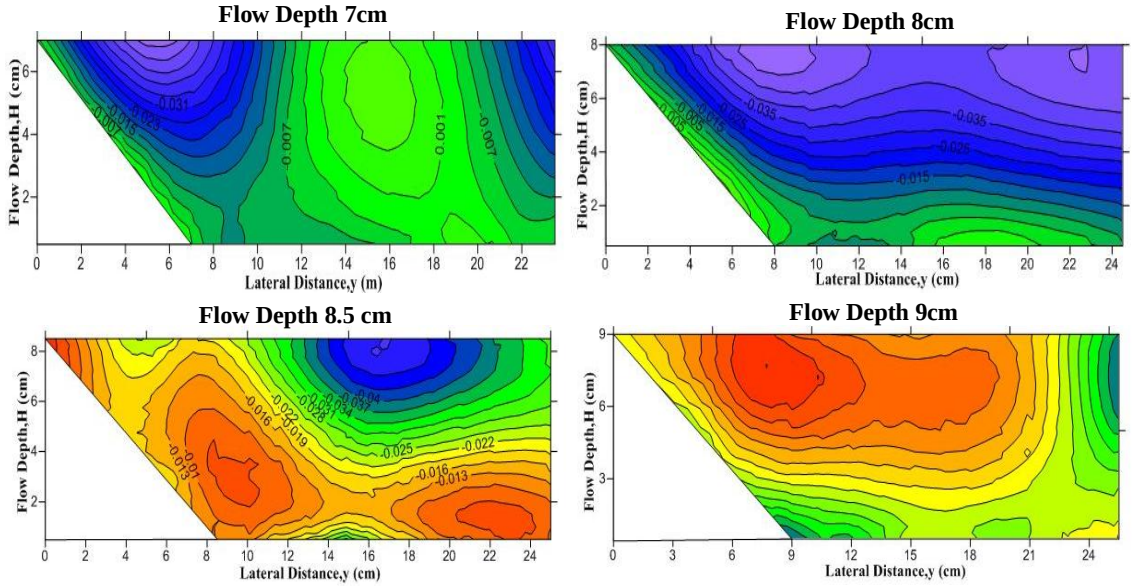

Figure 4.19: Velocity contours in Z-direction (along the vertical direction)

- Using surfer the longitudinal velocity contours in x direction, transverse velocity contours in both y direction and z direction for rough (type-1) trapezoidal channel from experimental observation have been graphically presented in figure 4.17 to 4.19. For rough channels the maximum longitudinal velocity in X-direction occurs at central portion and spreads towards side bank. Due to the higher roughness the magnitude of velocities are lower as compared to smooth channel for all flow depths.

- Similar results have been found for transverse velocity in y direction as found for smooth channel.
- For Z-direction the peculiar results have been observed and for lower depth of flow the minimum velocity occurs at interface region due to low effect of roughness. But for higher depth of flow the maximum velocity occurs at interface region and upper portion as effect of roughness reduces from bottom to top region.

4.7.5 Velocity Contours For Rough trapezoidal Channel (Type-2)

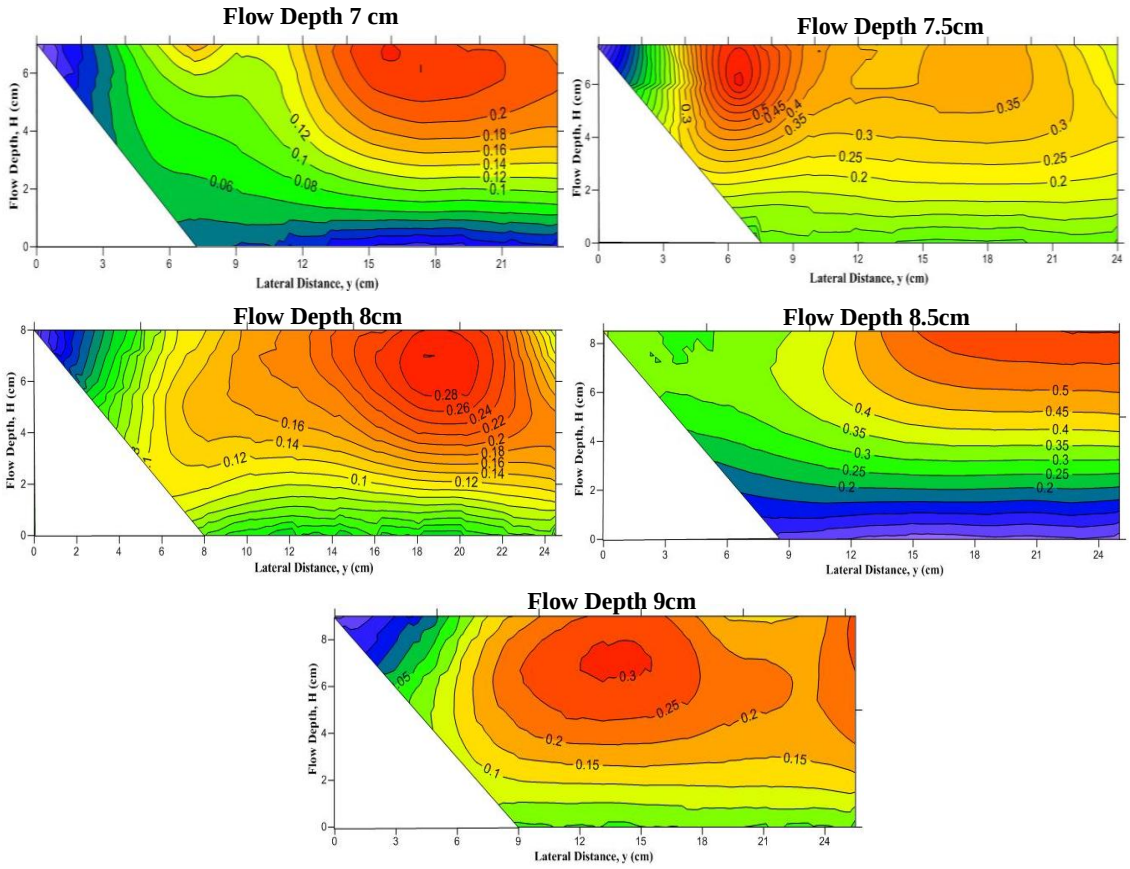

Figure 4.20: Velocity contours in X-direction (along the flow direction)

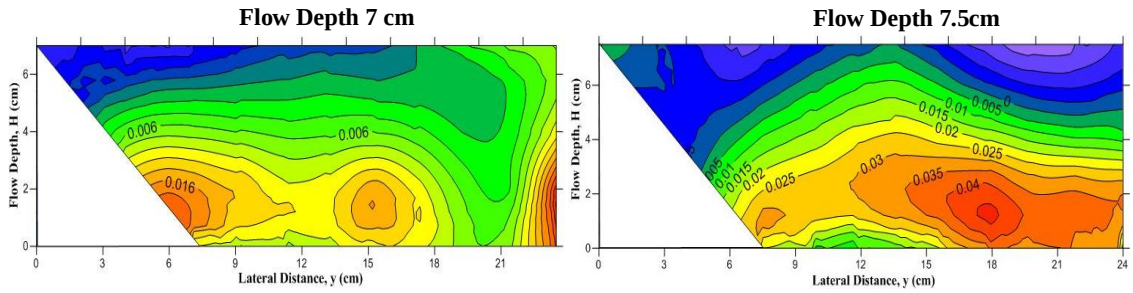

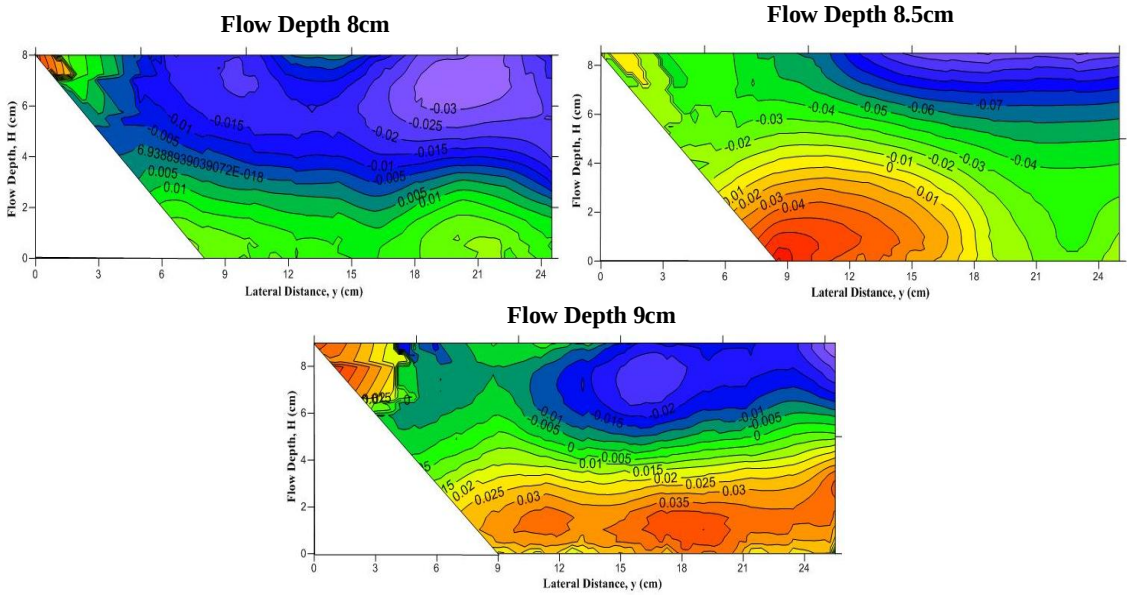

Figure 4.21: Velocity contours in Y-direction (along the transverse direction)

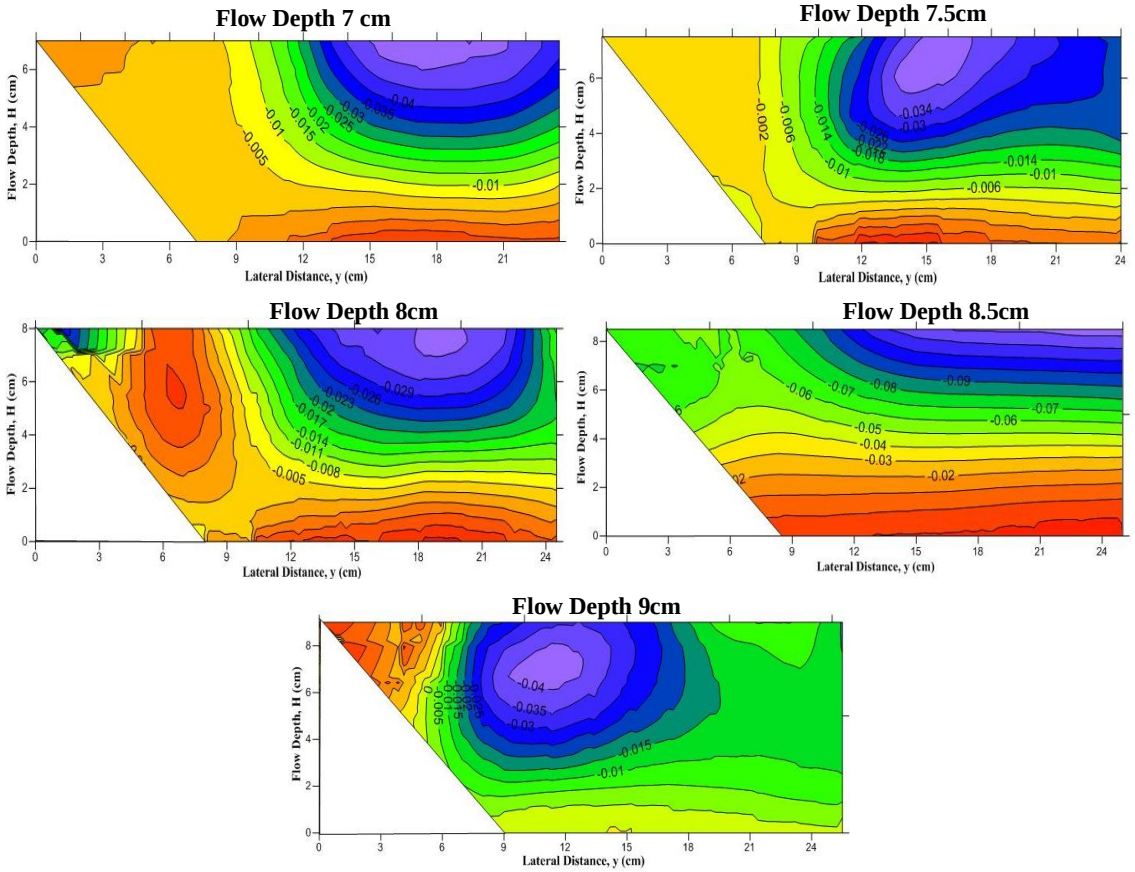

Figure 4.22: Velocity contours in Z-direction (along the vertical direction)

- Using surfer the longitudinal velocity contours in x direction, transverse velocity contours in both y direction and z direction for rough (type-2) trapezoidal channel from experimental observation have been graphically presented in figure 4.20 to

4.22. For this type of rough channels the maximum longitudinal velocity in X-direction occurs at central portion of main channel for all flow depth. But in case of higher depth the maximum velocity occurs at upper part of central portion. Due to the higher roughness the magnitude of velocities are lower as compared to smooth channel for all flow depths.

- The results have been found for transverse velocity in y direction velocity magnitude maximum as found at central region and junction of main channel and side wall at bottom of the channel. Maximum velocity occurred near the boundary region as compared to the upper portion of channel.
- For Z-direction the results have been observed that similar to transverse velocity in y direction and for lower depth of flow the minimum velocity occurs at interface region due to low effect of roughness. But for higher depth of flow the maximum velocity occurs at interface region and upper portion as effect of roughness reduces from bottom to top region.

Chapter-5

Theoretical Analysis and Discussions

5.1 Depth Averaged RANS Equation

5.1.1 Reynolds time averaged concept

The turbulence appears in a flow system, because of fluctuating velocity and pressure with time and space almost too complicated for modelling. However when averaged over time, the random terms show signs of required behaviour. Reynolds (1884) was the first researcher who realized this generation and applied this concept to purpose a time averaged approach. Base on his observations he suggested that all flow quantities can be expressed as the summation of mean and fluctuating flow. The fluctuating velocity components can be defined in terms of the average velocity and a fluctuating component shown in figure 5.1:

$$u = \bar{u} + u'; v = \bar{v} + v'; w = \bar{w} + w' \tag{5.1}$$

Time averaged components are

$$\bar{u} = \frac{1}{\Delta t}\int_t^{t+\Delta t} u\, dt \neq 0 ; \overline{u'} = \frac{1}{\Delta t}\int_t^{t+\Delta t} u'\, dt = 0 ; \overline{uu'} = \frac{1}{\Delta t}\int_t^{t+\Delta t} u\, u'\, dt = 0 \tag{5.2}$$

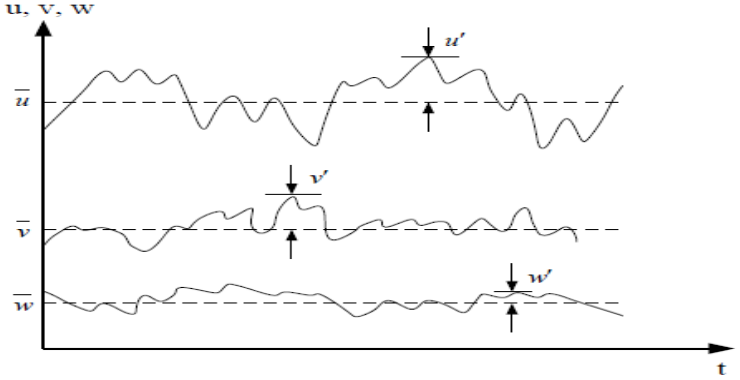

Figure 5.1: Concept of mean and fluctuating turbulence velocity components (Sharifi, 2008)

Reynolds (1884) recognized in turbulent flow, fluctuation in flow cause shear stress by the transfer of momentum and demonstrated that turbulent stresses, τ^R also known as Reynold stress were proportional to the time averaged of the product of velocity fluctuation within

the flow (Nezu and Nakagawa, 1993; Nezu, 2005). These Reynolds stresses in stream wise direction are:

$$\tau_{xz}{}^{R} = \bar{\rho}\overline{u'w'},\ \tau_{xy}{}^{R} = \bar{\rho}\overline{u'v'},\ \tau_{xx}{}^{R} = \bar{\rho}\overline{u'^{2}} \tag{5.3}$$

These above reynolds stresses were calculaed earlier in above section from experimentation data of three direction velocity measured with micro-ADV.

5.2 Eddy Viscosity Coefficient

In a laminar flow condition, the internal tangential shear stresses can be related to the linear dynamic viscosity through Stokes's law (Batchelor, 1967). In the mid-nineteenth century, some investigators were suggested "eddy viscosity" concept in turbulent flow which is an important factor to propose a general relationship of shear stress and shear strain, to relate the mean rate of deformation to the turbulent stresses (Schlichting, 1979, Davidson, 2004):

$$\tau_{xz}{}^{R} = \bar{\rho}\overline{u'w'} = \varepsilon_t\left(\frac{\partial u}{\partial x} + \frac{\partial w}{\partial z}\right) = (\mu_l + \mu_t)\left(\frac{\partial u}{\partial x} + \frac{\partial w}{\partial z}\right) \tag{5.4}$$

where the eddy viscosity ε_t is the sum of the laminar viscosities (μ_l) and turbulent viscosities (μ_t). The eddy viscosity is observed as a coefficient of momentum transfer intimating the transfer of momentum from lower velocity to its higher and vice versa (Finnmore and Franizi, 2002).

Variations of eddy viscosity along the lateral directions of the experimental channels are given below in a chronologic order.

5.2.1 Rectangular Smooth Channel

The variation of eddy viscosity co-efficient due to formation of eddies in flow pattern with the lateral distance throughout the cross section of rectangular smooth channel were given in figure 5.2.It can be observed that the variation of eddy viscosity for given flow depth.

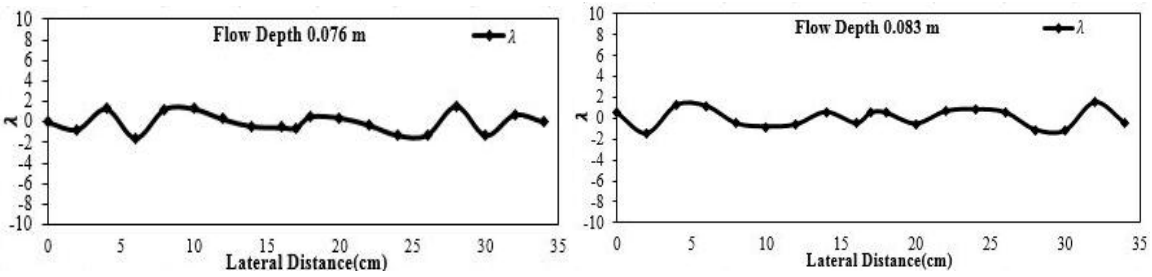

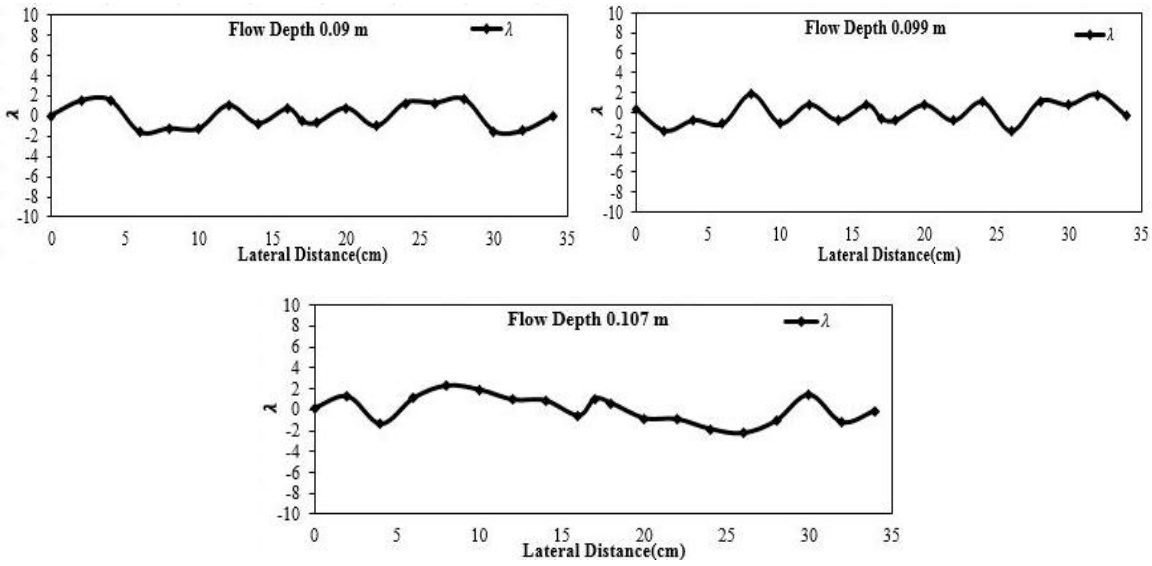

Figure 5.2: Eddy viscosity co-efficient of different flow depths in smooth rectangular channel

5.2.2 Trapezoidal Smooth Channel

The variation of eddy viscosity co-efficient due to formation of eddies in flow pattern with the lateral distance throughout the cross section of trapezoidal smooth channel for different flow depths were presented in figure 5.3. It can be observed that from given variation of eddy viscosity coefficient at the side wall region higher magnitude of λ as compared to central region of channel where approximate constant values of λ in smooth trapezoidal channel.

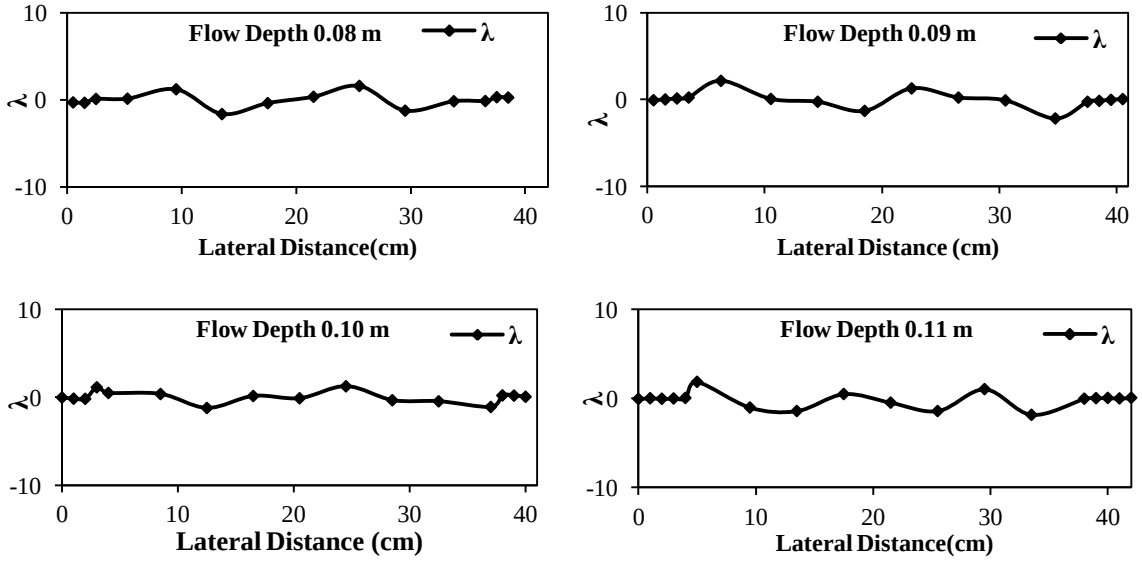

Figure 5.3: Variation of eddy viscosity co-efficient of different flow depths in smooth Trapezoidal channel

5.2.3 Trapezoidal Rough Channel (Type-1)

The variation of eddy viscosity co-efficient due to formation of eddies in flow pattern with the lateral distance throughout the cross section of trapezoidal rough channel (type-1) were shown in figure5.4. It can be observed that the variation of eddy viscosity at the central region as compared to the smooth channel of same geometry higher magnitude due to the higher roughness value. Fluctuation in variation was frequent along the lateral distance due to the roughness surface.

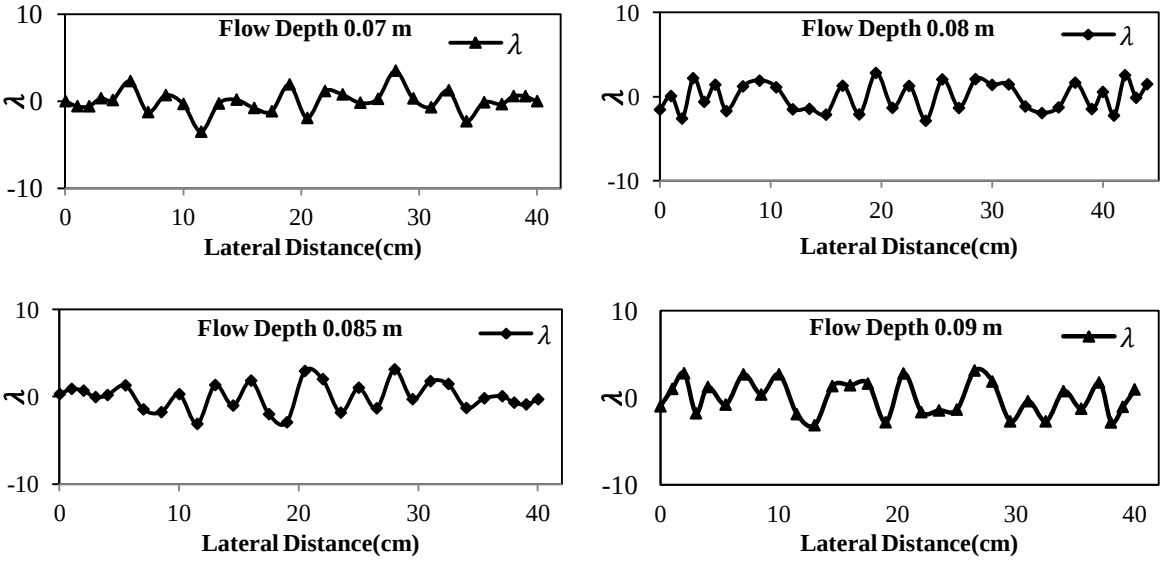

Figure 5.4: Variation of eddy viscosity co-efficient of different flow depths in trapezoidal rough (type-1) channel

5.2.4 Trapezoidal Rough Channel (Type-2)

The variation of eddy viscosity co-efficient due to formation of eddies in flow pattern with the lateral distance throughout the cross section of trapezoidal rough channel (type-2).shown in figure 5.5. It was observed that magnitude of λ varies with higher value as compared to the type-1 rough material, because roughness of type-2 rough experimental channel is more than type-1 rough channel.

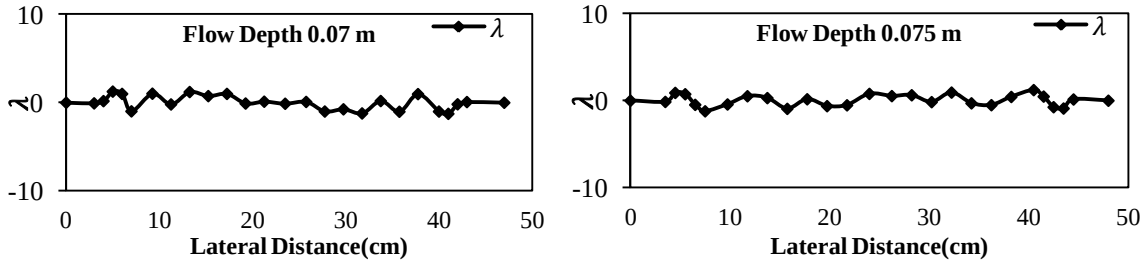

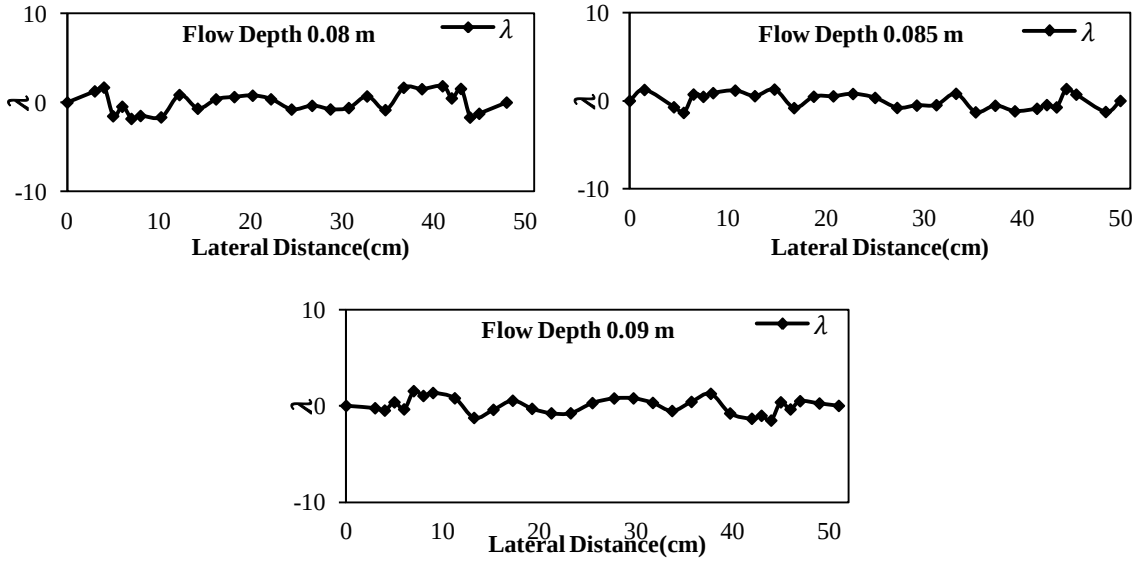

Figure 5.5: Variation of eddy viscosity co-efficient of different flow depths in trapezoidal rough (type-2) channel

Obsevations:-

1 For smooth channel in all flow depths the variation of eddy viscosity is less as compared to rough channel.

2 Due to effect of roughness, formation of eddy is more in rough channel in smooth channel. Value of eddy viscosity increases as increase in roughness value. So in trapezoidal channel eddy viscosity variation have been observed quit different from rectangular channel due to two different flow criteria zones.

3 In rectangular smooth open channel the eddy viscosity varies from -1.8 to +1.4 as minimum to maximum value.

4 It is observed that variation of eddy viscosity in smooth channel varies from -1 to +1 and for rough (type-1) channel varies from -2.5 to +2.4 and for rough (type-2) channel varies from -2.8 to +2.4 as minimum to maximum value respectively. There is a larger variation in rough channel as compared to smooth channel.

5 But Finally it is observed that average eddy viscosity for a perticular channel is nearly a constant value for all flow depths.

5.3 Global and local friction factors

The boundary shear stress distribution (τ) across the wetted perimeter of the flow section of simple main channel was measured by Preston tubes. This was done to evaluate or determine the interaction mechanism on the distribution of boundary shear stress across

the wetted flow perimeter. As per Patel (1965), the difference in static and dynamic pressure values (Δp) observed respectively in the static holes and dynamic holes of the Preston tube immersed in the boundary layer of the flowing liquid can be used to measure indirectly the point boundary shear stress over the solid boundary with an accuracy of +/- 6%.For mathematical computations of the boundary shear stress, Patel (1965) suggested a number of relationships which are as follows

$$y^* = 0.50x^* + 0.037, \quad 0 \le y^* < 1.50 \text{ or } 0 \le x^* \le 2.90 \tag{5.4a}$$

$$y^* = -0.0060x^{*3} + 0.1437x^{*2} - 0.1381x^* + 0.8287, \quad 1.50 \le y^* < 3.50 \text{ or } 2.90 \le x^* \le 5.60 \tag{5.4b}$$

$$x^* = y^* + 2log_{10}(1.95y^* + 4.02), \quad 3.50 \le y^* < 3.50 \text{ or } 5.60 \le x^* \le 7.60 \tag{5.4c}$$

With $x^* = log_{10}\left(\frac{(\Delta p)d^2}{4\rho v^2}\right)$ (5.4d)

and $y^* = log_{10}\left(\frac{\tau_b d^2}{4\rho v^2}\right)$ (5.4e)

Where, *d is* the external diameter of the Preston tube is 0.0047m and *v is* the kinematic viscosity for the water is 1×10^{-4} m^2/s.

Boundary shear (τ_b) from point to point along the bed of the channels are found out using Preston tube techniques by using Patel's calibration equation (5.4a) to equation (5.4e). Boundary shear stress $\tau_b$can be evaluated in lateral direction from point to point by using the equation (5.4e). Knowing the depth averaged velocity and boundary shear stress, the global friction factor is evaluated for respective flow conditions of channels are found out using the equation 5.5.

$$f_{global} = \frac{8\tau_{b,avg}}{\rho {U_{mean}}^2} \tag{5.5}$$

Where: $\tau_{b,avg}$ is boundary shear stress over whole channel wetted perimeter, f_{global} is global friction factor,ρ is density of water and U_{mean} is mean velocity of the flow for a particular flow depth.

Then local friction factor is evaluated for respective flow conditions of the channels from point to point along the bed as per equation given below in equation 5.6:

$$f_{local} = \frac{8\tau_{b,local}}{\rho {U_d}^2} \tag{5.6}$$

Where:τ_b is boundary shear stress of any desire point , $f_{local}$is local friction factor,ρ is density of water and U_d is depth averaged velocity.

5.3.1 Variation of global Friction Factors

Variation of global friction factor observed with aspect ratio for both smooth and rough channels shown in figure 5.6 to 5.8. Global friction factor calculated using the equation 5.5 for experimental channels and other investgators channel data of both smooth and rough surfaces.

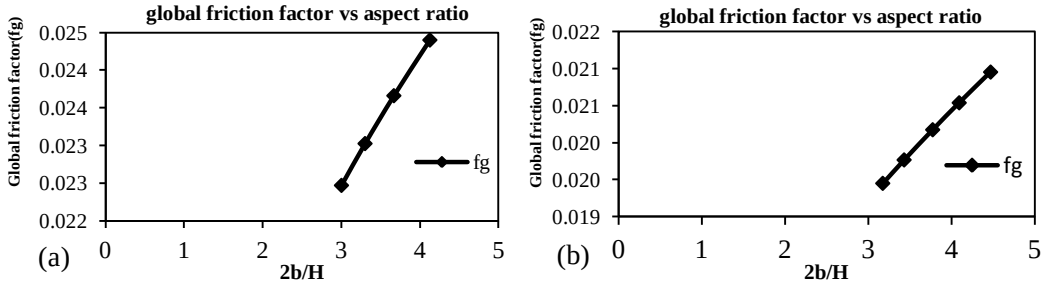

Figure 5.6: Variation of global friction factor of experimental channels (a) Trapezoidal smooth channel (b) Rectangular smooth channel

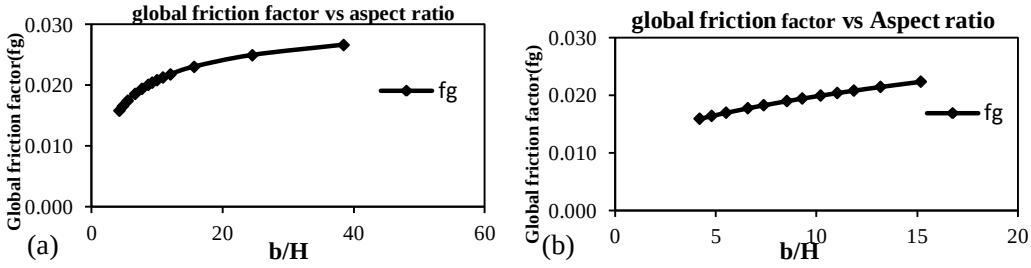

Figure 5.7:.Variation of global friction factor (a) Rectangular smooth channel (Tang, 1999) (b) Rectangular smooth channel (Atabay,2001)

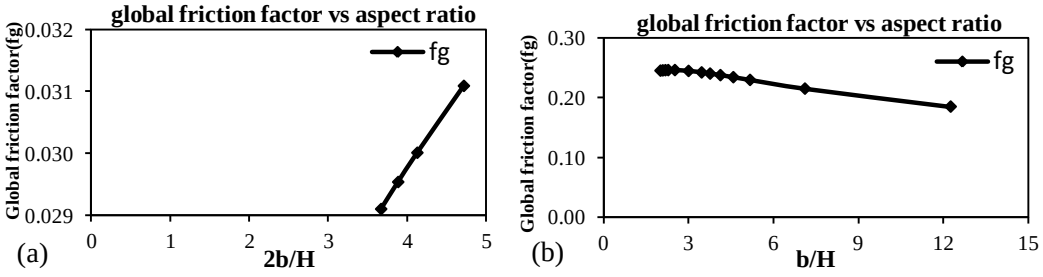

Figure 5.8: Variation of global friction factor (a) Trapezoidal rough channel (experimental channel) (b) Rectangular rough channel (Tang, 1999)

5.3.2 Variation of local Friction Factors

To find out the point to point friction factor value along the cross section of channel, a relationship between the boundary shear stress and depth averaged velocity has been considered. By using this relationship the local friction value at every vertical section can

be evaluated using equation (5.6), if the measured boundary shear stress and depth averaged velocity at the respective vertical section are known to us. Variation of local friction factor along the lateral direction of experimental channels and for rectangular smooth channel (Atabay, 2001) shown in figure 5.9 and 5.10 respectively.

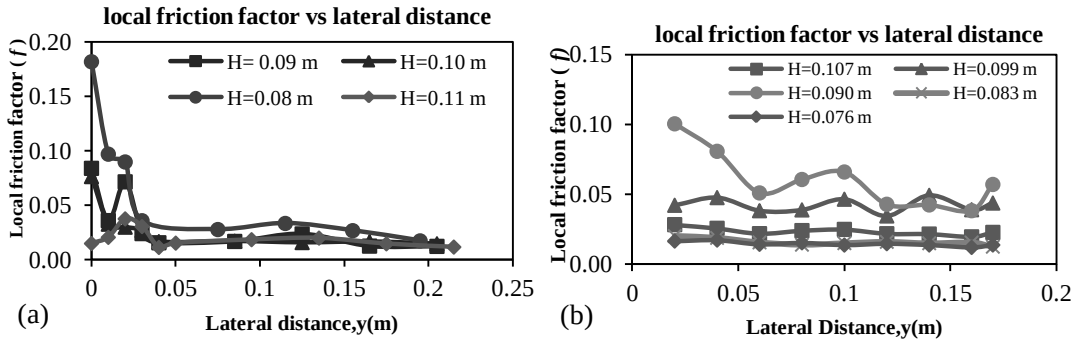

Figure 5.9: Variation of local friction factor of experimental channels (a) Trapezoidal smooth channel (b) Rectangular smooth channel

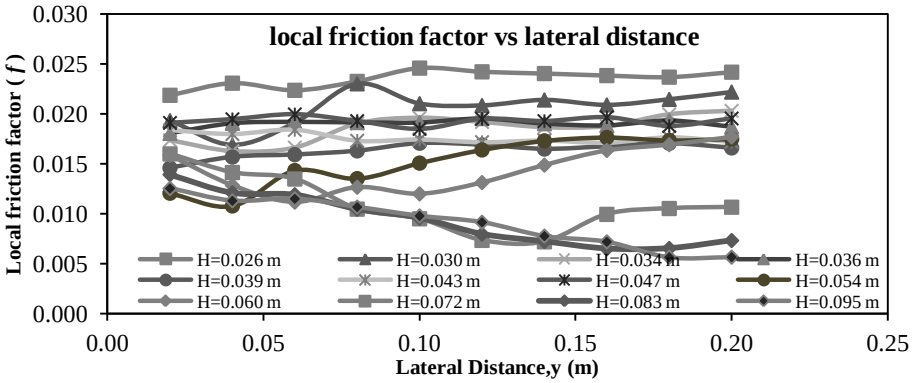

Figure 5.10: Rectangular Smooth channel (Atabay, 2001)

Observations

In constant flow domain the friction factors value remains constant for whole cross-section but in trapezoidal channel it varies greatly in side wall or varying flow domains, it because of the turbulence and vertices formation .So it is no need to calibrate the friction factor, because it remains constant and it also depend upon the manning's *n* which is constant for a channel through out the whole lateral and longitudinal section.

5.4 Secondary Flow Phenomena

Secondary current is caused by anisotropic of turbulent velocity.Further, turbulent structure such as secondary current (which is generally driven by the anisotropy and in-homogeneity of turbulence) creates velocity dip and affects the flow. Although, the influence of secondary flows for river processes has long been recognized, but their origin,

mechanics, effects and co-relations with primary mean flow and turbulence are still a matter of debate. Hence in this study an effort has made to recognize the affect of the turbulence in simple open channel.

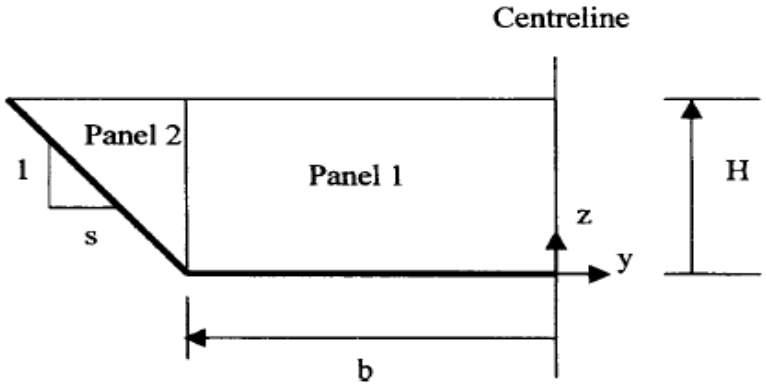

Figure 5.11: Cross-section of trapezoidal channel, with side slope 1:s (Omran,2005)

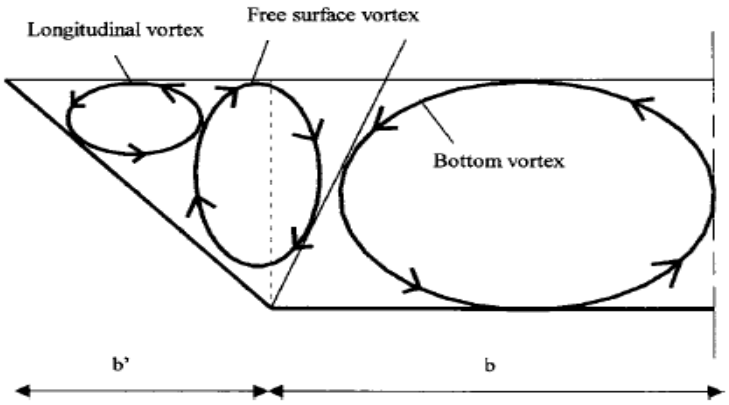

Figure 5.12: Secondary flow cells in half trapezoidal channel (Omran, 2005)

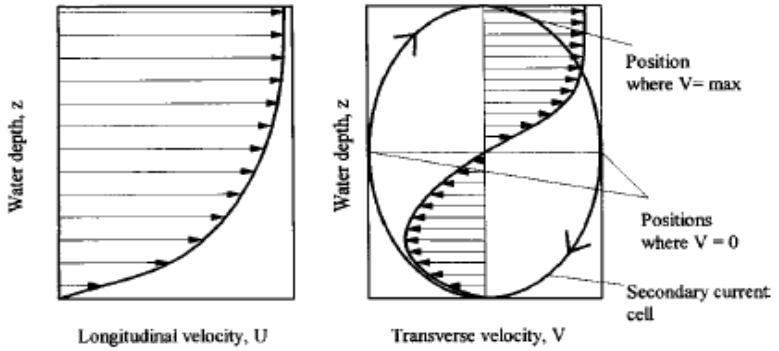

Figure 5.13: Longitudinal and transverse velocity profiles (Omran, 2005)

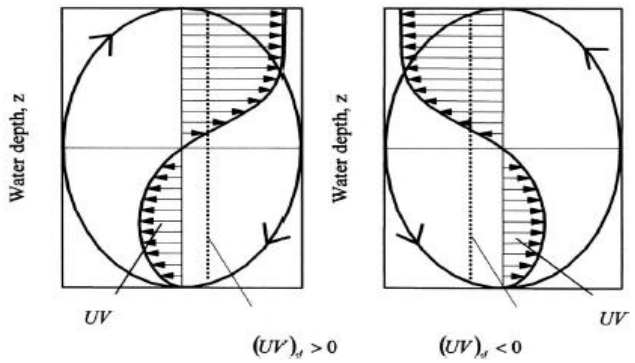

Figure 5.14: Signs of the depth-averaged term(UV)d, (Omran,2005)

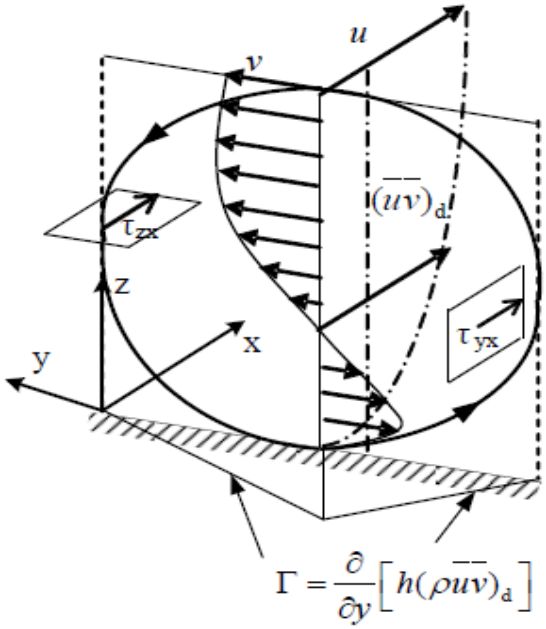

Figure 5.15: Visualisation of the averaged secondary flow term (Chlebek and Knight, 2006)

5.5 Secondary Current Patterns

The secondary flows continuously transport momentum from the centre to the corners generate high velocities there. Secondary current is taking place always at resultant of transverse and lateral direction of primary flow. Secondary current is an important component which is considered in every numerical approach to quantify the accurate flow of the particular channel. Secondary currents are responsible to formation different type of secondary cells in different zones doe rectangular and trapezoidal channels are given in this research work. The velocity vector diagrams are produced the secondary cells in constant depth domain in case of rectangular channel and in both constant and side slope domain in trapezoidal channels are shown as given figures for different flow depths.

5.6 Mechanism of secondary currents

5.6.1 Longitudinal Vorticity Equation

The production of turbulence induced secondary currents in straight channel with rectangular and trapezoidal cross section was explained by longitudinal vorticity equation The distribution of difference $\left(\overline{w^2} - \overline{v^2}\right)$of the normal stresses play an vital role has been already studied by Einstein and Li (1965). The secondary current patterns in an open channel flow verified experimentally in the present study.

The longitudinal vorticity equation in fully developed turbulent flow as given below in equation 5.7

$$\mathrm{V}\frac{\partial \xi}{\partial y} + \mathrm{W}\frac{\partial \xi}{\partial z} = \frac{\partial^2}{\partial y \partial z}\left(\overline{v^2} - \overline{w^2}\right) + \left(\frac{\partial^2}{\partial z^2} - \frac{\partial^2}{\partial y^2}\right)\overline{vw} + \mathrm{v}\nabla^2\xi \qquad (5.7)$$

In which

$$\xi \equiv \frac{\partial W}{\partial y} - \frac{\partial V}{\partial z} \qquad (5.8)$$

The last term of equation (5.7), the viscous form term was neglected except very near the wall .The convection term of the left hand side can be approximately neglected according to the examination of Nezu and Nakagawa (1984). Among the three terms of right side in equation 5.7, first term is the production term of vorticity which promotes generation of secondary currents. The extreme left side term of equation 5.7 is convection term of vorticity or advection of vorticity which shows that secondary currents exist.

The Reynolds stress $-\overline{vw}$ can be expressed in terms of eddy viscosity as follows:

$$-\overline{vw} = \varepsilon_{yz}(\partial W/\partial y) + (\partial V/\partial z) \qquad (5.9)$$

Then the secondary current velocity components *V* and *W* are expressed using also stream function ψ as follows:

$$V = {}^{\partial\psi}/_{\partial z} \text{and} W = {}^{\partial\psi}/_{\partial y}$$

ε_{yz} remains unknown, since the measurement of $-\overline{vw}$are quite difficult in open channel flows. So the distribution of difference $\left(\overline{w^2} - \overline{v^2}\right)$ that determined the structure of the secondary currents as discussed by Gerard (1978).

Basic Equations

The equation of motion in a fully developed wide channel flow are given by (Nezu and Nakagawa, 1989)

$$V\frac{\partial U}{\partial y} + W\frac{\partial U}{\partial z} = g\sin\theta - \frac{1}{\rho}\frac{\partial P}{\partial x} - \frac{\partial \overline{uv}}{\partial y} - \frac{\partial \overline{uw}}{\partial z} + v\nabla^2 U \quad (5.10)$$

$$V\frac{\partial V}{\partial y} + W\frac{\partial V}{\partial z} = -g\cos\theta - \frac{1}{\rho}\frac{\partial P}{\partial y} - \frac{\partial \overline{v^2}}{\partial y} - \frac{\partial \overline{vw}}{\partial z} + v\nabla^2 V \quad (5.11)$$

$$V\frac{\partial W}{\partial y} + W\frac{\partial W}{\partial z} = -\frac{1}{\rho}\frac{\partial P}{\partial z} - \frac{\partial \overline{vw}}{\partial z} - \frac{\partial \overline{w^2}}{\partial y} + v\nabla^2 W \quad (5.12)$$

$$\frac{\partial}{\partial x}\left(\frac{\partial P_*}{\partial x}\right) = \frac{\partial}{\partial y}\left(\frac{\partial P_*}{\partial x}\right) = \frac{\partial}{\partial z}\left(\frac{\partial P_*}{\partial x}\right) = 0,$$

$$\therefore -\frac{1}{\rho}\frac{\partial P_*}{\partial x} = \frac{1}{\rho}\frac{\partial P}{\partial x} + g\sin\theta \equiv C\ (const) \quad (5.13)$$

5.7 Secondary current vectors

The secondary current vectors were calculated that the resultant of lateral and transverse direction velocity components by using the equation

Resultant vector = $\sqrt{V^2 + W^2}$ (5.14)

The following figure 5.16 to figure 5.19 are shown for secondary current vector for both geometry of rectangular and trapezoidal channel with smooth and roughened surface.

5.7.1 Rectangular Smooth Channel

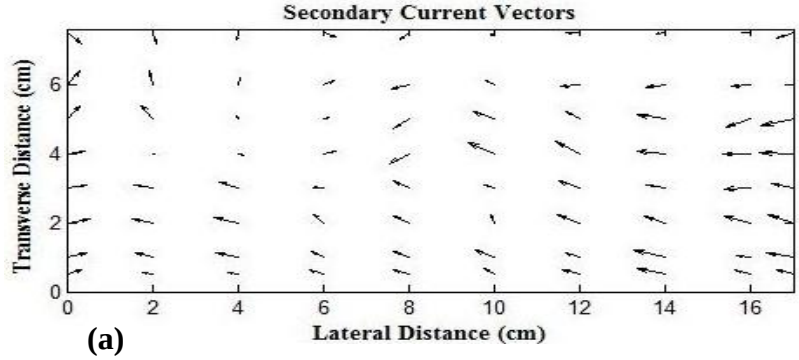

(a)

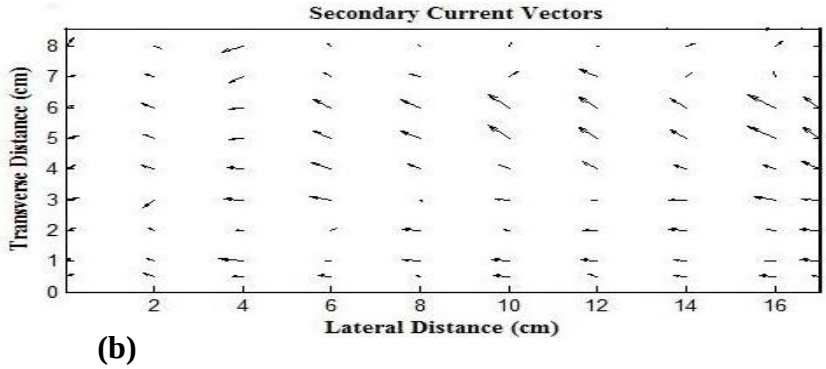

(b)

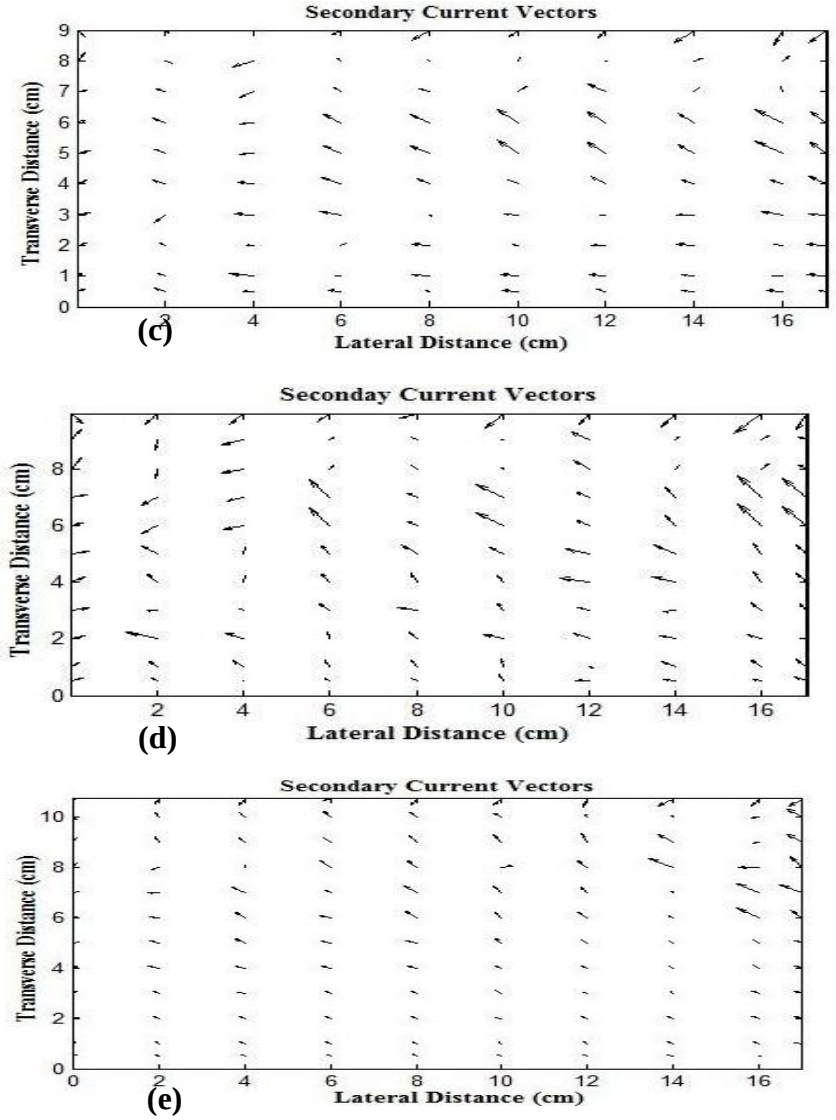

Figure 5.16: Secondary current vectors of different flow depths for rectangular smooth channel (a) 0.076m, (b) 0.0.83m, (c) 0.09m, (d) 0.099m, (e) 0.107m

Observations in Rectangular Smooth Channel

In this research work, left half of the channel is considered for evaluation of secondary currents shown in figure 5.16.The above velocity vector figures are showing that the cellular secondary currents induced due to velocity components of *V* and *W*. It was observed that maximum secondary currents are moving toward the vertical side wall from the centre of the channel. It also observed that few secondary currents are try to move away from the side wall due to the obstruction of flow obstructed by the boundary creates vortices. The magnitude of secondary current is quite small at boundary as compared to nearer the free surface due to the free movement of intermolecular particles in a flow field. Otherwise uniform in magnitude of secondary current has been observed at the central

region of the channel. As flow depth increases the magnitude of secondary flow also decreases respectively due to low effect of boundary friction at higher flow depths. So in rectangular channel formation of secondary cells are not clearly observable due to one zone of flow (i.e. constant flow domain) where less boundary and wall effects are affecting to the flow structures.

5.7.2 Trapezoidal Smooth Channel

Trapezoidal channel is the second geometry used in this research work to observe the effect of secondary current and formation of secondary cells different roughness. First it was considered that how a smooth trapezoidal channel created secondary current and secondary cells in the given channel. Left half of the channel has been taken in to consideration for all cases of trapezoidal channels also.

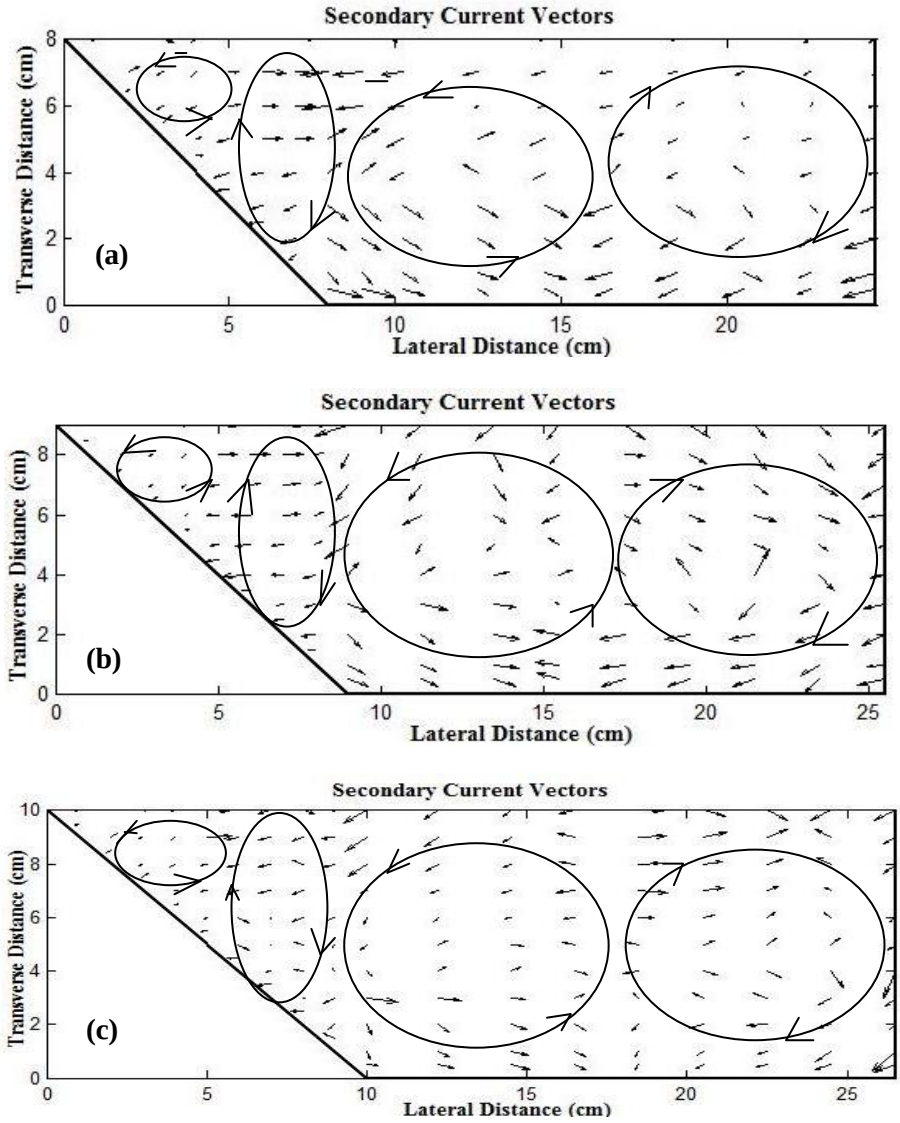

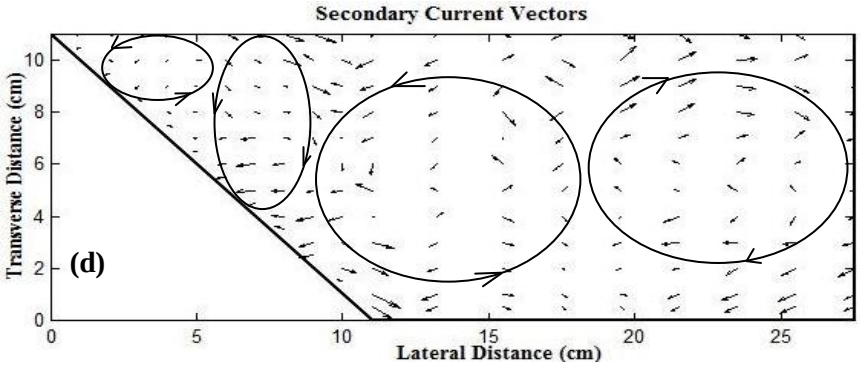

Figure 5.17 : Secondary current vectors of different flow depths for trapezoidal smooth channel (a) 0.08m (b) 0.09m (c) 0.10m (d) 0.11m

5.7.3 Trapezoidal Rough Channel (Type-1)

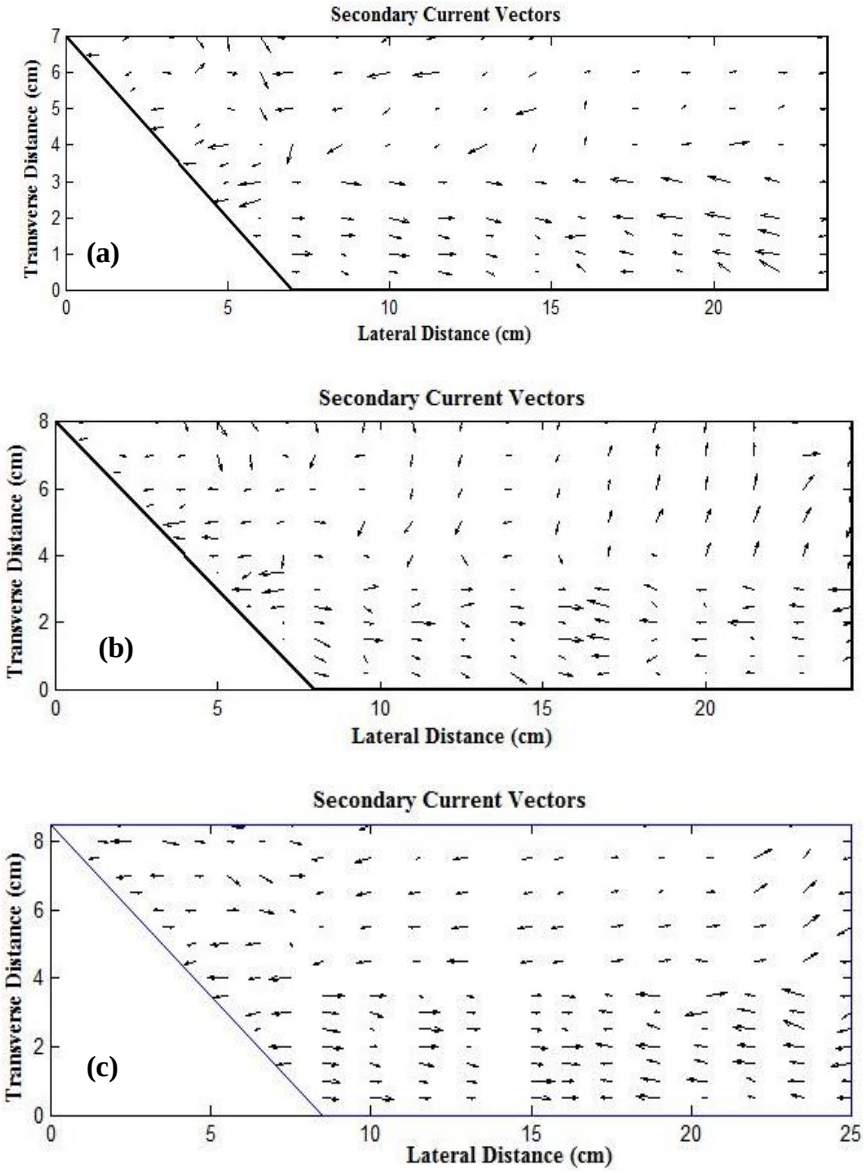

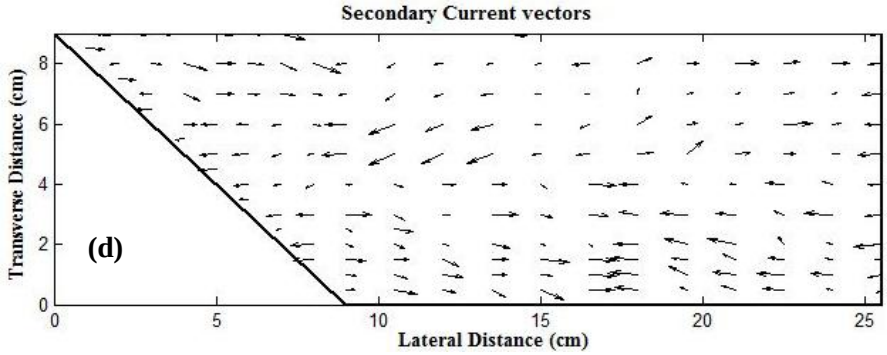

Figure 5.18 : Secondary current vectors of different flow depths for trapezoidal rough (type-1) channel (a) 0.07m (b) 0.08m (c) 0.085m (d) 0.09m

5.7.4 Trapezoidal Rough Channel (Type-2)

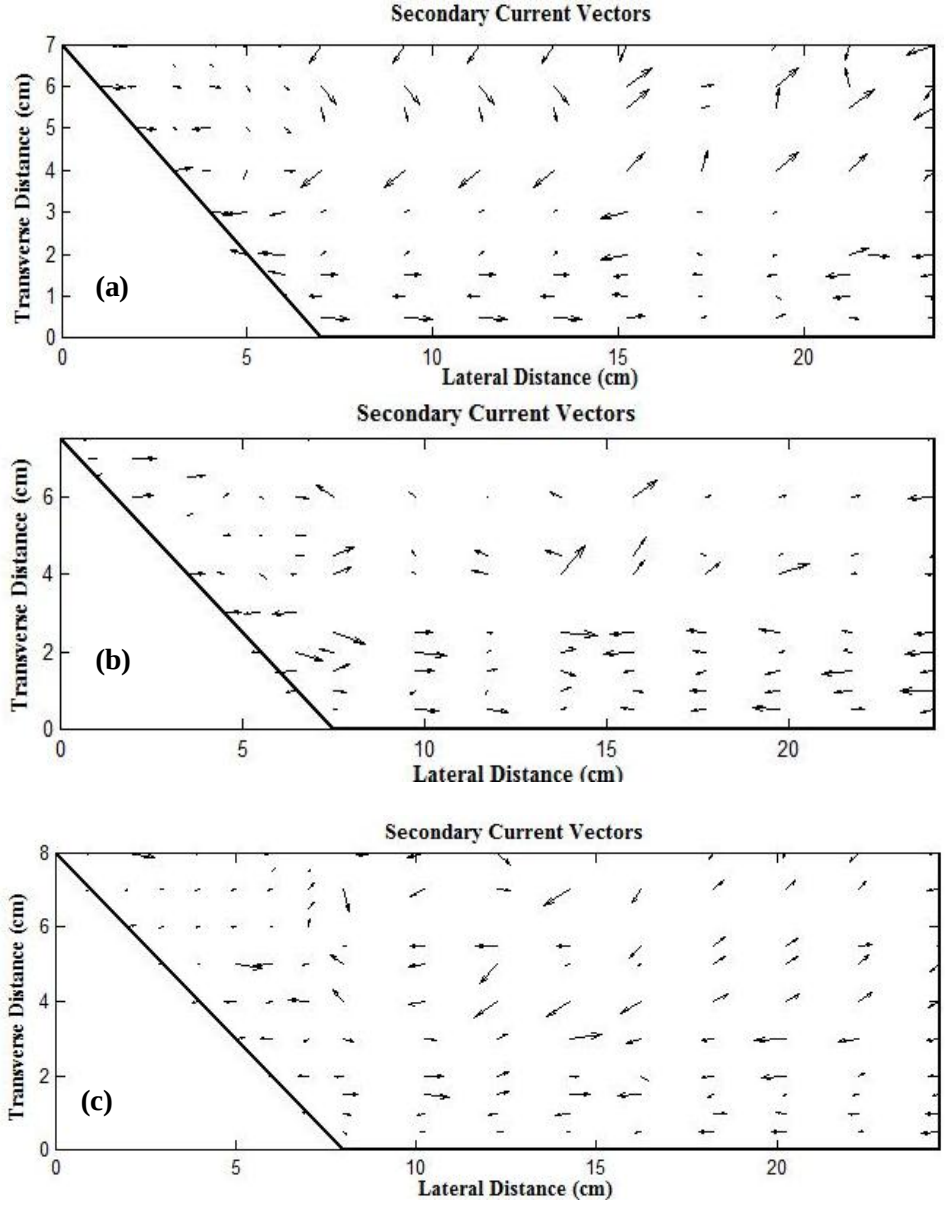

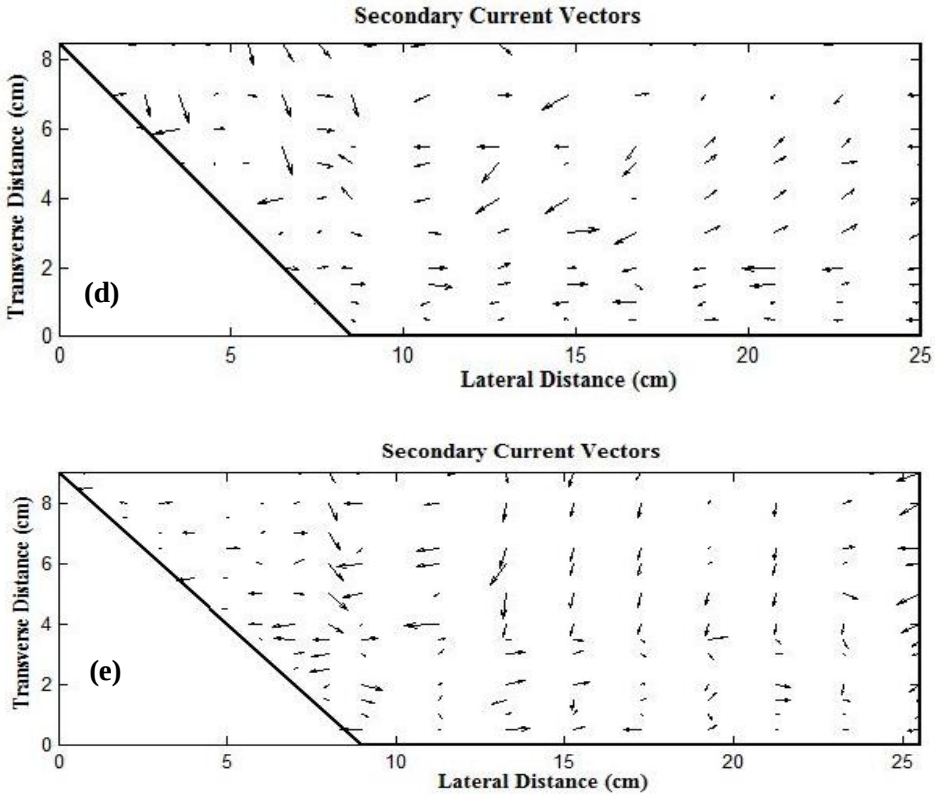

Figure 5.19 : Secondary current vectors of different flow depths for trapezoidal rough (type-2) channel (a) 0.07m (b) 0.075m (c) 0.08m (d) 0.085m (e) 0.09m

Observations in Trapezoidal Channel

- Formation of secondary cells due to secondary vector diagram plotted by taking the two fluctuating velocity of transverse and vertical direction are shown in figure 5.17. The secondary cells are produced with reverse rotating cells and numbers of the cells are four in the left half of the channel. For figure 5.18 and 5.19 same type of secondary cells are produced as shown in trapezoidal smooth channel concerning secondary current behaviours, but size of secondary cells may different for rough trapezoidal channels.
- It has been observed that numbers of secondary cells of reverse rotating cells in constant flow domain are two and another cell of clockwise rotating cell near the interface between constant and variable flow domain due to large momentum transfer between two different flow zones which divided the flow in to two parts with an inclined interface. Again another cell has been produced due to wall effect and water molecules with counter-clockwise rotation.

- The above velocity vector figures are showing that the cellular secondary currents induced in two different regions. The width of corner (side wall) secondary cell spread up to the line between the interface of side wall and bed. The maximum strength is always observed at the interface between the main channel and the side wall in trapezoidal channel for smooth and rough cases. The magnitude of secondary flow in the main flow region must be higher than that in the near wall region. The secondary currents are larger near the bed than the free surface.
- The side wall secondary currents are spreading to the width of 1.19 H, 1.17 H, 1.13 H and 1.12 H in 8 cm, 9 cm, 10 cm and 11 cm of flow depth respectively from left most corner for smooth channel. The side wall secondary currents are spreading to the width of 1.357 H, 1.375 H, 1.353 H and 1.389 H in 7 cm,8 cm,8.5 cm and 9 cm of flow depth respectively from left most corner for rough channel.
- The secondary current cells have a greater effect on τ_b than on U_d since the perturbations in the former distribution are more pronounced. The number of secondary current cells is found to depend on the channel aspect ratio.
- As per Tominaga et. al. (1989) also observed that the numbers of secondary cells are produced with the effect of flow aspect ratio for simple prismatic channels. For 2b/H $\leq$ 2.2, the number of secondary current cells in a simple trapezoidal channel was found to be equal to three, with two located over the side slope region and one over the flat bed region. For 2b/H >2.2, the number of secondary current cells in a simple trapezoidal channel was found to be equal to four, with two located over the variable flow domain (i.e. side slope region) and two over the constant flow domain (i.e. flat bed region). So from experimental observation we observed same numbers of secondary cells were produced in respective regions.
- The actual pattern of secondary current cells in a simple rectangular channel can be replaced by three equivalent cells, spread over the half width of the channel in order to simulate the U_d distribution accurately. The sign of secondary current term, Γ should be determined from the location and rotation of the secondary current cells.

Chapter-6

Methodology and Model Development

6.1 Shiono and Knight Method (SKM)

6.1.1 Background

The Shiono and Knight method (SKM) (1988; 1990; 1991) is a lateral distribution method based on the depth averaged Reynolds Averaged Navier-Stokes (RANS) equations. The quasi 2-D model includes some of the key 3-D flow structures that occur in rivers and simple or compound channels and is able to predict the lateral variation of depth-averaged velocity and boundary shear distributions within natural river channels of any cross section shape. Its promising results for both laboratory channels and natural rivers have been led it to being adopted by the UK's Environmental agency for use in its 'Conveyance and Afflux Estimation System' software which is also popularly known as CEAS or CES software. (see also McGahey, 2006; McGahey et al.,2006;2008)

6.1.2 Governing Equation

The simplified form of Navier-Stokes equation in steady uniform flow is as follows:

$$\rho\left[v\frac{\partial u}{\partial y}+w\frac{\partial w}{\partial z}\right]=\rho g sin\theta+\frac{\partial \tau_{yx}}{\partial y}+\frac{\partial \tau_{zx}}{\partial z} \quad (6.1)$$

i.e., secondary flow = weight force +Reynolds stresses(lateral + vertical),where *u, v, w* are the local velocities in x (along the flow) , y (lateral) and z (vertical) directions respectively;$S_0= sin\theta$ is the longitudinal slope of bed;τ_{yx} and $\tau_{zx}$are the Reynolds stresses on plane perpendicular to the y and z directions respectively; ρ-the water density, and g is the gravitational acceleration.

Shiono Knight integrated the Navier-Stoke's equation that is the momentum equation over the flow depth *H*, mainly to find out the depth-averaged velocity distribution. The method of solving this equation is known as Shiono-Knight method. They provided a analytical solution for this model from which both depth-averaged distribution and boundary shear stress distribution can be simply found out.

Integrating the equation (6.1) over a flow depth *H*, Shiono and knight obtained a quasi 2-D equation indicated in equation(6.2)

$$\rho g H S_0 - \rho \frac{f}{8} {U_d}^2 \sqrt{1+\frac{1}{s^2}} + \frac{\partial}{\partial y}\left\{\rho \lambda H^2 \left(\frac{f}{8}\right)^{1/2} U_d \frac{\partial U_d}{\partial y}\right\} = \frac{\partial H(\rho UV)_d}{\partial y} \quad (6.2)$$

Where *H* is the depth of water in channel,$U_d$is depth averaged velocity components in *x* direction, S_0 is longitudinal bed slope, *f* is friction factor,*s* is side slope of channel and $\lambda$is dimensionless eddy viscosity.Subscript '*d*' denotes that the term is depth-averaged.

The right hand side of equation (6.2)is taken as secondary flow effect, which is also known as transverse gradient of secondary flow. Γ is the symbol to define the secondary flow parameter.

6.2 Calibrating Coefficients

The three calibrating coefficients are *f*, λ,Γ are defined as follows:

6.2.1 Darcy-Weisbach friction factor (*f*)

$$f = \frac{8gn^2}{R^{1/3}} \quad (6.3)$$

Also calculated by using following equation:

$$f = \frac{8\tau_b}{\rho {U_d}^2} \quad (6.4)$$

6.2.2 Eddy Viscosity Coefficient (λ)

Turbulent flow is the flow in which random motion of smaller or larger masses of the fluid is superimposed upon some simple pattern of flow. So in a flow the molecular viscosity with respect to turbulence is called eddy viscosity.Dimensionless eddy viscosity coefficient,λ depends on local shear velocity or average boundary shear velocity and flow depth *H*.

Then λ is calculated by using the following equations:

$$\tau_b = \left(\frac{f}{8}\right)\rho {U_d}^2 \quad (6.5)$$

$$\bar{\tau}_{yx} = \rho\, \bar{\in}_{yx} \frac{\partial U_d}{\partial y} \quad (6.6)$$

$$\overline{\epsilon}_{yx} = \lambda U_* H \tag{6.7}$$

$$\lambda = \frac{\overline{\epsilon}_{yx}}{U_* H} \tag{6.8}$$

6.2.3 Secondary flow parameter (Γ)

Secondary flow parameter Γ is defined by the equation:

$$\Gamma = \frac{\partial}{\partial y}[H(\rho UV)_d] \tag{6.9}$$

6.2.4 Secondary flow coefficients

Secondary flow coefficients (K_1 and K_2) were evaluated from experimental data and then calibrated. After calibration the obtained value of K_1 and K_2 with flow aspect ratio (2b/h) are plotted in figure

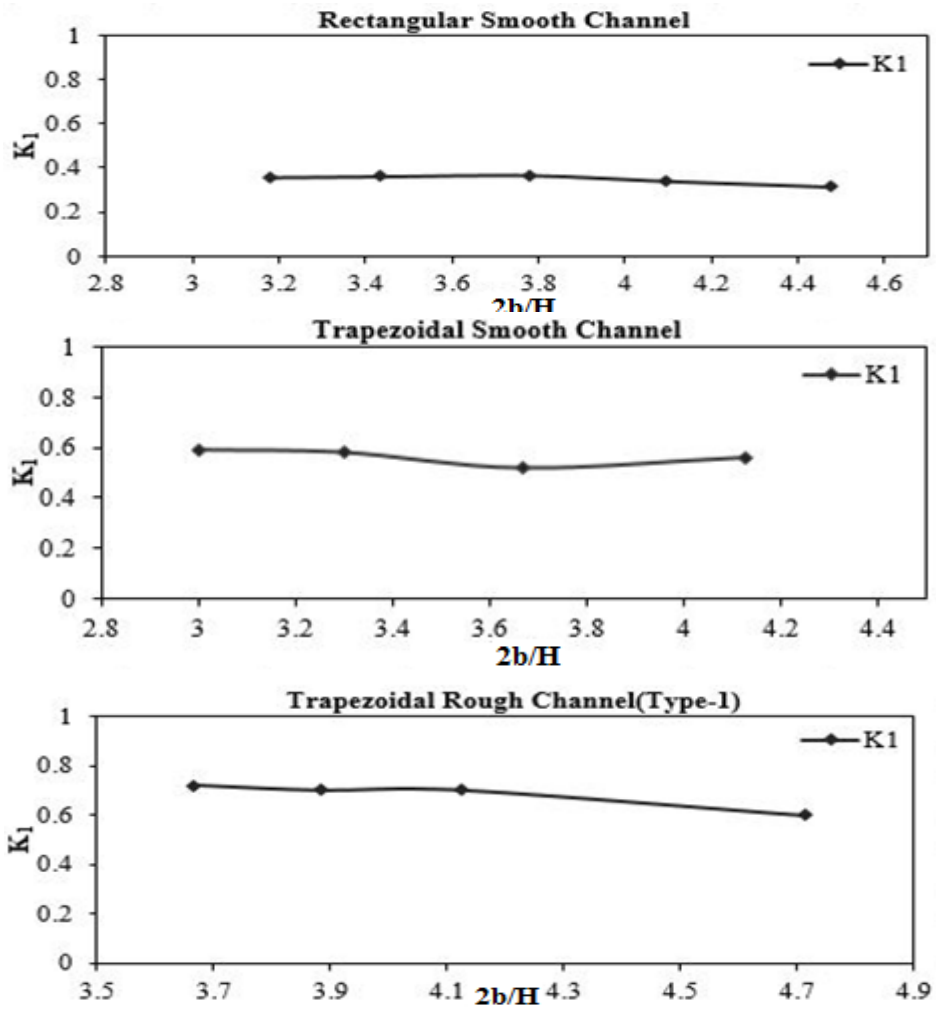

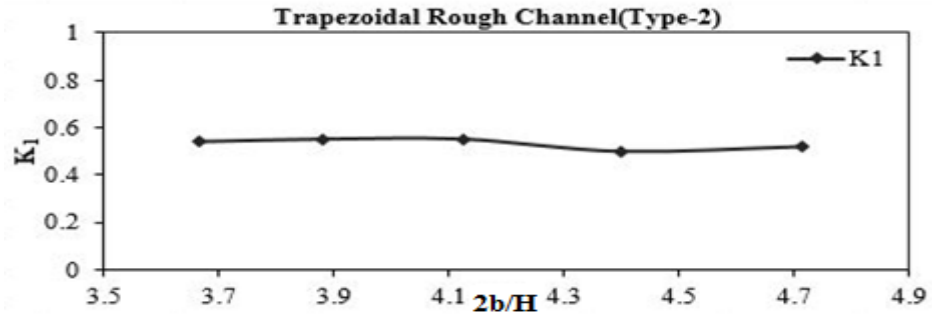

Figure 6.1: Variation of Secondary coefficient K_1 with aspect ratio (2b/H)

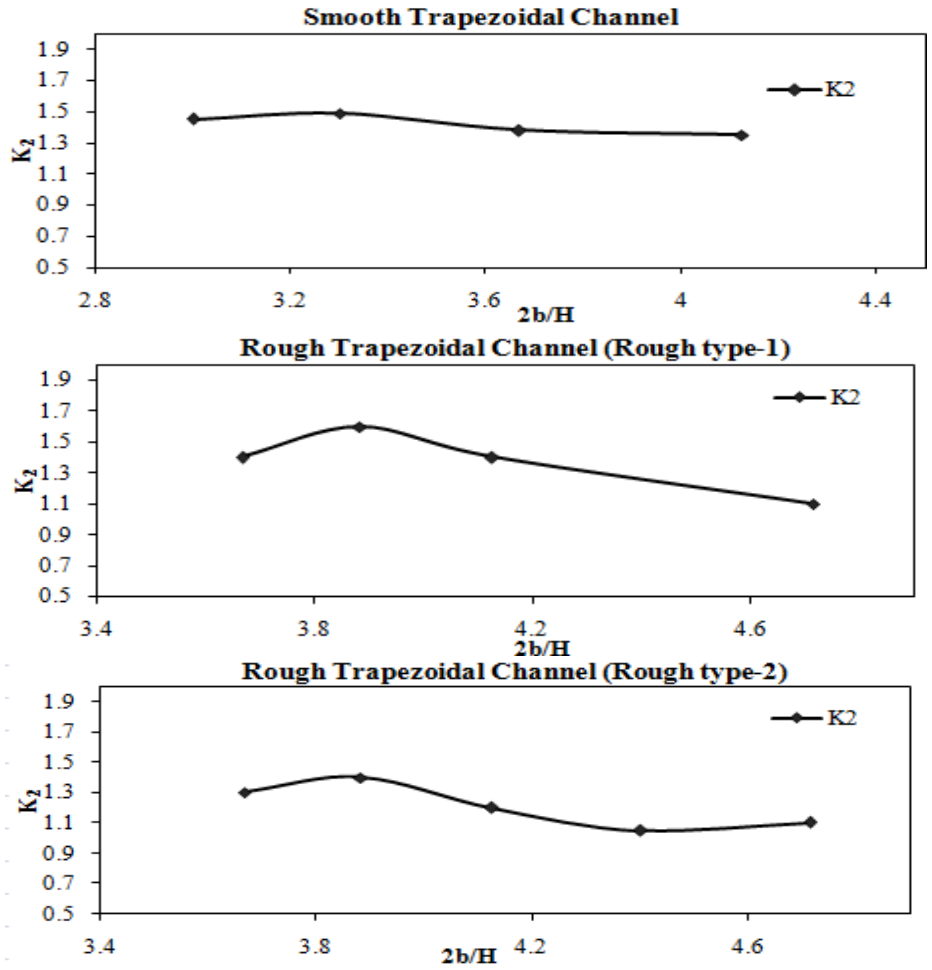

Figure 6.2: Variation of Secondary coefficient K_2 with aspect ratio (2b/H)

Secondary flow coefficients and eddy viscosity of experimental channels with flow aspect ratio are tabulated in table 6.1. Eddy viscosity values were taken as constant for respective flow depths in although it was varied with a lateral direction of channel. For calibrating purposes it was considered a single value for a particular flow depth. Eddy viscosity was dependent on flow depth and roughness type in simple prismatic channels observed in this work

Table 6.1: Secondary flow co-efficient and eddy viscosity of experimental channels

Geometry Type	Roughness Type	Aspect Ratio (2b/H)	Secondary Flow Coefficients		λ
			Constant Flow domain(K_1)	Variable Flow domain (K_2)	
Rectangular	Smooth	3.178	0.356	-	0.74755
Rectangular	Smooth	3.434	0.360	-	-0.3517
Rectangular	Smooth	3.778	0.365	-	-0.1688
Rectangular	Smooth	4.096	0.340	-	-0.3298
Rectangular	Smooth	4.474	0.315	-	-0.0577
Trapezoidal	Smooth	3.000	0.590	1.45	-0.02211
Trapezoidal	Smooth	3.300	0.580	1.49	0.053194
Trapezoidal	Smooth	3.667	0.520	1.38	0.13204
Trapezoidal	Smooth	4.125	0.660	1.35	-0.15541
Trapezoidal	Rough(Type-1*)	3.667	0.720	1.4	0.266497
Trapezoidal	Rough(Type-1)	3.882	0.700	1.6	-0.37075
Trapezoidal	Rough(Type-1)	4.125	0.700	1.4	-0.14804
Trapezoidal	Rough(Type-1)	4.714	0.600	1.1	-0.19146
Trapezoidal	Rough(Type-2*)	3.667	0.540	1.3	0.083642
Trapezoidal	Rough(Type-2)	3.882	0.550	1.4	0.400802
Trapezoidal	Rough(Type-2)	4.125	0.550	1.2	-0.18408
Trapezoidal	Rough(Type-2)	4.400	0.500	1.05	-0.07343
Trapezoidal	Rough(Type-2)	4.714	0.520	1.1	0.433024

Type-1* small gravel of size 7 mm to 20 mm (n=0.02),Type-2* plastic mat of thickness 15mm (n=0.024)

6.3 Multi Variables Regression Analysis

6.3.1 General

In statistical modelling, regression analysis is a statistical process for estimating the relationships among variables. It includes many techniques for modelling and analysing several variables, when the focus is on the relationship between a dependent variable and one or more independent variables (or predictors). More accurately, regression analysis helps to understand how the value of dependent variable changes when any one of the independent variables is varied, while the other independent variables are kept fixed.

Regression analysis is widely used for prediction and forecasting. Also used to understand which among the independent variables are related to dependent variable, and to explore the forms of these relationships.

Multiple variable regression analysis is a powerful technique used for predicting the unknown value of a variable from the known value of two or more variables. By multiple regression, we can model with just one dependent and two or more independent (exploratory) variables. The variable whose value is to be predicted is known as dependent variable and the variables whose known values are used for prediction are known independent (exploratory) variables.

Once a multiple regression equation has been developed, then one can check how good that model (in terms of predictive ability) by examining the coefficient of determination (R^2). R^2value always lies between 0 and 1.

Multiple regression analysis is used when one is interested in predicting continuous dependent variables from a number of independent variables.

6.3.2 Model Development

In this present study, a number of possible single regression models considering different one to one relationships (e.g., exponential, power, linear or logarithmic) between dependent parameter and independent parameters were tested. Based on a criteria, the selection of best regression models were achieved i.e., the highest coefficient of determination (R^2) values. Two preferred input variables were useful for this study since each variable was controlling the shear distribution. Multi linear regression analysis (MLA) complies these two independent variables with model up the dependent variable. Finally, through multi linear regression analysis, the resulted output with high coefficient of determination.

The experimentally measured velocity associated with the both rectangular and trapezoidal channel with different roughness of smooth and rough configuration. The independent variables were two dimensionless parameters defined using the cross-section geometric dimensions (*b* and *y*) and flow depths (*z* and *H*). Experimental velocity data were arranged and then drawn the vertical and lateral velocity distribution along the cross-section of channel at desired locations (i.e. 0.2H,0.4H,0.6H,.08H and 0.95H). Then for vertical velocity profile the logarithmic equations were obtained for every position along the lateral distance for all flow depths. Then one equation would be taken where R^2 is

maximum (i.e.R^2≈0.95) among all the vertical velocity profiles, that reliable profile was taken for regression analysis. For lateral velocity profile five different equations of power function were taken whose R^2 is maximum(i.e.R^2≈0.99,0.96,0.97,0.94 and 0.96 for 0.2H,0.4H,0.6H,0.8H and 0.95H respectively). These independent parameters were used as ratio of $\left(\frac{y}{b}\right)$and $\left(\frac{z}{H}\right)$ which required for finding the ratio of $\frac{U}{\bar{U}}$.Then local velocity *U* was determined which is required to find the depth averaged velocity distribution for all given depths of NITR channel, FCF channel and other researcher's data. So finally five equations were developed by multi-variable regression model given in equation 6.10 to equation 6.14.These equations obtained from multi-variable regression analysis were given large R^2 value for all depths of NITR, FCF and other researcher's data. The multi-variable regression model was tested for reliability and the error analysis also done with actual data which is obtained from experiment.

$$\left(\frac{U}{\bar{U}}\right)_{0.2H} = 0.44073 - 0.01678\ln\left(\frac{z}{H}\right) + 0.55092\left(\frac{y}{b}\right)^{0.1577} \quad (6.10)$$

$$\left(\frac{U}{\bar{U}}\right)_{0.4H} = 1.00863 + 0.38096\ln\left(\frac{z}{H}\right) + 0.4595\left(\frac{y}{b}\right)^{0.2473} \quad (6.11)$$

$$\left(\frac{U}{\bar{U}}\right)_{0.6H} = 0.56066 - 0.207178\ln\left(\frac{z}{H}\right) + 0.4818\left(\frac{y}{b}\right)^{0.2725} \quad (6.12)$$

$$\left(\frac{U}{\bar{U}}\right)_{0.8H} = 0.503536 - 0.03894\ln\left(\frac{z}{H}\right) + 0.6823\left(\frac{y}{b}\right)^{0.2114} \quad (6.13)$$

$$\left(\frac{U}{\bar{U}}\right)_{0.95H} = 1.2633 + 1.40896\ln\left(\frac{z}{H}\right) + 0.5683\left(\frac{y}{b}\right)^{0.1305} \quad (6.14)$$

6.4 Validation of Proposed Model

In this section the predicted model has been compared and validated with experimental or actual data with SKM, FCF data series and Tominaga et al. (1989) data series successively. Validation of proposed model has been done for check the approximation of the model with other researcer's method and with other available data sets. This secion has been presented the comaprison of experimental (or actual) results, SKM with proposed or predicted model in rectangular and trapezoidal cases with smooth and rough surfaces and also predicted model has been validated with FCF (series A) and Tominaga et. al (1989) data series with inabnk flow.

6.4.1 Smooth Rectangular Channel

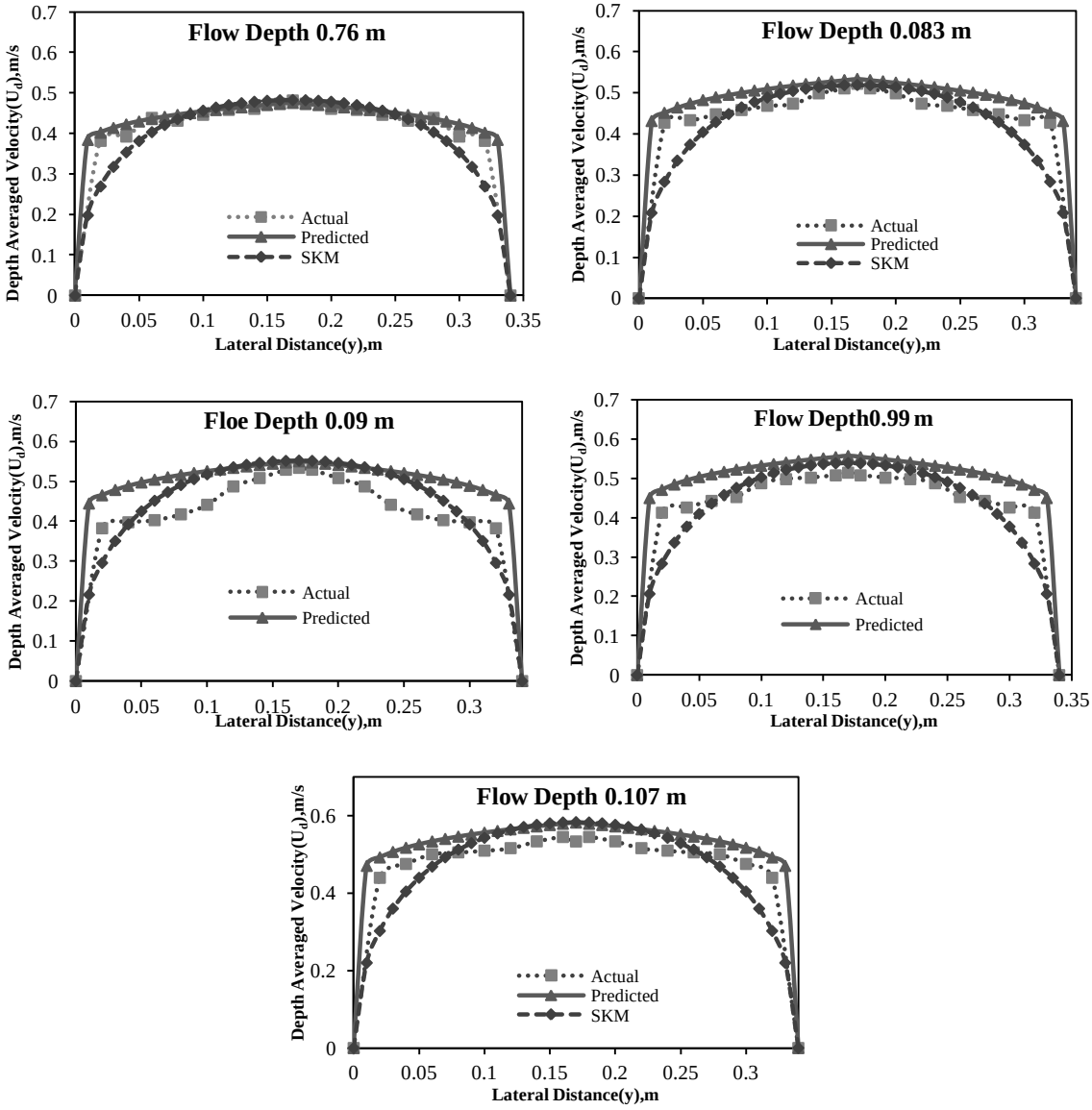

Figure 6.3: Depth averaged velocity of different flow depths

6.4.2 Trapezoidal smooth Channel

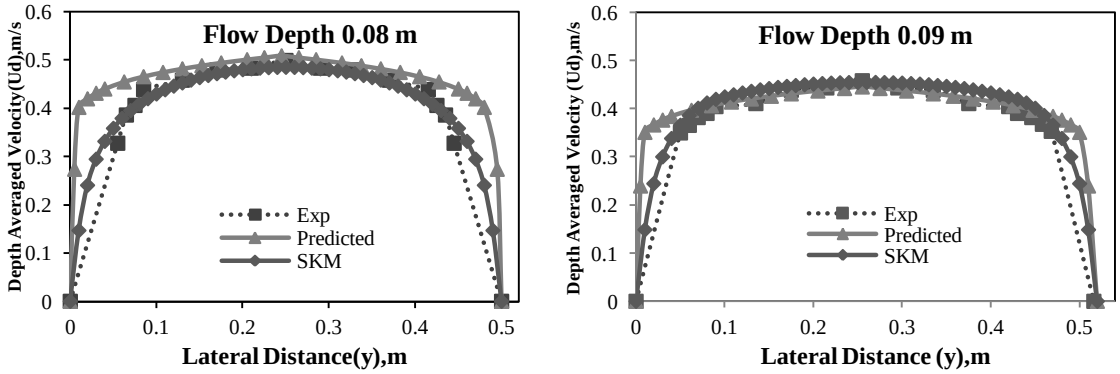

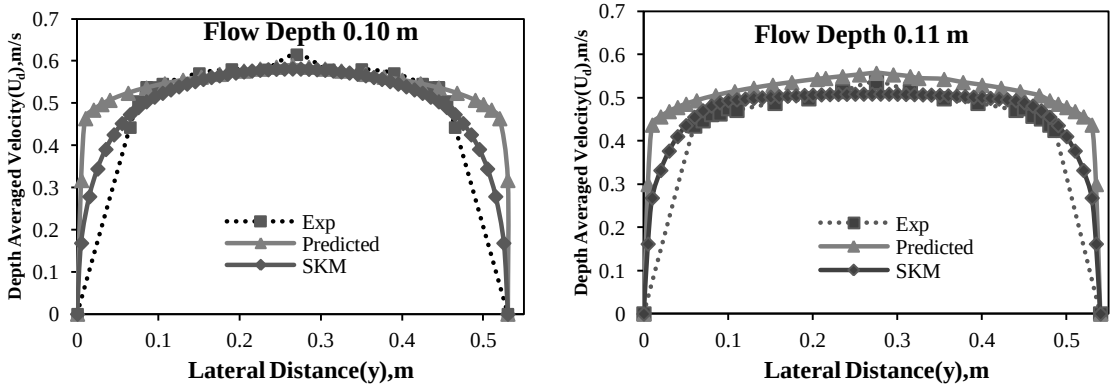

Figure 6.4: Depth averaged velocity of different flow depths

6.4.3 Trapezoidal Rough Channel (Rough type-1)

Rough type-1 used roughness material as small gravel of size varied 7mm to 20 mm with manning's *n* value was 0.02. The predicted model was compared with experimental data series and also well compared with SKM.

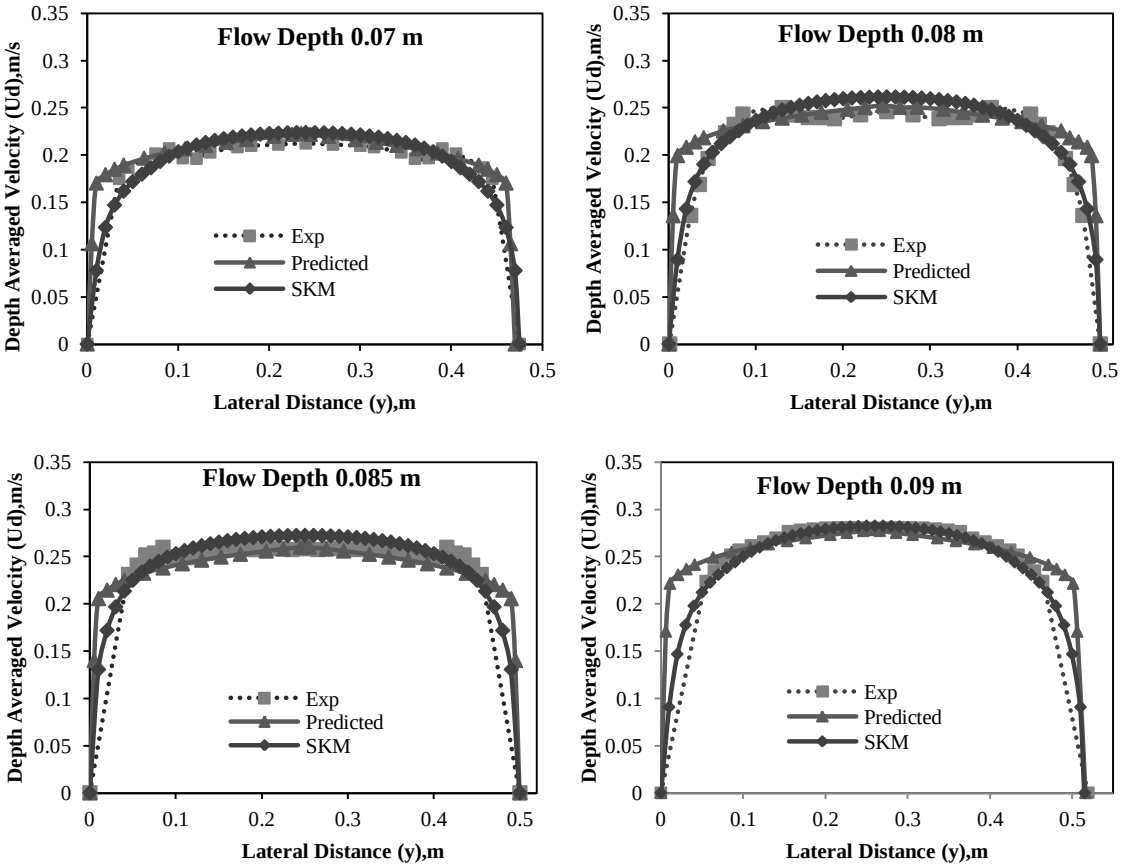

Figure 6.5: Depth averaged velocity of different flow depths

6.4.4 Trapezoidal Rough Channel (Rough type-2)

Trapezoidal rough channel (type-2) used plastic mat as roughness material of thickness 15 mm with manning's *n* was 0.024. The predicted model was compared with experimental data series and also well compared with SKM. The depth averaged velocity for different flow depths (i.e. H=0.07m, 0.075m, 0.08m .085m, 0.09m) along the lateral distance are shown in figure 6.6.

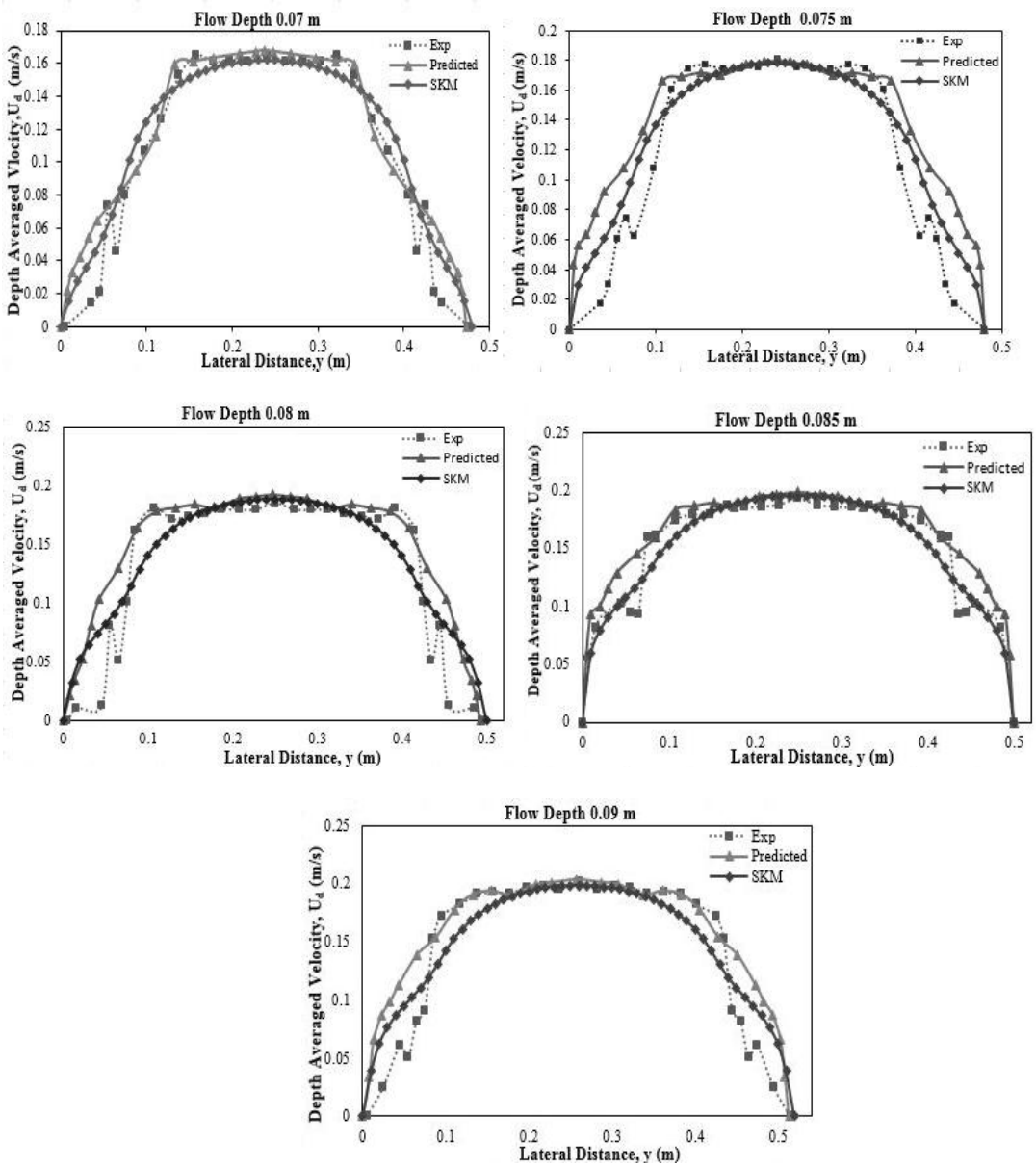

Figure 6.6: Depth averaged velocity of different flow depths

6.5 Discussions

- The model has been applied to the present experimental channels having both smooth and rough surfaces. The capability of developed equations has been verified with experimental finding and has been also well compared with SKM. SKM shows good prediction of depth averaged velocity near the central region of the channel fails to provide at side of the channel. SKM also found under predict depth averaged velocity near the wall and over predicts near the central region in all cases at lower depths.
- The present equation is better than SKM, however the present equation is found over predict at higher flow depths and shows a good agreement of depth averaged velocity at lower flow depths. This happened for both rectangular and trapezoidal cases.
- For rough channels SKM was again found to over predict near central region and also over predicts near well region except junction between bed and side wall. Near the junction there is a transition at over and under predictions. For higher flow depths of rough channels SKM under predict the depth averaged velocity between junctions of trapezoidal channels and over predicts along the side walls.

6.6 FCF Channel Series and Tominaga et al (1989) data series

The UK Flood Channel Facility (FCF) was originally set up by the Science and Engineering Research Council (SERC) at Hydraulic Research, Wallingford in 1986. The main aim of the studies in the FCF was to investigate the flow phenomena in rigid boundary and skewed channel (Series A), rigid boundary meandering channel (Series B) and loose boundary of straight and meandering channel (Series C). This experimental investigation would allow academics or researchers to study the conveyance of river channels, one stage channels (i.e. Flow considered in main channel only), two stage channels and floodplain behaviour, river flooding issue and sediment transport and morphology (Ervine et al., 2000; knight et al.,1999).

The UK Flood Channel Facility (FCF) is a large scale national facility for undertaking experimental investigations of inbank and overbank flows in rivers. The FCF was 56 m long and 10 m wide with usable length of 45m. The longitudinal bed slope was 1.027×10^{3}.

The entry of flow was carefully controlled by an inlet weir and stilling boom, and downstream water levels controlled by 5 tailgates. The flow was re-circulating pumps with maximum discharge of 1.1 m^3/s. The photograph of experimental channel and layout of FCF shown in figure 6.7.

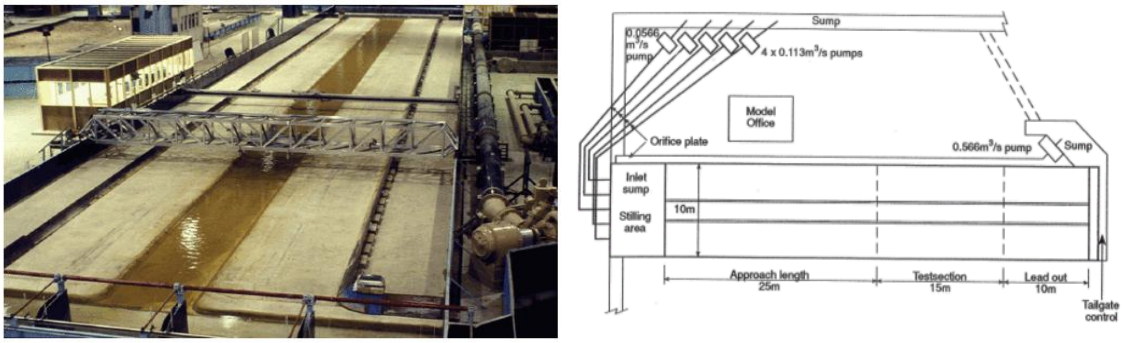

Figure 6.7: Photo of experimental channel and layout of SERC Facility at Wallingford, UK

Tominaga et. al (1989) experimental set up

The experimental apparatus and procedure for Tominaga et al. (1989) were mentioned below. Experiments were conducted in a tilting flume with 12.5 m length and 0.4m×0.4m cross-section. A fully developed, uniform flow was established at the test section 7.5 m downstream from the entrance of channel by adjusting the bed slope and the moveable weir at the channel bed. Filters were set up in the settling tank to remove the suspended impurities. Experiments were carried out into three groups. The first group consisted of experiments in smooth rectangular open channels (Tominaga and Ezaki (1987)). While channel width of channel *B* was fixed, the flow depth *H* was changed in order to examine the effect of aspect ratio *B/H* on secondary currents. The second and third groups are consisted of smooth and rough trapezoidal channel respectively. The details of geometrical and hydraulic parameters of Tominaga et. Al. (1989) has been used in this present study.

Table 6.2: Details of geometrical and hydraulic parameters of Tominaga et.al. (1989) used

Case	Channel Geometry	Channel width, *B*(m)	Flow Depth, *H*(m)	Discharge, *Q* m^3/s	Aspect ratio. $A_r=B/H$	Mean Velocity, U_m(m/s)	Bed slope
S2	Rectangular	0.4	0.1015	7.58	3.94	0.1868	0.000138
T13	Trapezoidal	0.248	0.11	10.55	2.2	0.3936	0.000359

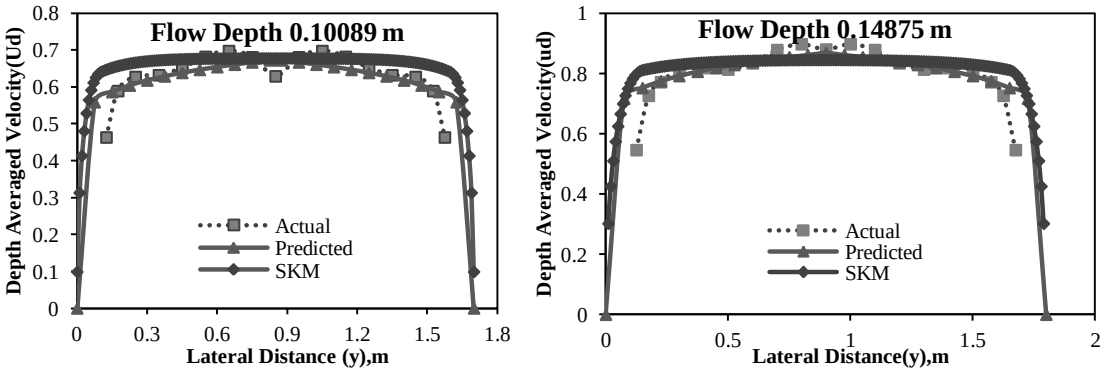

Figure 6.8: Depth averaged velocity of FCF Channel series of inbank conditions

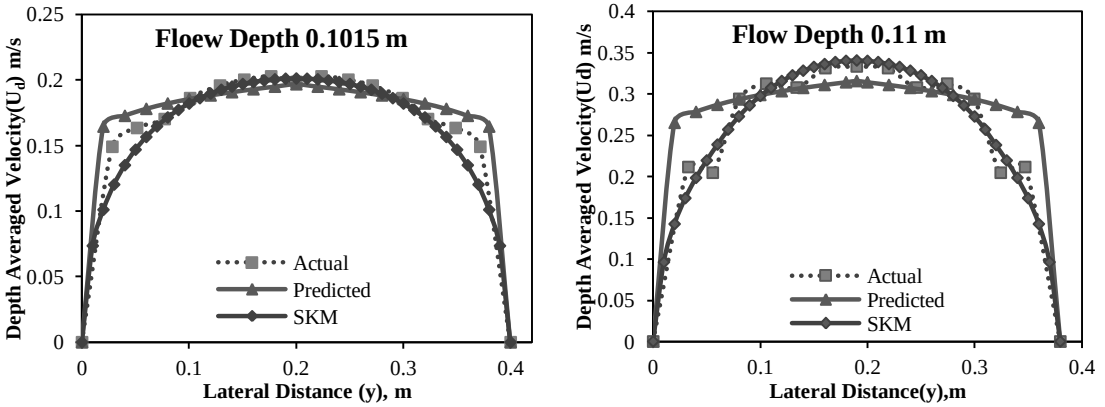

Figure 6.9: Depth averaged velocity of Tominaga et al.(1989) series of inbank conditions

6.7 Application of Model to Natural River Data Sets

A new model is examined as efficient if it can predict accurately when apply to field data. Applications of this model to two natural river data sets namely Senggai (B) and Senggai are presented in this section. These two natural rivers located in Kuching, the capital city of Sarawak state, Malaysia. The morphological cross-sections of rivers are presented in figure 6.10 and 6.11. It presents that these rivers are almost straight and uniform in cross-section. But the configurations of natural rivers are generally unsymmetrical and uneven surface compared to laboratory channels. So it is a very rigorous task to validate the developed model with any natural rivers. The geometrical perimeter and hydraulic area of the rivers are changed to an accessible shape that the original perimeter and original area of cross section remains same. The geometric, hydraulic and surface properties of natural river data sets are mentioned in table 6.3.

Table 6.3: Geometric properties and surface conditions used for natural river data

Geometrical Properties	River Senggai(B)	River Senggai
Bank Full Depth,h(m)	1.306	1.06
Top Width,T(m)	5.285	5.5
Bed Slope(S_0)	0.001	0.001
Surface Condition(main channel)	Erodible Soil	Erodible Soil
Surface Condition(side bank)	Long Vegetation	Erodible Soil
Manning's *n*(main channel)	0.082	0.082
Manning's *n*(side bank)	0.25	0.082

Figure 6.10: Morphological cross-section of River Senggai B (Hin et al. 2008)

Figure 6.11: Morphological cross-section of River Senggai (Hin et al. 2008)

6.7.1 River Senggai (B)

River Senggai (B), actual cross sectional geometry shown in figure 6.12. It was quite even, so this cross-section can be considered directly for validation. The observed depth averaged velocity(U_d) along the lateral cross section of river Senggai (B) for two inbank depths of flow (H=0.698m and 1.088) found from previous literature are considered for validation of the new approach. The value of lateral U_d resulted from present approach

along with the values from SKM for these typical depths have been compared with field measurements. It is found that two methods approximately predict the $U_d$value nearer to observed values.

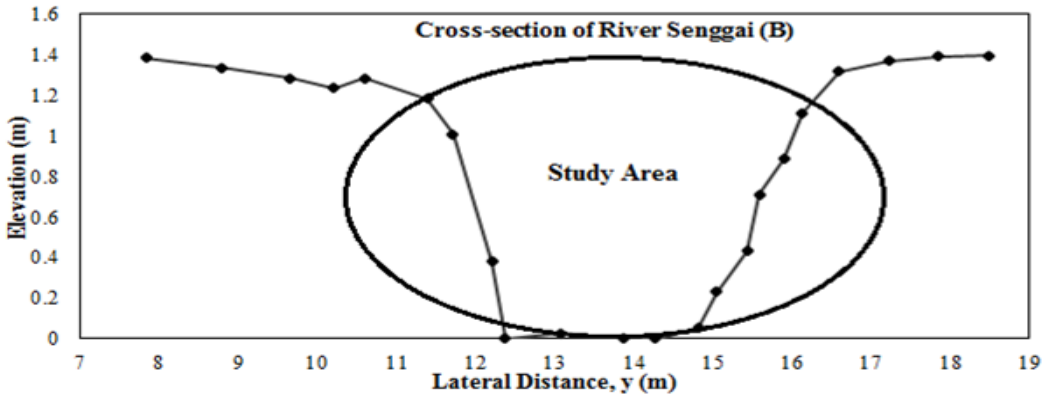

Figure 6.12: Actual Cross-section of River Senggai (B)

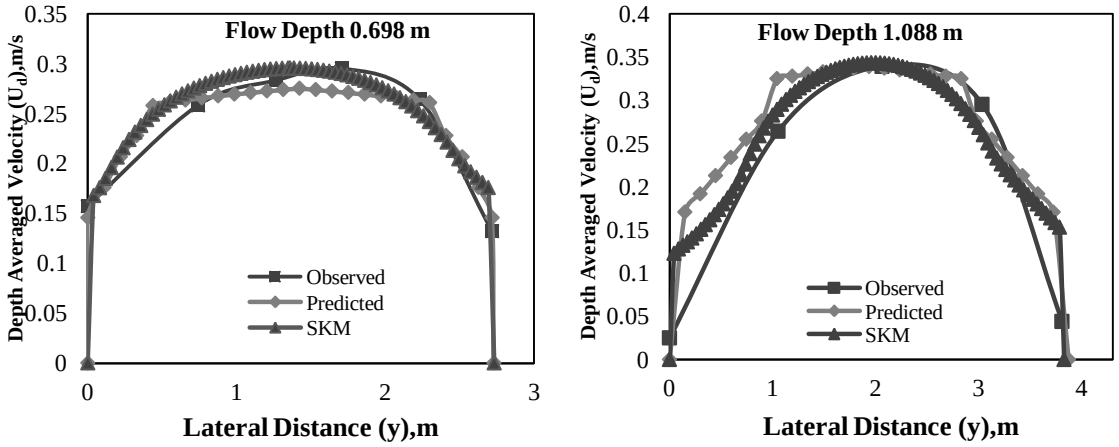

Figure 6.13: Depth averaged velocity of river Senggai (B)

6.7.2 River Senggai

River Senggai is irregular in its geometry mainly in the bed of the main channel. So it was quite difficult to take approximate depth from actual cross-section of river Senggai (figure 6.14) for comparison with predicted model and SKM. So to overcome from this difficulty a modified geometry was considered with approximate same perimeter and same cross-sectional area as compared with actual cross-sectional geometry shown in figure 6.15.

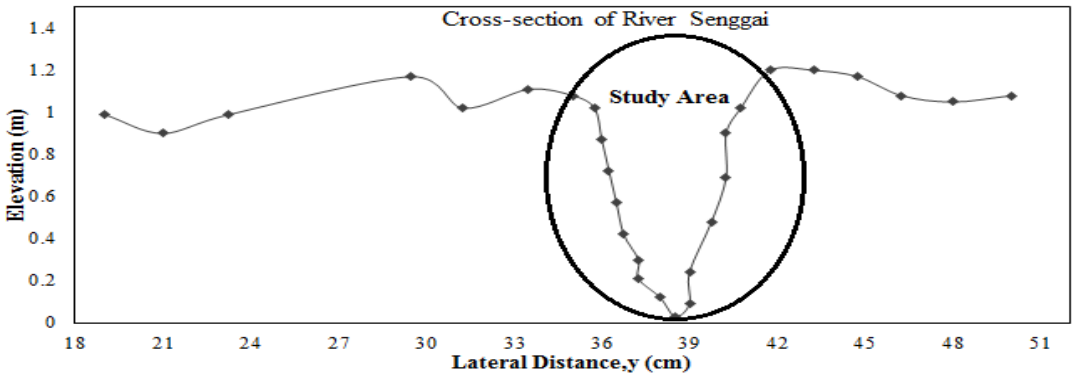

Figure 6.14: Actual Cross-section of River Senggai

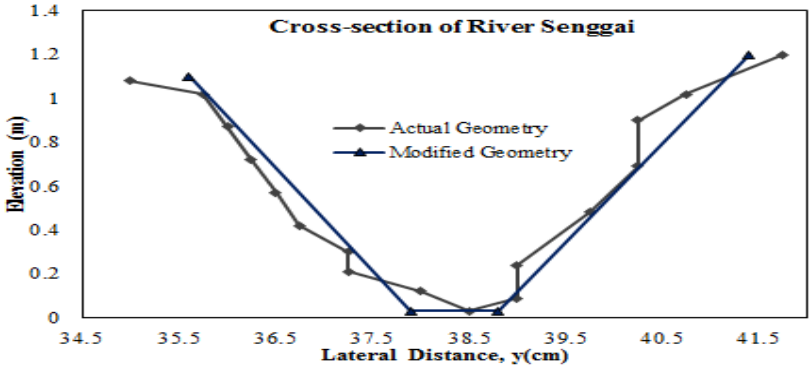

Figure 6.15: Modified Cross-section of River Senggai equivalent to actual area

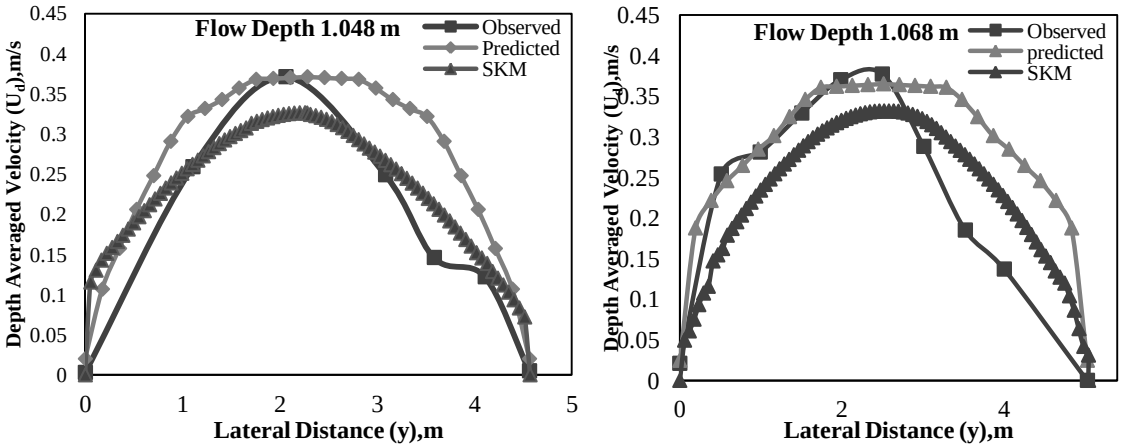

Figure 6.16: Depth averaged velocity of river Senggai

River Senggai is very irregular in cross sectional geometry. So the observed $U_d$value is uneven throughout the cross section. The observed depth averaged velocity(U_d) along the lateral cross section of river Senggai for two inbank depths of flow (H=1.048m and 1.068) found from previous literature are considered for validation of the new approach. The value of lateral U_d resulted from present approach over estimates the observed values.It has been also observed the SKM is found to under estimate the observed values.

Chapter-7

Conclusions and Scope of future work

7.1 Conclusions

Experimental investigation has been carried out in different smooth and rough channels having both rectangular and trapezoidal cross section to study the secondary flow phenomena in an open channel flow. The analytical model of SKM requires three appropriate calibrating coefficients for solution. The dependency of these parameters on the prophesy of depth averaged velocity are analysed and observed. Reviewing all the aspects regarding these parameters some conclusions are made and summarised below:

1 Variation of eddy viscosity (λ) along the lateral direction of the channels were observed in rectangular and trapezoidal channels with smootha nd rough surfaces. It was observed that the variation in magnitude of λ for rough channels higher than compared to the smooth channels.In smooth open channels variation of λ was nearly constant along the lateral direction except at the side wall region (where applicable,i.e. in case of trapezoidal cases) for different flow depths. Variation of λ in rough open channels were higher as compred to the smooth open channel of same geomety.Also it was observed that for higher roughness the variation of λ increases in magnitude due to more turbulence between the intermolucar particles.

2 Friction factor (*f*) varies along the lateral direction also observed from observed experimenatl data sets along with other researchers data series.Friction factor observed with two different criteria as global friction factor (f_g) evaluted from a perticular flow depth of the given channel geometry by calculating manning's *n* and hydraulic radius (R). Local friction factor (f_l) also evaluated from point to point by calcualting the depth averaged velocity and boundary shear stress from observed and measured data sets. In constant flow domain the friction factors value remains constant for whole cross-section but in trapezoidal channel it varies greatly in side wall or varying flow domains, it because of the turbulence and vertices formation .So it is no need to calibrate the friction factor, because it remains constant and it

also depend upon the manning's *n* which is constant for a channel through out the whole lateral and longitudinal section.

3 The secondary flow coefficients K_1 and K_2, which were responsible for secondary flow calibrated successfully and used as input parameter in analytical solution of SKM to modify the SKM for accurate prediction in depth averaged velocity. It was observed that for rectangular channel in constant flow domain only, K_1 varied with flow aspect ratio almost constant value due to less turbulence occurrences, while in trapezoidal channel small deviation can be observed varied with flow aspect ratio due to more turbulence than rectangular channel the total flow were responsible for two different regions i.e. constant flow domain and variable flow domain. K_2 was an another secondary flow coefficient which can be only observed in variable flow domain in case of trapezoidal channel for both smooth and rough open channels. Value of K_2 was more as compared to vale of K_1 due to momentum transfer between two different regions were occurred.

4 Three dimensional turbulent structures were investigated experimentally and calibrated numerically for secondary currents .The effects of the free surface, the channel shape and the boundary roughness on secondary currents were also studied experimentally. The secondary currents mechanism was also discussed by using basic vorticity equation.

5 Secondary currents structure in trapezoidal channel is different from rectangular open channel flows. A vortex with reverse rotation of free surface vertex is generated at the interface region between variable flow domain (i.e. side wall) and constant flow domain (i.e. free surface). It also has been observed, the structures of secondary currents are not appreciably changed although the boundary roughness conditions varied along the width of channel. But span-wise vertex scale increases as the flow aspect ratio increases. Three dimensional structures of the primary mean velocity, the turbulence intensities and secondary current coefficients are considered for accurate prediction of depth averaged velocity (U_d).

6 Multiple linear regression has been applied to model these calibrating coefficient friction factor (f), non dimensionless eddy viscosity (λ) and secondary flow parameter (Γ) with secondary flow coefficients K_1& K_2. Using these calibrating co-efficient the modified SKM is found to provide better depth averaged velocity

distribution as compared to the SKM method. Also the predicted method has been well validated against experimental channel data sets, FCF data, other researcher's data, and natural river data of river Sengai (B) and river Senggai.

7.2 Scope of future work

The followings are the scope of future work concerning the present research work:

1. The present research has been done for smooth and rough inbank flow. This research can extend to mobile bed cases, where the secondary currents are predominant due to the transport of sediments.
2. Also the present research can be extended to investigate of flow mechanism affected by secondary currents in meandering open channel.
3. The further work can be done in compound channel flow with different configuration like prismatic and non prismatic in cross-section throughout its length.
4. Also a refinement to the present model can be investigated by considering a large numbers of data in smooth and rough channel flow.

References

[1] A. R. Zarrati, Y. C. Jin and S. Karimpour. "Semi analytical model for shear stress distribution in simple and compound open channels." *Journal of Hydraulic Engineering* vol. 134, no. 2, 205-215, 2008.

[2] A. Tominaga, I. Nezu, K. Ezaki, and H. Nakagawa. "Three-dimensional turbulent structure in straight open channel flows." *Journal of hydraulic research*, vol.27, no. 1, pp. 149-173, 1989.

[3] D. Knight, and A. Shamseldin, eds. *River basin modelling for flood risk mitigation*. CRC Press, 2005.

[4] D. Knight, and A. Shamseldin,.eds.,"River basin modelling for flood risk mitigation." CRC Press, 2005.

[5] D. W Knight, H. S. Patel, J. D. Demetriou, and M. E. Hamed. "Boundary shear stress distributions in open channel and closed conduit flows." *Proceedings of Euromech 156-The Mechanics of Sediment Transport*, 33-40, 1982.

[6] D. W Knight., and R. H. J. Sellin. "The SERC flood channel facility." *Water and Environment Journal*, vol. 1, no. 2, 198-204, 1987

[7] D. W. Knight, K. W. H. Yuen, and A. A. I. Alhamid. "Boundary shear stress distributions in open channel flow." *Physical mechanisms of mixing and transport in the environment* 51-87, 1994.

[8] D. W.Knight, and J. B. ABRIL C. "Refined calibration of a depth-averaged model for turbulent flow in a compound channel." *Proceedings of the Institution of Civil Engineers. Water, maritime and energy*, vol. 118, no. 3, 151-159, 1996.

[9] D. W.Knight, and K. Shiono. "Turbulence measurements in a shear layer region of a compound channel." *Journal of hydraulic research*, vol. 28, no. 2, 175-196, 1990.

[10] D.W. Knight, M. Omran, and X. Tang. "Modeling depth-averaged velocity and boundary shear in trapezoidal channels with secondary flows." *Journal of Hydraulic Engineering*, vol.133, no. 1, 39-47, 2007.

[11] G. K. Batchelor, "An introduction to fluid dynamics." *Cambridge University Press. Cambridge. UK*, vol. 515, P13, 1967.

[12] G. V. Wilkerson and J. L. McGahan. "Depth-averaged velocity distribution in straight trapezoidal channels." *Journal of Hydraulic Engineering*, vol. 131, no. 6, 509-512, 2005.

[13] H. Nakagawa and I. Nezu. "Experimental investigation on turbulent structure of backward-facing step flow in an open channel." *Journal of Hydraulic Research* vol. 25, no. 1, 67-88, 1987.

[14] H. Schlichting, "Boundary ayer ¹heory.",McGraw Hill, Newyork, 459-465,1979.

[15] I. Nezu, "Open-channel flow turbulence and its research prospect in the 21st century." *Journal of Hydraulic Engineering*, vol.131, no. 4, 229-246, 2005.

[16] I. Nezu, A. Kadota, and H. Nakagawa. "Turbulent structure in unsteady depth-varying open-channel flows." *Journal of Hydraulic Engineering* 123, no. 9 752-763, 1997.

[17] I. Nezu, and H Nakagawa, "Turbulence in open channels." *AA Balkema, Rotterdam, The Netherlands*, 1993.

[18] I.Nezu, "Open-channel flow turbulence and its research prospect in the 21st century." *Journal of Hydraulic Engineering*, vol. 131, no. 4 229-246, 2005.

[19] I.Nezu, H. Nakagawa, and G.H. Jirka. "Turbulence in open-channel flows." *Journal of Hydraulic Engineering*, vol. 120, no. 10, pp.1235-1237, 1994.

[20] J. Chlebek, "Modelling of simple prismatic channels with varying roughness using the SKM and a study of flows in smooth non-prismatic channels with skewed floodplains." PhD diss., University of Birmingham, 2009.

[21] J. Chlebek and D. W. Knight. "A new perspective on sidewall correction procedures, based on SKM modelling." *RiverFlow*, vol.1, pp. 135-144, 2006.

[22] J.Guo, and P. Y. Julien. "Shear stress in smooth rectangular open-channel flows." *Journal of hydraulic engineering* vol. 131, no. 1, 30-37, 2005.

[23] K. Ansari, H. P. Morvan, and D. M. Hargreaves. "Numerical investigation into secondary currents and wall shear in trapezoidal channels." *Journal of Hydraulic Engineering*, vol. 137, no. 4, 432-440, 2011.

[24] K. Shiono and D. W. Knight. "Turbulent open-channel flows with variable depth across the channel." *Journal of Fluid Mechanics*, vol. 222, 617-646, 1991.

[25] K. Shiono and T. Feng. "Turbulence measurements of dye concentration and effects of secondary flow on distribution in open channel flows." *Journal of Hydraulic Engineering*, vol. 129, no. 5, 373-384, 2003.

[26] K. Shiono, and D. W. Knight. "Mathematical models of flow in two or multi stage straight channels." In *Proc. Int. Conf. on River Flood Hydraulics*, 229-238, 1990.

[27] K. Shiono, and D. W. Knight. "Two-dimensional analytical solution for a compound channel." In *Proc., 3rd Int. Symp. on refined flow modeling and turbulence measurements*, 503-510. 1988.

[28] K. Shiono, and Donald W. Knight. "Turbulent open-channel flows with variable depth across the channel." *Journal of Fluid Mechanics* 222 (1991): 617-646.

[29] K. Yang, N. Ruihua, L. Xingnian, and C. Shuyou. "Modeling depth-averaged velocity and boundary shear stress in rectangular compound channels with secondary flows." *Journal of Hydraulic Engineering*, vol. 139, no. 1, pp. 76-83, 2012.

[30] K.V.N Sarma, P. Lakshminarayana and NS LakshmanaRao. "Velocity distribution in smooth rectangular open channels." *Journal of Hydraulic Engineering* 109, no. 2 270-289, 1983.

[31] M. Jesson, , M. Sterling, and J. Bridgeman. "Modeling Flow in an Open Channel with Heterogeneous Bed Roughness." *Journal of Hydraulic Engineering*, vol. 139, no. 2, pp. 195-204, 2012

[32] M. N. Omran, "Modelling stage-discharge curves, velocity and boundary sheer stress distributions in natural and artificial channels using a depth-averaged approach." PhD diss., University of Birmingham, 2005.

[33] O. Reynolds, "An experimental investigation of the circumstances which determine whether the motion of water shall be direct or sinuous, and of the law of resistance in parallel channels." *Proceedings of the royal society of London*, vol. 35, no. 224-226 84-99, 1883.

[34] P. Davidson, *Turbulence: an introduction for scientists and engineers*. Oxford University Press, USA, 2015.

[35] P. R Wormleaton,. "Floodplain secondary circulation as a mechanism for flow and shear stress redistribution in straight compound channels." *Coherent flow structures in open channels* (1996): 581-608.

[36] P.M. Steffler, N. Rajaratnam, and A. W. Peterson. "LDA measurements in open channel." *Journal of Hydraulic Engineering* ,vol 111, no. 1, 119-130, 1985.

[37] Patel, V.C. Calibration of the Preston tube and limitations on its use in pressure gradients. *Journal of Fluid Mechanics*, vol. 23, no. 01, 185-208, 1965.

[38] S. Atabay, Stage-discharge, resistance and sediment transport relationships for flow in straight compound channels.Doctoral dissertation, University of Birmingham. 2001.

[39] S. Sharifi, "Application of evolutionary computation to open channel flow modelling." PhD diss., University of Birmingham, 2009.

[40] V.C Patel, "Calibration of the Preston tube and limitations on its use in pressure gradients." *Journal of Fluid Mechanics*, vol. 23, no. 01, 185-208, 1965.

[41] V.T. Chow, "Open channel hydraulics." McGraw-Hill, New York, 1959
[42] X. Tang, Derivation of the wave speed-discharge relationship from cross-section survey for use in approximate flood routing methods, 1999.

Dissemination

1. "Prediction of depth averaged velocity in smooth open channel flow", ISH, *Journal of hydraulic Engineering*, Taylor & Francis (Communicated),2016
2. "Variation of local friction factor in an open channel flow", Accepted for Indian journal of science & technology, through NCTACE-2016.
3. "Apparent shear in an asymmetric compound channel" *River Flow 2016, International conference on Fluvial Hydraulics (July12-15), St. Louis, USA. (Accepted).*
4. "Prediction of Interacting length for evaluation of Discharge in symmetric and asymmetric compound channel" *20th International Conference on Hydraulics, Water Resources and River Engineering (HYDRO-2015).*
5. "Depth averaged velocity distribution for symmetric and asymmetric compound channel.*" 1st International Conference on Micro-electronics, computing & Communication Systems (MCCS-2015), (Accepted for Springer proceedings).*
6. "Flow computation in symmetric and asymmetric compound channels using Conveyance Estimation System."*1st International Conference on Nano-electronics, Circuits & Communication Systems (NCCS-2015), (Accepted).*